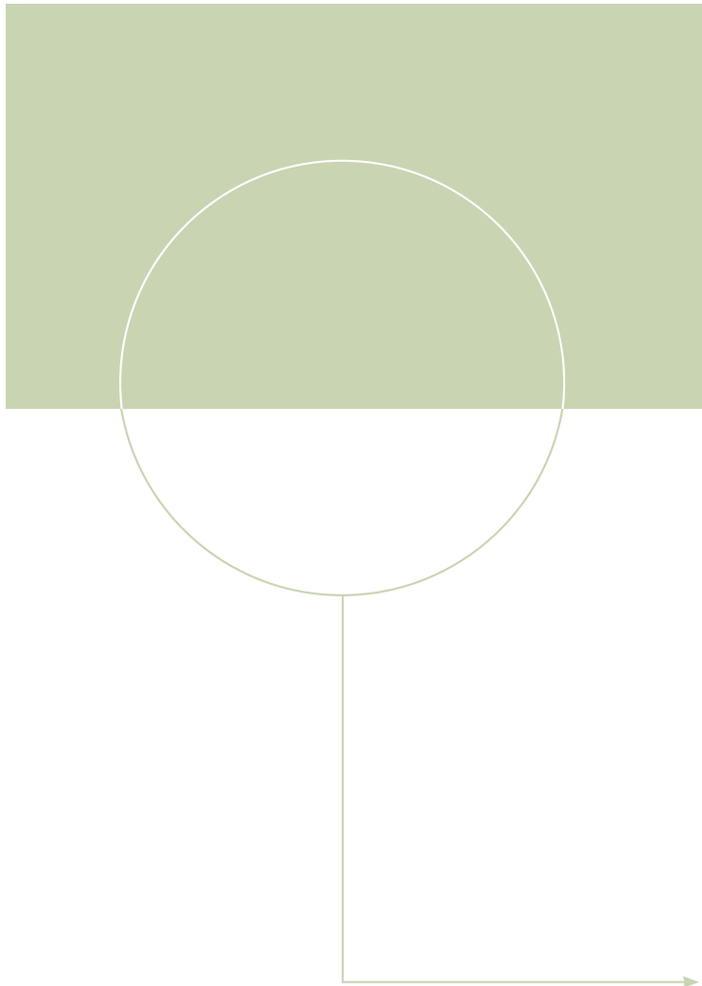

Master's thesis

2019

Ellinor Bratt Sletfjerding

NTNU
Norwegian University of
Science and Technology
Faculty of Engineering
Department of Civil and Environmental Engineering

Ellinor Bratt Sletfjerding

Smart vapour barriers in compact timber-framed roofs

Parameter analysis and field measurements

June 2019

NTNU
Norwegian University of
Science and Technology

NTNU
Norwegian University of
Science and Technology

NTNU

Norwegian University of
Science and Technology

Smart vapour barriers in compact timber-framed roofs

Parameter analysis and field measurements

Ellinor Bratt Sletfjerding

Civil and environmental engineering
Submission date: June 2019
Supervisor: Stig Geving, IBM
Co-supervisor: Lars Gullbrekken, SINTEF

Norwegian University of Science and Technology
Department of Civil and Environmental Engineering

Preface

This is a master thesis written at the Department of Civil and Environmental Engineering of the Norwegian University of Science and Technology (NTNU) in Trondheim, Norway. I have investigated the functionality of a smart vapour barrier in compact timber-framed roofs through a parameter analysis and on-site measurements of two pilot projects. The pilot projects are constructed by Klima2050 in collaboration with Statsbygg, Skanska Husfabrikken and Bakke Bygg.

I want to thank Bakke Bygg, Skanska Husfabrikken and Klima2050 for providing me with the necessary details of the constructions in the field study. In addition, I want to thank Sivert Uvsøkk, a senior research scientist working for SINTEF, and Lars Gullbrekken, a research scientist working for SINTEF Klima2050. Thank you for the guidance and discussions regarding my results. Lars Gullbrekken has provided me with details of the pilot projects and counselled me throughout the semester. I also want to thank Professor Stig Geving by the Department of civil and environmental engineering, NTNU, for guidance and for helping me organising my thesis throughout the semester.

Ellinor Bratt Sletfjerding

Trondheim, 04. juni 2019

Abstract

Various studies have concluded that a compact timber-framed roof with a Smart Vapour Barrier (SVB) can increase the climate robustness of the construction. In addition, it can decrease the height of the roof assembly, the use of materials, construction time and create economic gains.

This study aims to determine the robustness of a compact timber-framed roof with SVB and identify parameters that can improve the drying potential and the risk of mould. WUFI 2D is used in a parameter analysis to simulate different constructions with various materials and climates. The effect of sun exposure, internal conditions, initial conditions, type of construction and the choice of materials are investigated. The results of the different scenarios are compared with a reference construction.

The results of the parameter analysis show that built-in moisture, internal moisture load and the external climate are driving factors for increasing the drying process. In addition, the type of materials used in the construction are important to consider. The type of SVB is essential and the results show that with low vapour diffusion resistance values for high Relative Humidity (RH) is increasing the drying potential and allows more moisture to dry towards the internal air. Most of the scenarios are at risk of mould. The study identifies that external temperature, cloud index and latitude are all factors that should be considered in regard to mould growth. The most favourable scenario is located in Oslo with low internal moisture load, low built-in moisture and using an SVB with low vapour diffusion resistance for high RH.

Two pilot projects created by Klima2050 for different climates have been analysed in order to understand how the constructions respond to real climates. The two projects are located in Longyearbyen (constructed by Statsbygg) and Lund Vest near Oslo (constructed by Bakke Bygg). Both projects are constructed with sensors measuring the moisture content in the timber structure, the RH and temperature of the air in the insulation. The constructions have been simulated in WUFI 2D with climate data measured on-site, aiming to verify material data.

The analysis period is over one winter. The results show that the initial moisture content is well below the critical limit and that the buildings were built in dry conditions. There is little to no risk of mould growth due to the low moisture content in the timber structure. Based on the result of the parameter analysis, the project located in Lund Vest has a drying potential due to the area it is situated. The construction in Longyearbyen, however, should be investigated further. Because of high latitude, it has reduced direct solar radiation.

Sammendrag

Flere studier har konkludert med at et kompakt tretak med Smart Dampsperre (SDS) kan øke klimarobustheten. I tillegg minkes høyden på taktkonstruksjonen, bruken av materialer, byggetiden og kan dermed gi økonomisk gevinst.

Denne studien undersøker hvilke parametere som kan øke robustheten til et kompakt tretak med SDS og vurdere om en slik konstruksjon fungerer for Nordiske klima. Målet er å vurderer risiko for muggvekst og potensialet konstruksjonen har for å tørke. WUFI 2D er brukt i en parameter analyse for å simulere ulike konstruksjoner og klima. Effekten av solstråling, innvendige vilkår, startbetingelser, type konstruksjon og materialbruk er studert. De ulike scenarione er sammenlignet med en standardisert konstruksjon.

Resultatene fra parameteranalysen viser at startfukt, innvendig fuktnivå og utvendig klima er de drivende faktorene for å øke robustheten til taket. I tillegg er det identifisert at materialbruk er viktig å vurdere. Parameteranaysen viser at en SDS med lav dampdiffusjonsmotstand for høye verdier av Relativ Fuktighet (RF) gir et bedre resultat fordi den tillater mer fuktighet å tørke mot innelufta. De fleste av scenarioene har risiko for muggvekst i den øvre delen av konstruksjonen. Studien viser at utetemperaturen sammen med skydekkeindeksen og breddegraden har betydning for muggvekst. Det gunstigste scenarioet er lokalisert i Oslo, har lavt innvending fuktnivå, lavt startfukt i trematerialene og en SDS som har lav dampdiffusjonsmotstand verdi som gir gode muligheter for uttørkning mot innelufta.

I tillegg er to pilotprosjekter, konstruert av Klima2050 for to ulike klima, analysert for å forstå hvordan konstruksjonene fungerer i praksis. Prosjektene er lokalisert i Longyearbyen (bygget av Statsbygg) og i Lund Vest nær Oslo (bygget av Bakke Bygg). Begge prosjektene inneholder sensorer som måler trefuktigheten i bjelkene, RF og temperatur i isolasjonen. Konstruksjonen er brukt i en simulering med WUFI 2D med klimadata som er målt på stedet. Målet med simuleringen er å verifisere materialparameterne i prosjektene.

Analyseperioden er delt over en vinter. Resultatene fra målingene viser at startfuktinnholdet i bjelkene er lavt og at byggeprosessen har skjedd under tørre omstendigheter. De viser lite til ingen risiko for muggvekst på grunn av lite fuktinnhold. Basert på resultatene fra parameterundersøkelsen har prosjektet i Lund Vest stor uttørkningsevne på grunn av at bygget er plassert i nærheten av Oslo. Prosjektet lokalisert i Longyearbyen derimot, bør følges nøye med for å vurdere hvordan taket responderer til lav solhøyde og lite direkte solstråling.

Contents

Chapter 1: Introduction

An environmental vulnerability report on buildings describes how climate change can affect Norwegian buildings in the future. The report predicts that the future climate will be warmer, wetter and wilder, resulting in increased risk of mould in Norwegian buildings (Flyen, C. et al., 2010). This is demonstrated in figure 1.1. Today there are around 615 000 buildings in Norway that are at risk of mould, and more buildings will fall under this category if building methods are not improved (Flyen, C. et al., 2010). Therefore, future buildings should adapt to decrease the risk of building damage due to climate change.

In order to meet the future climate, SINTEF has established a research centre called Klima2050. The aim of Klima2050 is to reduce societal risks that are a result of the changing climate. Resilient buildings, stormwater management, measures for prevention of water triggered landslides and decision-making processes are among the topics that Klima2050 is investigating (Klima2050, 2019). The study presented in this paper is in collaboration with Klima2050 and is focusing on moisture resilient buildings. To study the topic in practice, Klima2050 is collaborating with the private sector to form pilot projects. Two of these are being studied in this paper.

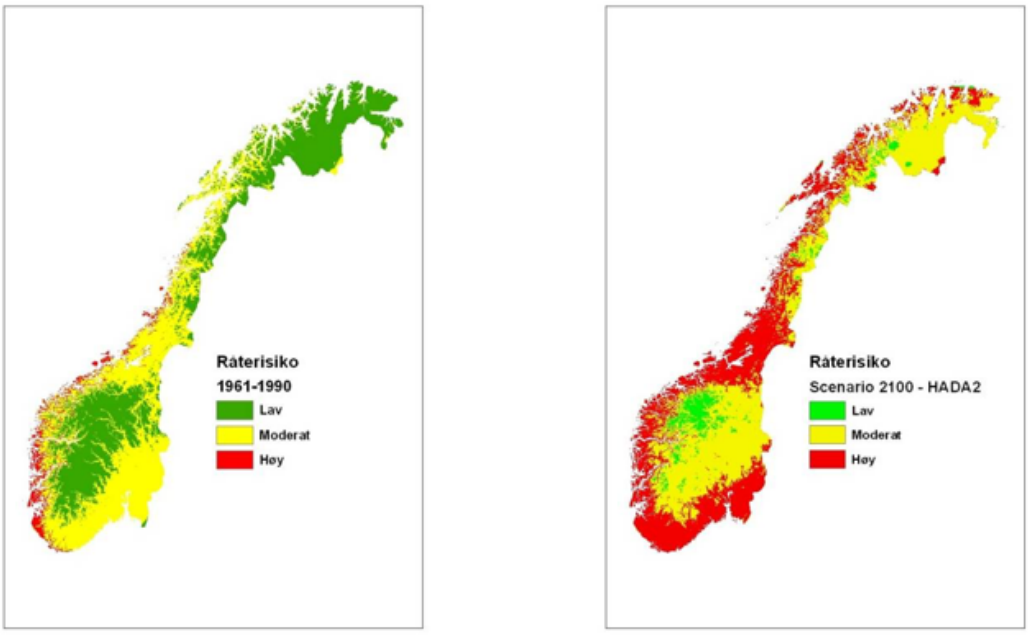

Figure 1.1: The potential risk of mould in Norwegian buildings today (left) and for future scenarios (right), marked in red (high), yellow (moderate) and green (low) (Flyen, C. et al., 2010)

1.1 Project aim and purpose

This paper will investigate the robustness of a compact timber-framed roof using a Smart Vapour Barrier (SVB). Many laboratory and simulation studies show that the use of an SVB in compact timber-framed roofs can increase the robustness of the construction and create drying potential. Thus, the technology has come far enough to be implemented in pilot projects.

The aim of this project is to identify:

- parameters that are affecting the drying potential of a compact timber framed roof with SVB
- any risk of mould in the constructions that er being studied
- the robustness of a compact timber framed roof with SVB of two pilot projects with on-site measurements
- material data in the pilot projects with Wärme Und Feuchte Instationär: Transient Heat and Moisture (WUFI)

1.2 Background

1.2.1 Moisture in buildings

Construction robustness is an important issue regarding moisture damage. Studies show that moisture is considered the biggest problem regarding building damage (Holme, J. and Geving, S., 2018). Flat roofs are especially weak constructions regarding water accumulation, and timber constructions are weak regarding the risk of mould.

Moisture accumulates in a construction in different ways and it is important to understand these mechanisms to prevent damages. Some of these transport mechanisms are given in the list below. This study focuses on water vapour diffusion and it is assumed no air nor water leakage into the construction.

- Air leakage moving water in form of liquid into the construction
- Damage on the envelope that allows rain water into the construction
- Capillary suction in the materials
- Moisture convection, water vapour that is transported by air leakage
- Water vapour diffusion from the internal air into the construction

The hygroscopic properties of wood vary according to species and depend on relative humidity (RH). Wood absorb and desorb moisture to reach equilibrium with the surrounding air. Figure 1.2 shows the absorption and desorption curve of spruce. The hygroscopic area of wood is when it is absorbing moisture in the pore walls. This is normally when RH is below 98% (SINTEF byggforsk, 2018a). The pores are being filled due to capillary suction when RH is above 98%.

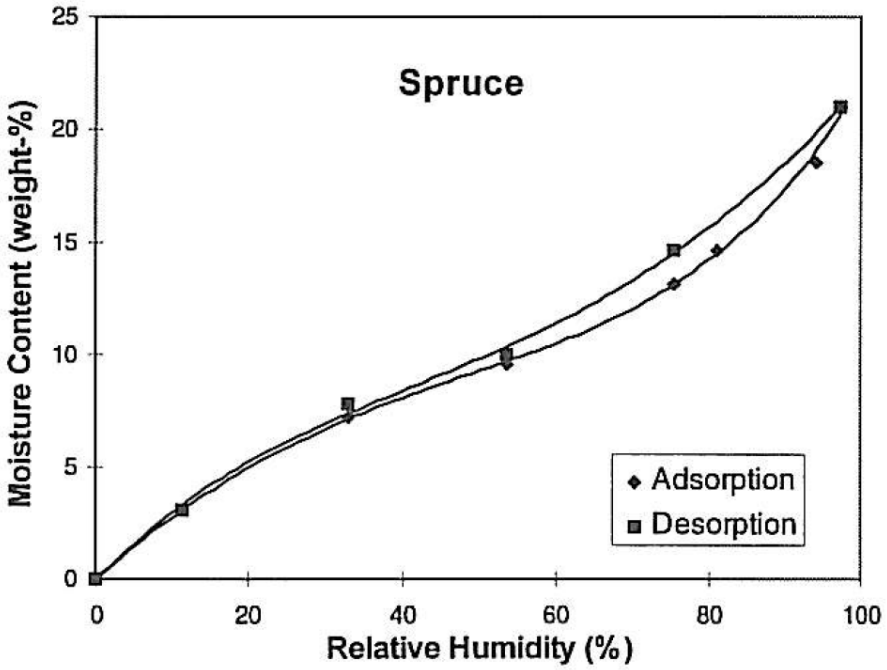

Figure 1.2: Sorption curve for spruce (Bergheim, E, Geving, S, and Time, B, 1998)

1.2.2 Risk of mould and rot decay

Wood is a material that can absorb and store water, and will over time reach equilibrium with the ambient air. The critical moisture level is a limit that should not be exceeded to avoid damage.

Table 1.1 describes different organisms that can damage building components due to moisture. This study focuses mainly on the risk of mould, but the accumulation of moisture over time can lead to decay of the wooden material. Development of mould in a construction needs moisture, heat, nutrient (biological material) and time. When the temperature decreases to 0°C, the growth stops. However, it can continue to grow when the conditions are suitable. If the temperature increases above 25-30°C, the growth decreases, and if it reaches 40-50°C, the mould dies (SINTEF byggforsk, 2005).

Development of mould depends on various factors such as wood species, surface quality, fungus species and the length of the periods allowing mould to develop (Viitanen, 1994). The potential of mould growth can be divided into 6 indexes, where 0 is no growth and

6 is heavy growth. Various studies have investigated how to model the potential for mould growth. The VTT model is a dynamic model that considers the time where the conditions, RH and temperature, are suitable for mould growth and calculates the mould growth index accordingly. Figure 1.3 shows a modelled coherence of time, temperature and RH. A laboratory study investigating the mould development in a wall assembly finds that spruce reach a mould index between 2-3 during the spring (Viitanen, 1994). The simulated exposure conditions were 60-95% RH and 2-10℃ and the indexes correspond to $<$10% coverage of mould on a surface (microscopical/visual). Another study investigating the factors affecting the development of mould concludes that spruce sapwood is at risk of mould when the RH is above 80% and temperature between 5℃ and 50℃ over a longer period of time (Viitanen, 1994). However, based on figure 1.3, when the conditions are close to the limit, the period needed for mould to develop is long.

Table 1.1: Damage on building components due to moisture (Viitanen, H. et al., 2003)

Organisms	**Damage**	**RH [%]**	**Temperature [℃]**
Bacteria	Biocorrosion of different materials, smell and health problems	RH $>$ 97%, wet material	ca -5 to +60
Mould fungi	Surface growth on different materials, smell and health problems	RH $>$ 75%	ca 0 to + 50
Blue-stain fungi	Blue-stain of wood and permeability change	RH $>$ 95%	ca -5 to + 45
Decay fungi	Different type of decay in wood (soft rot, brown rot or white rot) and strength loss of materials.	RH $>$ 95%	ca 0 to +45
Algae and lichen	Surface growth of different materials on outside or weathered material	Wet materials, also nitrogen and low pH are needed	ca 0 to +45
Insects	Different type of damages in organic materials, surface failures or strength loss.	RH $>$ 65% depends also on environment	ca 5 to +50

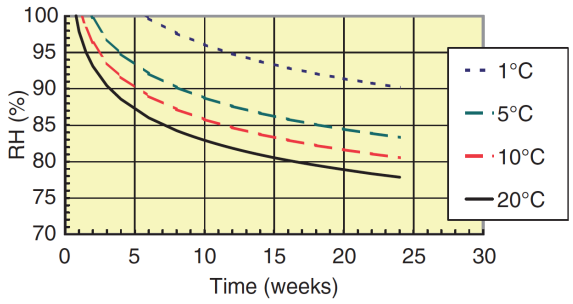

Figure 1.3: Time dependent mould development (Viitanen, H. et al., 2003)

1.2.3 Smart vapour barriers (SVB)

SVB is a vapour barrier with varying diffusion resistance depending on RH. There are many different types with various values of diffusion resistance and some of these are presented in table 1.2. In theory, the SVB has low diffusion resistance for high RH and reversibly for low RH. Moisture reduces the bonds keeping the molecules together and increases the volume. The expanding pores allow more moisture to pass. Reversibly, pores become smaller with decreasing RH which prevent moisture to pass.

μ is the water vapour resistance factor which indicates the material's reluctance to let water vapour pass through. s_d value is the vapour diffusion resistance measured in m and is given as the equivalent air layer thickness. The latter value is the water vapour resistance factor times the thickness of the material.

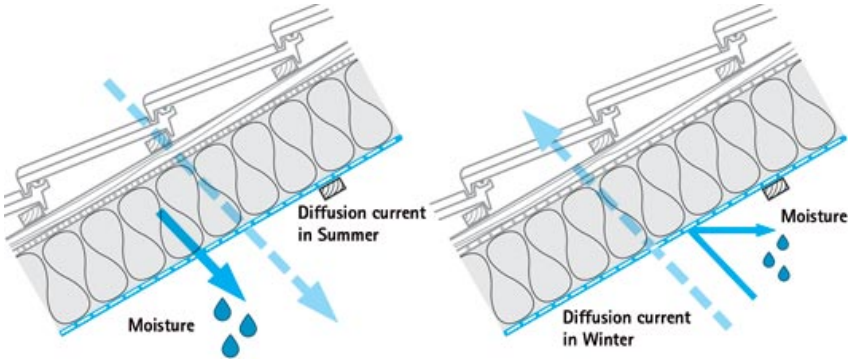

Figure 1.4: Direction of vapour pressure gradient in the summer and winter season (Crosson, N., 2008)

The diffusion current, vapour pressure gradient, is depending on the partial vapour pressure on each side of the material. The partial vapour pressure is a function of temperature and water vapour concentration, where it increases with increasing temperature and water vapour concentration (Thue, J. V., 2016). A compact wooden roof is in general constructed with a water tight membrane on top and therefore has no water sources from the external ambient. The direction of the vapour gradient is pointing towards the side

with the lowest partial vapour pressure, and therefore towards the area in the construction with the lowest temperature. Figure 1.4 shows how the pressure gradient is changing according to season. In summer, the solar radiation heats up the roofing membrane and cause an inward vapour pressure gradient. The average RH on both sides of the SVB is high which allows the construction to dry towards the internal air. In winter, however, the vapour pressure gradient is pointed towards the external air. Hence, the average RH on both sides of the SVB should be low, so that the corresponding s_d value is high. This prevents moisture diffusion into the roof construction.

In short, the technology of an SVB can increase the drying potential and reduce the risk of mould. Therefore, compact wooden roofs have a potential to increase the climate robustness of new constructions.

1.2.4 Compact timber framed roofs

Timber is a preferred material to use in Nordic buildings due to its low environmental impact, its ease of utilisation and its local accessibility. It is an organic material that is at risk of mould and rot within humid environments. Mould grows easy in hot and wet locations, and due to the prediction of a hotter, wetter and wilder climate in the future, the risk of mould will increase.

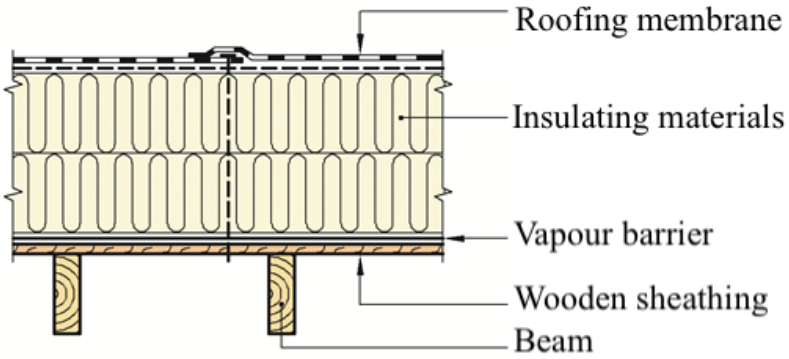

Figure 1.5: Composition of a traditional compact timber framed roof (SINTEF byggforsk, 2018b)

A traditional flat compact wooden roof, as shown in figure 1.5, has all the insulation above the wooden sheathing and the vapour barrier is placed underneath the insulation. The roofing membrane is water tight to prevent water from coming into the construction from the external environment. The vapour barrier, usually a foil with high s_d, is preventing vapour diffusion from the inside air into the construction (SINTEF byggforsk, 2018b). In short, the insulation is placed between two vapour-tight membranes and organic materials should not be installed here in case of built-in moisture content.

By moving the insulation beneath the wooden sheathing and in between the beams, roof height and material use decreases. This solution requires a drying potential to prevent

mould growth in the timber frame. A solution is shown in figure 1.6, where a water tight roofing membrane is placed on top and an SVB underneath the insulation.

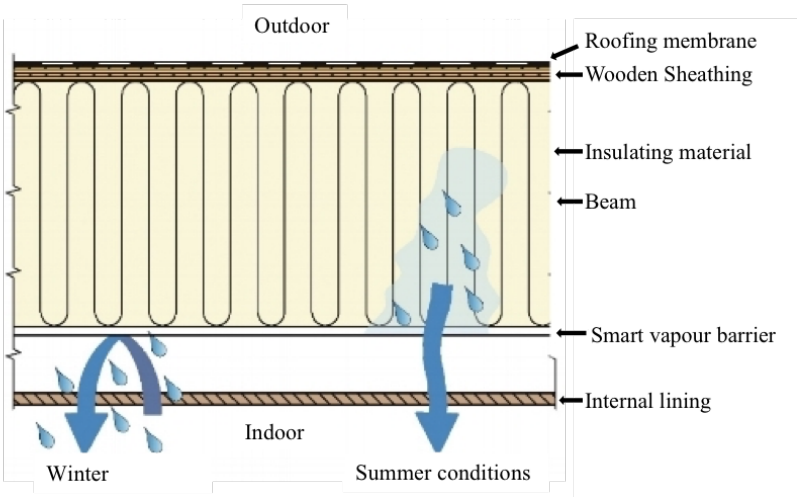

Figure 1.6: Composition of a compact timber framed roof with SVB (Klima2050, 2018)

1.3 Parameters affecting the drying potential

Various conditions and parameters can affect the drying potential. As described in chapters 1.2.2 and 1.2.3 the moisture in the materials will distribute within the roof assembly according to the vapour pressure gradient and material properties. The aim of having a roof assembly with SVB is to create possibilities for the timber elements to dry. Therefore, it is important to optimise a construction so that the drying potential is sufficient. The following is a description of various parameters that are identified to affect the robustness of a timber-framed roof with SVB. However, other parameters, such as good craftsmanship and accumulation of snow on top of the roof, can also be of importance regarding the robustness of the roof construction.

1.3.1 Type of smart vapour barrier

There are different kinds of SVBs with various ranges of s_d values available on the market today. Laboratory studies analysing the use of the different SVBs in table 1.2, conclude that the least vapour open SVB for low RH, and most vapour open for high RH is the most effective in flat roofs for Nordic climates (Geving, S, Thorsrud, E, and Uvsøkk, S., 2014; Geving, S., Stellander, M., and Uvsløkk, S., 2013; Geving, S, Thorsrud, E, and Uvsøkk, S., 2013). The two materials showing the best drying potential over one summer had sd $= 0,2$m (NovaFlex) and sd $= 0,05$m (AirGuard Smart) at the minimum. Furthermore, the constructions with AirGuard Smart, sd $= 0,05-102$m and polyethylene (PE) foil had the least water accumulation during winter.

Table 1.2: Types of SVBs (Geving, S., Stellander, M., and Uvsløkk, S., 2013)

Name	$\mathbf{s_d = 0.2m}$	**Material**
Delta-Novaflex, MemBrain, Difunorm Vario	0,2-5 m	Polyamide
Intello (Pro Clima, 2006)	0,25 - 26 m	Polyethylene copolymer
AirGuard Smart	0,05-102 m	Polyvinyl alcohol film
Hygrodiode 200A	1-20m	A laminated composition of synthetic fibres with capillary properties, Pe-foil and polyamide

1.3.2 Insulation material

Hygroscopic insulation has the ability to absorb and store moisture, and then release it when the conditions are dryer. A typical hygroscopic insulation material is wood fibre. Mineral wool, however, is not a hygroscopic material and has no capillary suction properties. Studies have concluded that using an SVB combined with hygroscopic insulation have little effect. The results show that hygroscopic insulation decreases the risk of mould due to the ability to store water trapped in the construction, and decrease RH in the critical areas (Langerock, C. et al., 2017; Werther, N., Winter, S., and Sieder, M., 2010; Ghazi Wakili, K. and Frank, T., 2004).

1.3.3 Internal cladding

An internal resistance higher than the value of the SVB with the corresponding average RH can reduce the drying potential and trap moisture between the SVB and the internal lining. However, a laboratory study concludes that a painted ceiling, $s_d = 0.135$m has an insignificant effect (Thorsrud, E., 2013).

The use of wooden panels as internal lining can also impact the drying potential because of its hygroscopic properties. A WUFI study demonstrated that the wooden panel works as a buffer in the same way as the SVB, and the use of an SVB was unnecessary in combination with wooden panels (Ghazi Wakili, K. and Frank, T., 2004).

1.3.4 Sun exposure

Shading is an important factor for the drying potential of a timber-framed roof. The surface temperature is lower in shaded areas compared to sun-exposed areas. This means that the vapour pressure gradient decreases, which reduces the drying potential. Laboratory studies conclude that 40% of the drying rate is reduced compared to unshaded conditions for all SVBs tested. The same study identifies that Delta-Novaflexx, $s_d = 0,2-5$m,

and Airguard Smart, $s_d = 0,05 - 102$m have sufficient drying potential. However, a field test including WUFI simulations concludes that the surface temperature is not high enough for a sufficient drying potential when using Photovoltaic (PV) panels that shade the roof assembly (Bludau, C., Schmidt, T., and Künzel, H. M., 2010).

Compact wooden roofs can come with different top layers, for example, green roofs, insulation or gravel. It is shown in a test house study, that applying an additional layer resembles shaded conditions. The temperature of the roofing membrane decreases and so does the drying potential during summer (Werther, N., Winter, S., and Sieder, M., 2010).

Another study identifies a correlation between air tightness and shaded conditions and concludes that shading is not a critical factor if the construction is air tight. However, shading is strongly affecting the drying potential when the construction is less air tight (Nusser, B. and Teibinger, M., 2013). Air leakage can cause moisture problems regarding convection as described in chapter 1.2.1. In case of shading, the temperature of the air reduces and RH increases, followed by water condensing. In Nordic climates, shading can be an issue due to seasonal variations of sun exposure.

1.3.5 Climate

External climate

Sun exposure and surface temperature are driving factors for the drying potential. Figure 1.7 shows climatic limits created in a WUFI study for different vapour barriers, an SVB, $s_d = 0,1-4,4$m, and a vapour barrier, $s_d = 3$m (Bludau, C. and Künzel, H. M., 2009). It is important to notice that this study only consider SVB with small maximum s_d values, in contrast to the requirement in Norway, $s_d = 10$m (Direktoratet for byggkvalitet, 2014). In theory, the climatic limit can change by using an SVB with higher maximum diffusion resistance. A parameter study concludes that using Novaflexx and Intello (see table 1.2) in Tromsø, Røros and Trondheim is critical because of reduced insulation capability and increase of mould growth in the wooden sheathing. The results show, however, that AirGuard Smart is the most favourable product to use in every climate (Thorsrud, E., 2013).

Figure 1.7: Geographical limits of the use of a vapour retarder, $s_d = 0,1 - 4,4$, and vapour barrier $s_d = 3$m (Bludau, C. and Künzel, H. M., 2009)

Internal climate

Because of the humidity dependency of an SVB, the internal climate is an important factor to consider. With high internal RH, the diffusion resistance can be lower than desired in the winter season. This effect was demonstrated in a parameter study, where it is concluded that higher internal moisture load increases the water accumulation in the roof assembly and therefore increases the risk of mould in the construction (Thorsrud, E., 2013).

1.3.6 Construction

How a roof is constructed varies from project to project. For example, the type of beams, the height of the insulation in the roof assembly and inclination. Different types of beams have different characteristics. The I-beam is composed of two flanges, one on top and one on bottom separated by a vertical wood board. A laboratory study concludes that the thickness of the insulation layer is influencing the fluctuation of the RH levels (Olsen, T. A., 2017). The results show that RH is higher for the test boxes with 20 cm insulation compared to the boxes with 30 cm in areas near the SVB. The laboratory study also includes a comparison between a solid-wood beam and an I-profiled beam. It concludes that the solid-wood beam works as a moisture buffer, it contributes by decreasing the RH fluctuations for areas close to the beam. However, the drying rate of an I-profile was higher, because it has more sides to dry from.

1.3.7 Initial conditions of construction materials

During the construction of a building, the materials can be exposed to a humid environment and rain which can result in high built-in moisture. It is desired to reduce the moisture content in the wooden elements beneath the critical limit described in chapter 1.2.2 before closing the construction.

In addition to high initial moisture content, the time in which closing the construction can be of importance. In case of possible built-in moisture, the drying potential should be high. It is normal to close a building during the fall. The reason for this is because it is intended to reduce the moisture uptake in the materials that can happen in case of rain, and reduced temperature. Towards winter, however, the solar exposure is limited in Nordic countries, which is required for a drying process.

Chapter 2: Parameter analysis

Various parameters that are assumed to affect the drying potential and the risk of mould in compact wooden roofs are being investigated. Sun exposure and material properties such as vapour diffusion resistance and moisture storage are affecting the drying potential in different ways as described in chapter 1.3. Parameters that are being studied in this paper is given in table 2.1.

Table 2.1: Parameter study, (*table continued on the next page*)

Parameter		**1**	**2**	**3**	**4**	**5**	**6**	**7**	**8**	**9**	**10**
Location	Trondheim	x	x	x	x	x	x	x	x	x	x
	Bergen		x								
	Oslo		x								
	Kise, Hedmark		x								
	Kristiansand		x								
	Kristiansund		x								
	Mo i Rana		x								
	Tromsø		x								
Moisture load	Low		x	x							
	Medium	x				x	x	x	x	x	x
	High				x						
Roof height	450 mm						x				
	350 mm	x	x	x	x			x	x	x	x
	250 mm					x					
Top insulation	0 mm	x	x	x	x	x	x			x	x
	50 mm							x			
	100 mm								x		
Beam (Spruce)	I									x	
	K	x	x	x	x	x	x	x	x		x
Insulation	Mineral wool	x	x	x	x	x	x	x	x	x	
	Wood fibre										x
Internal lining	s_d = 0.2m	x	x	x	x	x	x	x	x	x	x
	s_d = 1m										
Moisture content	18 % in beam	x	x	x	x	x	x	x	x	x	x
	20 % in wooden sheathing	x		x	x	x	x	x	x	x	x
	18 % in wooden sheathing		x								
	15 % in wooden sheathing										
	15 % in beam										
Date of closing	1st of October	x	x	x	x	x	x	x	x	x	x
	1st of January										
	1st of April										
	1st of July										
SVB	AirGuard Smart	x	x	x	x	x	x	x	x	x	x
	Majrex										
Inclination	0 °	x	x	x	x	x	x	x	x	x	x
	30 °										
	45 °										
	90°										
Orientation	North										

Table 2.1: Parameter study, (*continued*)

Parameter		**11**	**12**	**13**	**14**	**15**	**16**	**17**	**18**	**19**	**20**
Location	Trondheim	x	x	x	x	x	x	x	x	x	x
	Bergen										
	Oslo										
	Kise in Hedmark										
	Kristiansand										
	Kristiansund										
	Mo i Rana										
	Tromsø										
Moisture load	Low								x	x	x
	Medium	x	x	x	x	x	x	x			
	High										
Roof height	450 mm										
	350 mm	x	x	x	x	x	x	x	x	x	x
	250 mm										
Top insulation	0 mm	x	x	x	x	x	x	x	x	x	x
	50 mm										
	100 mm										
Beam (Spruce)	I										
	K	x	x	x	x	x	x	x	x	x	x
Insulation	Mineral wool	x	x	x	x	x	x	x	x	x	x
	Wood fibre										
Internal lining	s_d = 0.2m		x	x	x	x	x	x	x	x	x
	s_d = 1m	x									
Moisture content	18 % in beam	x	x		x	x	x	x	x	x	x
	20 % in wooden sheathing	x			x	x	x	x			
	18 % in wooden sheathing		x						x	x	x
	15 % in wooden sheathing			x							
	15 % in beam			x							
Date of closing	1st of October	x	x	x				x	x	x	x
	1st of January				x						
	1st of April					x					
	1st of July						x				
SVB	AirGuard Smart	x	x	x	x	x	x		x	x	x
	Majrex							x			
Inclination	0 °	x	x	x	x	x	x	x			
	30 °								x		
	45 °									x	
	90°										x
Orientation	North								x	x	x

2.1 Methodology

2.1.1 WUFI 2D

WUFI is a state of the art hygrothermal simulation tool that performs numerical simulations of heat and moisture transfer based on vapour diffusion and liquid transportation. An overview of the transport mechanisms included in WUFI calculations is shown in table 2.2. In this study, WUFI 2D is used which differ from WUFI 1D due to its possibilities to calculate moisture movement in two directions (Wufi, 2018).

Table 2.2: Transport mechanisms in WUFI calculations (Künzel, H. M., 1995)

	Included	**Not included**
Heat transfer	Heat conduction Enthalpy flows through moisture movement Heat radiation	Air flow
Vapour transfer	Vapour diffusion Solution diffusion	Moisture transport due to convection
Liquid transfer	Capillary conduction Surface diffusion	Hydraulic flow Seepage flow Electrokinesis and osmosis

A WUFI simulation requires standard material properties in addition to storage and liquid transport properties. The basic material data that are essential for the calculations are listed below. Other data are optional depending on the material and the purpose of the project.

- Bulk density, [kg/m^3]
- Porosity, [m^3/m^3]
- Heat capacity, [J/kgK]
- Heat conductivity (for dry material), [W/mK]
- Diffusion resistance factor (for dry material), [–]

Optional material properties include moisture dependent diffusion resistance factor, heat conductivity and properties connected to moisture storage as suction and redistribution. These properties are of different importance for various materials. Moisture storage as a function of RH needs to be considered carefully for wooden materials because of their hygroscopic properties, while the diffusion resistance function is important for materials such as a humidity dependent vapour barrier.

2.1.2 Material data

Table 2.6 describes the material data used in the analysis. Additional input data is shown in table 2.5.

User defined smart vapour barrier
The vapour barrier needs to be modelled with 1 mm thickness to avoid numerical problems during calculations. The two SVBs that are being investigated are user-defined based on the material called Intello created by Fraunhofer-IBP, Holzkirchen, Germany, and the values of s_d are modified as described in table 2.3 and 2.4. Both of the SVBs are in

reality direction dependent, which means that the diffusion resistance varies depending on the two sides of the SVB. In this study, the diffusion resistance is simplified for the average RH of both sides of the SVB.

Table 2.3: s_d values for Isola Du Pont™AirGuard smart generation 2 for average RH (Frey, N. and Geving, S., 2018)

Average RH [%]	**s_d [m]**	**μ [-]**
0	100	100000
12.5	90	90000
25	35	35000
37.5	13	13000
62.5	3.3	3300
75	0.21	210
90	0.2	200
100	0.2	200

Table 2.4: s_d values for SIGA™Majrex for average RH (Grunewald, J., 2016)

Average RH [%]	**s_d [m]**	**μ [-]**
0	35	35000
15	35	35000
40	11	11000
50	11	11000
70	3	3000
90	1	1000
100	1	1000

Table 2.5: Additional input data

Coefficients	**Unit**	**Value**	**Marks**
External			
Heat transfer coefficient	[W/m^{2}K]	25	Roof
s_d value	[m]	300	Bituminous felt with PVC
Short-wave radiation absorptivity	[-]	0.7	User defined
Long-wave radiation emissivity	[-]	0.9	Standard value
Adhering fraction of Rain	[-]	0	No absorption
Internal			
Heat transfer coefficient	[W/m^{2}K]	8	Indoor surface
s_d value	[m]	0.2	Paint with low s_d value
s_d value	[m]	1	Paint with high s_d value

Table 2.6: Material data

Material	Material in WUFI	Water vapour diffusion resistance factor [-]	Moisture storage function [kg/m^3]
Wooden sheathing			
Wood board	Scandinavian spruce transverse direction II[1]	108-27 (30-70% RH)	11.7-81.9 (10-97% RH)
Beam			
Solid-wood beam	Scandinavian spruce transverse direction II[1]	108-27 (30-70% RH)	11.1-81.9 (10-97% RH)
I-Profile	Scandinavian spruce transverse direction II[1]	108-27 (30-70 % RH)	11.1-81.9 (10-97% RH)
Insulation			
Mineral wool	Mineral Wool[2]	1.3	0
Wood fibre	Pavaflex[3]	1.35-1.58 (0-100% RH)	3.1-31.7 (50-97% RH)
Insulation with high compression strength	Mineral wool insulation board[4]	0.34	2-14.5-118 (50-93-99% RH)
Smart Vapour barrier			
Isola AirGuard Smart	Intello[5]	90000-210-200 (12.5-75-90% RH)	6.7-85 (80-100% RH)
SIGA Majrex	Intello [6]	35000-2000-1000 (15-70-100% RH)	6.7-85 (80-100% RH)
Internal Lining			
Gypsum board	Gypsum board[7]	8.3	4-11 (50-95% RH)

[1] NTNU Norwegian University of Science and Technology - Trondheim, Norway
[2] Frainhofer-IBP - Holzkirchen, Germany, changing the density according to product sheet (Glava, 2018[a])
[3] Fraunhofer-IBP - Holzkirchen, Germany
[4] Fraunhofer-IBP - Holzkirchen, Germany, changing the density according to product sheet (The Norwegian EPD Foundation, 2014)
[5] Fraunhofer-IBP - Holzkirchen, Germany, changing the vapour diffusion resistance factor according to product sheet (Grunewald, J., 2016)
[6] Fraunhofer-IBP - Holzkirchen, Germany, changing the vapour diffusion resistance factor according to product sheet (Frey, N. and Geving, S., 2018)
[7] Lund, Sweden

2.1.3 Initial conditions

Moisture content

The initial temperature is set to be 20 ℃ for the overall construction. The temperature will adjust according to the internal and external temperatures when the simulation starts. The initial moisture content in the wooden sheathing and beam as shown in table 2.7, are conservative values. These values are chosen in order to create a better understanding of the drying potential of a compact wooden roof with built-in moisture.

Table 2.7: Initial conditions

Materials used in WUFI	RH[%]	WC [kg/m^3]	T [°C]
Wooden sheathing	90	70.2 (18 weight%)	20
	95	78 (20 weight%)	20
	80	58.5 (15 weight%)	20
Solid-wood beam	90	70.2(18 weight%)	20
	80	58.5 (15 weight%)	20
I profiled beam	90	70.2 (18 weight%)	20
Wood fibre	50	3.1	20
Mineral wool	50	0.5	20

Initiation of the calculation

When the analysis starts, it is assumed that the building is inhabited. This means that the internal conditions are heated, and includes a moisture load due to human activities. The analysis initiates the 1st of October for the reference scenario. This date is used as a parameter in the analysis as shown in table 2.1, and is assumed to demonstrate the date of closing the construction scenarios. The analysis period is over three years in order to identify any trends in moisture content over the years.

2.1.4 Climate file

External

WUFI provides climate files from 10 different locations in Norway in a WUFI database which has been used in this parameter study. Two of these climates are excluded, Røros and Karasjok, due to numerical problems. Figure 2.1 shows the locations that are studied. Climatic traits are shown in table 2.8. The solar altitude varies greatly in Norway. In Trondheim, it varies between of the sun is around 50° and 3.35° . This impacts the solar radiation reaching the surface of the roof which is why it is important to consider when having inclined roofs.

Table 2.8: Climatic traits (Wufi, 2018)

Loaction	Mean temperature [°C]	Maximum temperature [°C]	Minimum temperature [°C]	Mean cloud index [-]
Trondheim	5.4	24.2	-13.8	0.74
Kristiansund	7.7	25.0	-6.4	0.77
Bergen	8.1	28.0	-9.7	0.71
Kristiansand	7.3	24.0	-16.3	0.65
Oslo	6.8	29.3	-14.8	0.67
Kise in Hedmark	4.6	26.5	-25.2	0.65
Mo i Rana	3.3	25.6	-20.2	0.71
Tromsø	2.1	22.0	-14.2	0.69

Figure 2.1: Location of climates simulated (Wikimedia Commons, 2019)

Internal

Internal moisture supply varies over the year and depends on the outdoor temperatures. The indoor humidity supplies used in the calculations are based on a study of the indoor air humidity in Norwegian houses. The study proposes values for low, middle and high moisture supply for different outdoor temperatures, based on 10 % critical values(Geving, S, Holme, J., and Jenssen, J.A., 2008). These values are higher than the mean value and can therefore be considered conservative. The study proposes "low" values for living rooms with low occupancy (>50 m^2/pers), "medium" values for living rooms with high occupancy and bedrooms, while "high" values are for bathrooms and laundry rooms. Furthermore, the indoor temperature is set as a constant temperature equal to 20 °C. The user-defined values created in WUFI for internal moisture supply is given in figure 2.2.

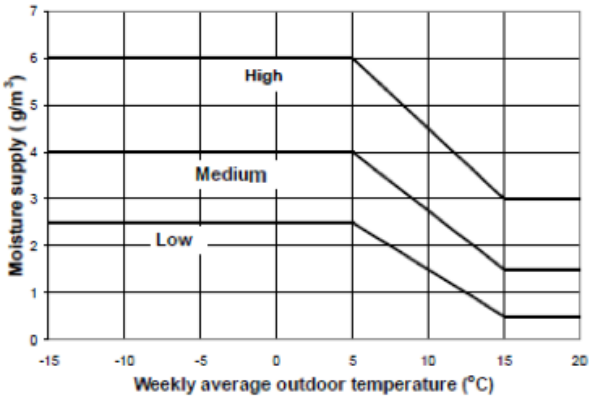

Figure 2.2: Internal moisture supply curve (Geving, S, Holme, J., and Jenssen, J.A., 2008)

2.2 Results

The results of the simulation are presented as figures with selected data from chosen monitor points. The trends are similar for all the scenarios. Therefore, the moisture content of various monitor points for the different scenarios are presented in appendix B. Based on the results, the most critical point regarding mould development is point 5. For each scenario, the parameters are presented in tables. Notice that the figures showing the total moisture content are presented as a percentage of change of total moisture content in the roof assembly. A model has a drying potential if the drying rate in summer is higher than accumulation in winter. The figures that describe the coherence of RH and temperature are showing the total temperature and RH on the left, and the value of temperature and RH only when both variables are above the corresponding critical value on the right. The arrow in the latter figure represents a period of possible mould development.

2.2.1 Reference scenario

The reference scenario is compared with the other scenarios where a parameter has been changed. In order to understand the impact of each parameter, it is important to investigate the results of the reference scenario. Table 2.9 shows the parameter data of this model which resemble the first column of table 2.1. Data is gathered from the selected points described in figure 2.4. Figure 2.3 shows that the roof construction has a drying potential, while figure 2.4 shows the moisture distribution in the wooden elements. Figure 2.5 shows the coherence of RH and temperature, where it seems that there is a period of around 5 months with possible mould development during the summer.

Table 2.9: Parameters

Parameter		**1**
Location	Trondheim	x
	Bergen	
	Oslo	
	Kise, Hedmark	
	Kristiansand	
	Kristiansund	
	Mo i Rana	
	Tromsø	
Moisture load	Low	
	Medium	x
	High	
Roof height	450 mm	
	350 mm	x
	250 mm	
Top insulation	0 mm	x
	50 mm	
	100 mm	
Beam (Spruce)	I	
	K	x
Insulation	Mineral wool	x
	Wood fibre	
Internal lining	$s_d = 0.2$m	x
	$s_d = 1$m	
Moisture content	18 % in beam	x
	20 % in wooden sheathing	x
	18 % in wooden sheathing	
	15 % in wooden sheathing	
	15 % in beam	
Date of closing	1st of October	x
	1st of January	
	1st of April	
	1st of July	
SVB	AirGuard Smart	x
	Majrex	
Inclination	0 °	x
	30 °	
	45 °	
	90°	
Orientation	North	

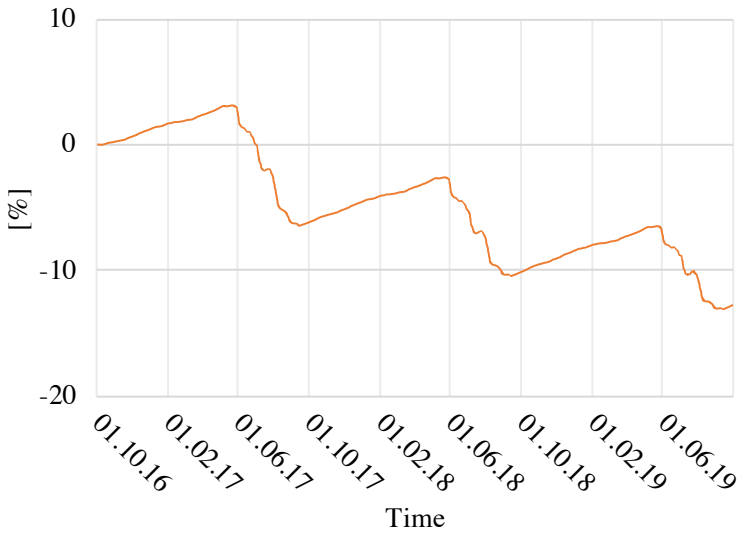

Figure 2.3: Percentage of change of the total moisture content in the roof assembly

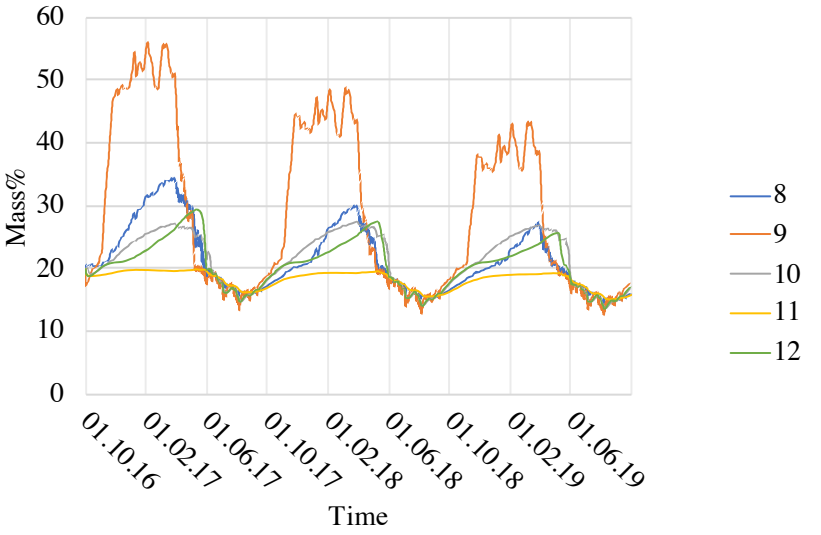

(a) Moisture content in the wooden sheathing

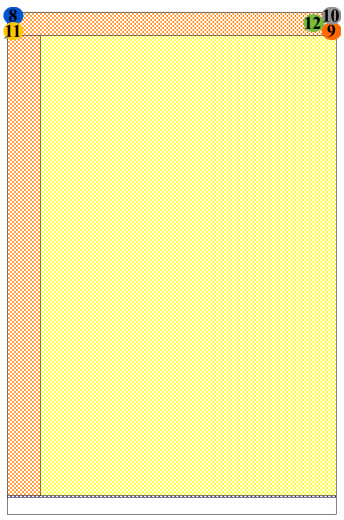

(b) Monitor points in the wooden sheathing

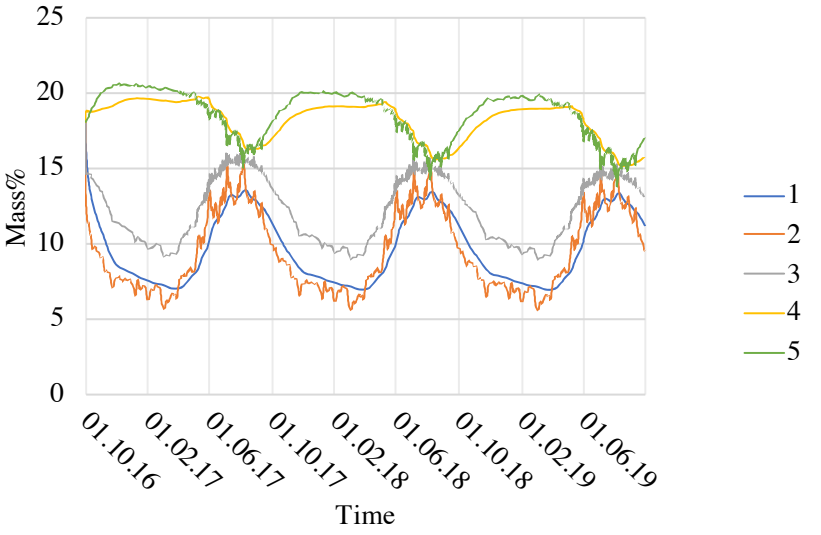

(c) Moisture content in the beam

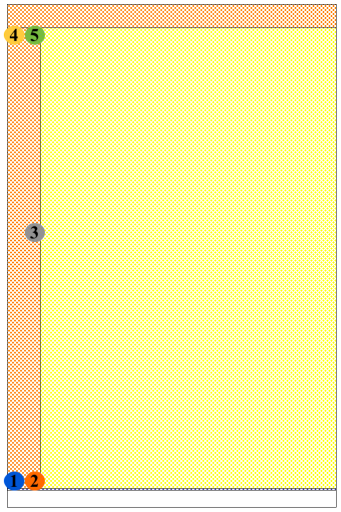

(d) Monitor points in the beam

Figure 2.4: Moisture content in various monitor points, calculated in mass%

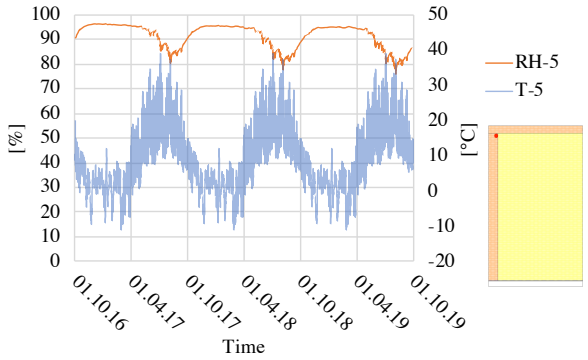

(a) RH and Temperature

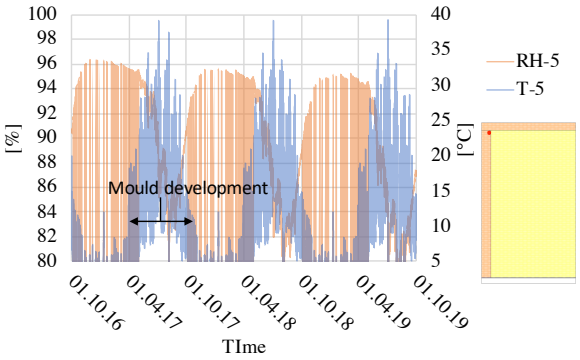

(b) RH > 80% and T > 5°C

Figure 2.5: RH and temperature for point 5

2.2.2 The effect of insulation above the wooden sheathing

Table 2.10 shows the parameters used for these scenarios. As seen in figure 2.6, the drying potential decreases by having insulation on top of the wooden sheathing. Figures 2.7 and 2.8 show the temperature and RH of the top beam close to the insulation. Here it is possible to see that RH decreases by increasing the insulation on top of the wooden sheathing and the period of possible mould development increases.

Table 2.10: Parameters

Parameter		**1**	**7**	**8**
Location	Trondheim Bergen Oslo Kise, Hedmark Kristiansand Kristiansund Mo i Rana Tromsø	x	x	x
Moisture load	Low Medium High	x	x	x
Roof height	450 mm 350 mm 250 mm	x	x	x
Top insulation	**0 mm** **50 mm** **100 mm**	**x**	**x**	**x**
Beam (Spruce)	I K	x	x	x
Insulation	Mineral wool Wood fibre	x	x	x
Internal lining	s_d = 0.2m s_d = 1m	x	x	x
Moisture content	18 % in beam 20 % in wooden sheathing 18 % in wooden sheathing 15 % in wooden sheathing 15 % in beam	x x	x x	x x
Date of closing	1st of October 1st of January 1st of April 1st of July	x	x	x
SVB	AirGuard Smart Majrex	x	x	x
Inclination	0 ° 30 ° 45 ° 90°	x	x	x
Orientation	North			

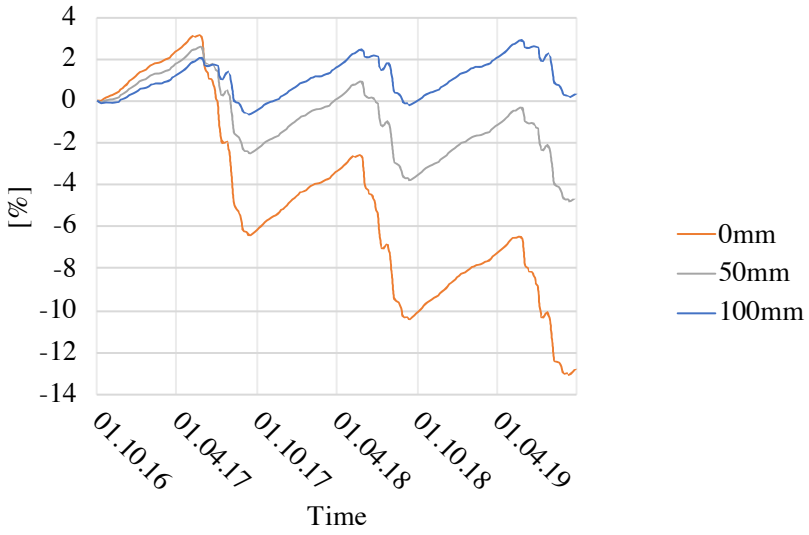

Figure 2.6: Percentage of change of the total moisture content in the roof assembly

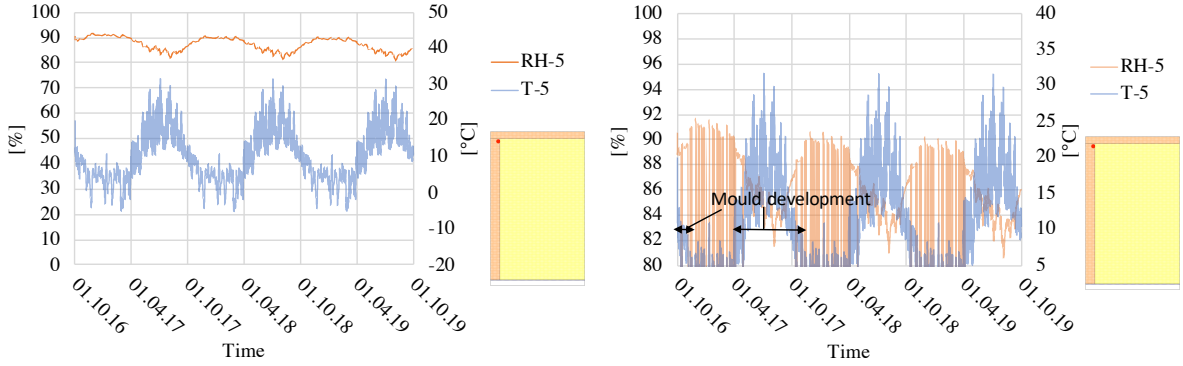

(a) RH and Temperature **(b)** RH $>$ 80% and T $>$ 5°C

Figure 2.7: Scenario: 50mm Insulation on top. RH and temperature for point 5

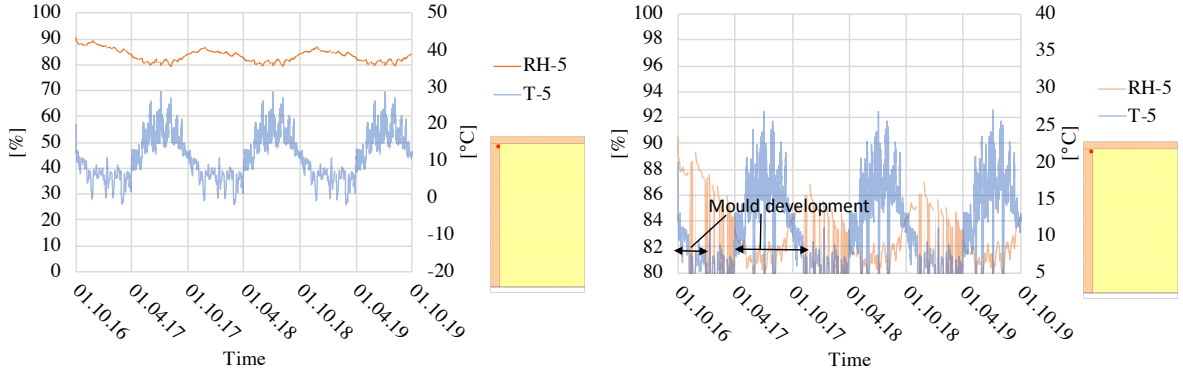

(a) RH and Temperature **(b)** RH $>$ 80% and T $>$ 5°C

Figure 2.8: Scenario: 100mm Insulation on top. RH and temperature for point 5

2.2.3 The effect of initial moisture content

Table 2.11 shows the parameters used for these scenarios. The effect of initial moisture content is investigated in order to identify the risk of mould due to high moisture contents. Figures 2.11 and 2.12 confirms that the risk of mould decreases with initial moisture content. Figure 2.9 shows that the scenario with 15 weight% has no drying potential. Additionally, figure 2.10 shows the average moisture content in equilibrium for the beam and the wooden sheathing.

Table 2.11: Parameters

Parameter		**1**	**12**	**13**
Location	Trondheim Bergen Oslo Kise, Hedmark Kristiansand Kristiansund Mo i Rana Tromsø	x	x	x
Moisture load	Low Medium High	x	x	x
Roof height	450 mm 350 mm 250 mm	x	x	x
Top insulation	0 mm 50 mm 100 mm	x	x	x
Beam (Spruce)	I K	x	x	x
Insulation	Mineral wool Wood fibre	x	x	x
Internal lining	s_d = 0.2m s_d = 1m	x	x	x
Moisture content	**18 % in beam** **20 % in wooden sheathing** **18 % in wooden sheathing** **15 % in wooden sheathing** **15 % in beam**	**x** **x**	**x** **x**	 **x** **x**
Date of closing	1st of October 1st of January 1st of April 1st of July	x	x	x
SVB	AirGuard Smart Majrex	x	x	x
Inclination	0 ° 30 ° 45 ° 90°	x	x	x
Orientation	North			

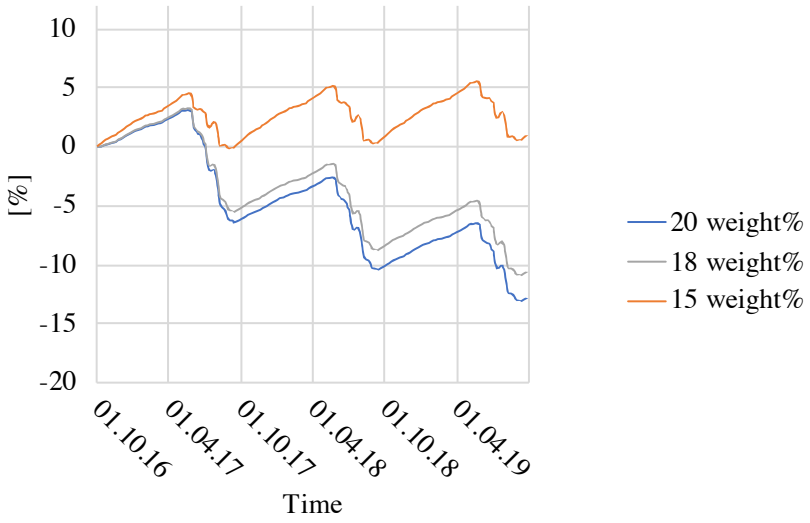

Figure 2.9: Percentage of change of the total moisture content in the roof assembly

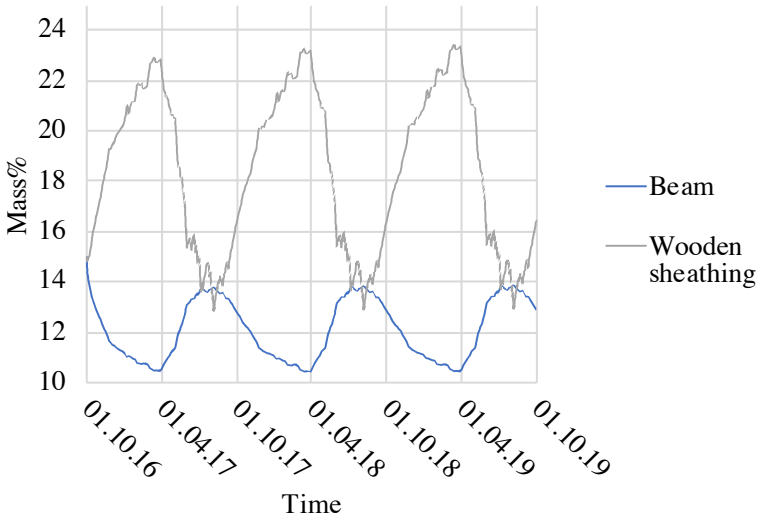

Figure 2.10: The average moisture content in the wooden sheathing and the beam for the scenario with 15 weight% initial moisture content

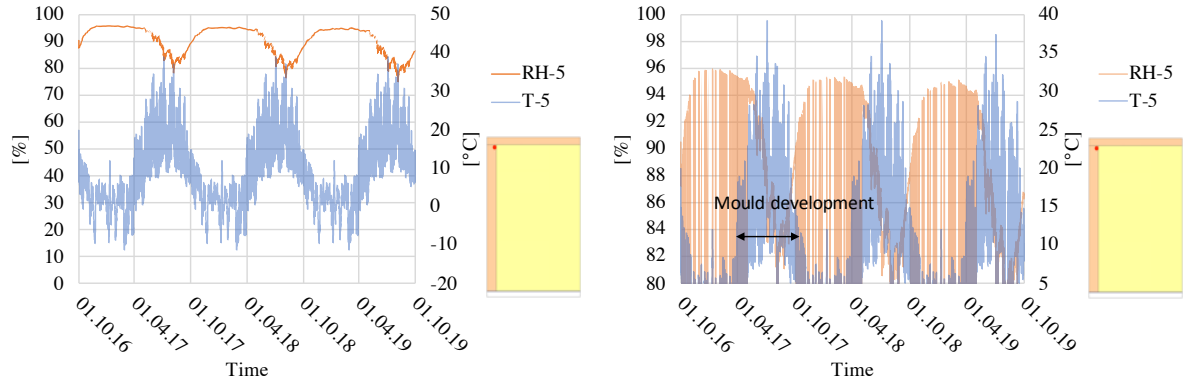

(a) RH and Temperature **(b)** RH $>$ 80% and T $>$ 5°C

Figure 2.11: Scenario: 18 weight%. RH and temperature for point 5

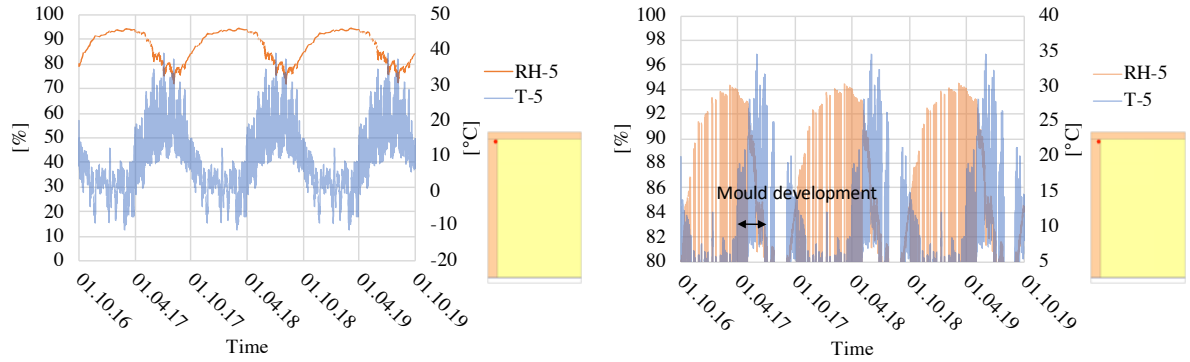

(a) RH and Temperature **(b)** RH $>$ 80% and T $>$ 5°C

Figure 2.12: Scenario: 15 weight%. RH and temperature for point 5

2.2.4 The effect of internal moisture load

Table 2.12 shows the parameters used for these scenarios. The effect of internal moisture load is investigated in order to identify how the SVB is reacting to different levels of internal RH. The roof construction accumulates moisture if the internal moisture load is high, as shown in figure 2.13. In addition, figures 2.14 and 2.15 show that the period with possible mould development increases with higher moisture load.

Table 2.12: Parameters

Parameter		**1**	**3**	**4**
Location	Trondheim Bergen Oslo Kise, Hedmark Kristiansand Kristiansund Mo i Rana Tromsø	x	x	x
Moisture load	**Low** **Medium** **High**	**x**	**x**	**x**
Roof height	450 mm 350 mm 250 mm	x	x	x
Top insulation	0 mm 50 mm 100 mm	x	x	x
Beam (Spruce)	I K	x	x	x
Insulation	Mineral wool Wood fibre	x	x	x
Internal lining	$s_d = 0.2$m $s_d = 1$m	x	x	x
Moisture content	18 % in beam 20 % in wooden sheathing 18 % in wooden sheathing 15 % in wooden sheathing 15 % in beam	x x	x x	x x
Date of closing	1st of October 1st of January 1st of April 1st of July	x	x	x
SVB	AirGuard Smart Majrex	x	x	x
Inclination	0 ° 30 ° 45 ° 90°	x	x	x
Orientation	North			

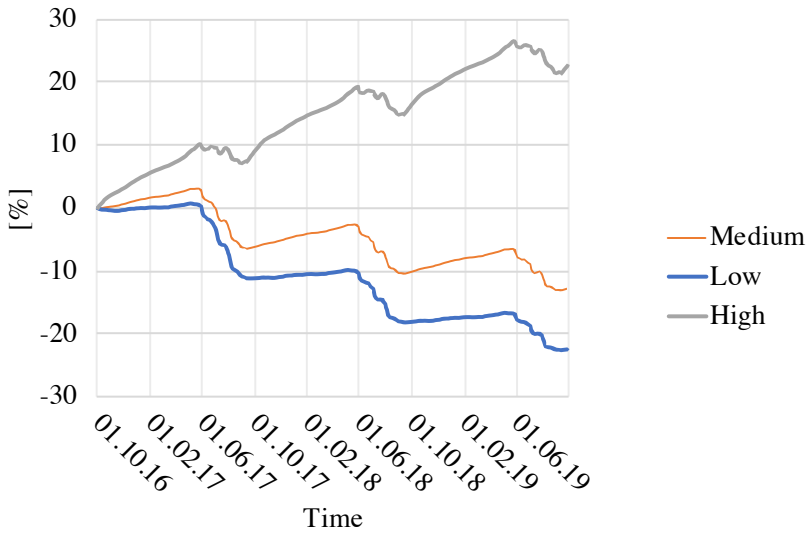

Figure 2.13: Percentage of change of the total moisture content in the roof assembly

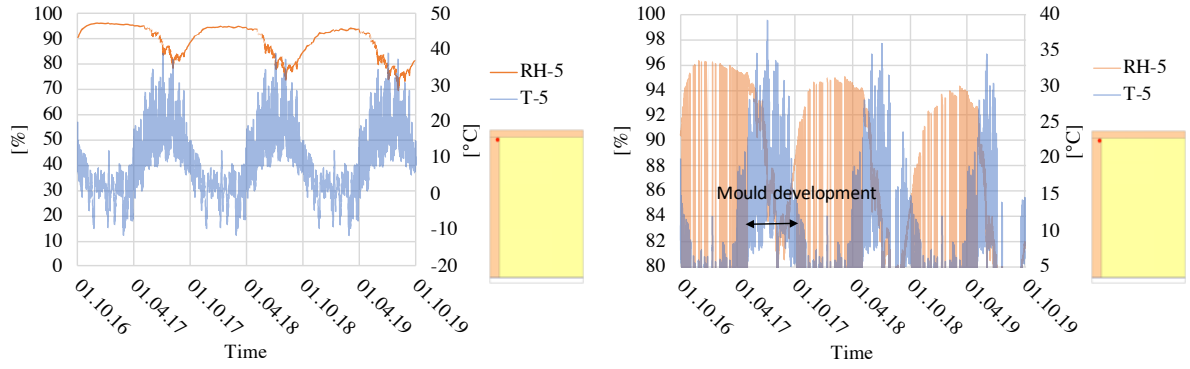

(a) RH and Temperature **(b)** RH $>$ 80% and T $>$ 5°C

Figure 2.14: Scenario: Low moisture load. RH and temperature for point 5

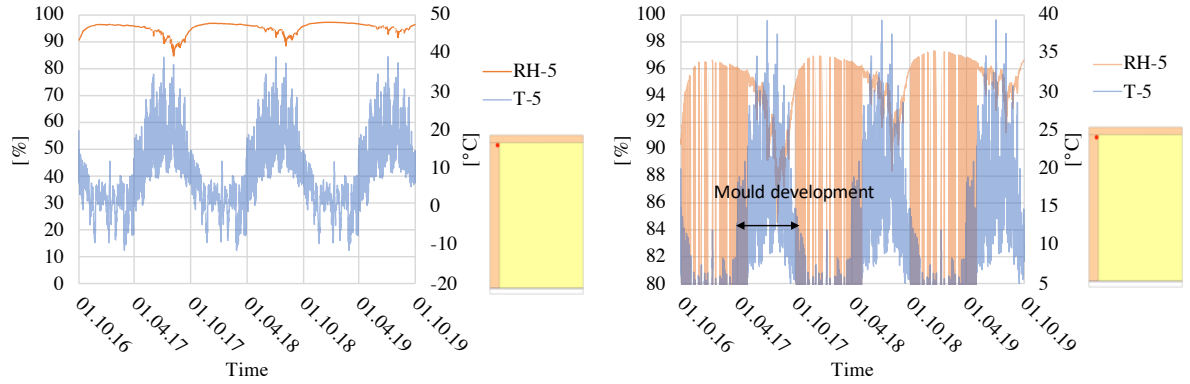

(a) RH and Temperature **(b)** RH $>$ 80% and T $>$ 5°C

Figure 2.15: Scenario: High moisture load. RH and temperature for point 5

2.2.5 The effect of initial date of the calculation

Table 2.13 shows the parameters used for these scenarios. Figure 2.16 shows that the scenario, 1st of April, has the highest drying potential. However, notice that the difference between the scenarios is decreasing every year. Figures 2.17, 2.18 and 2.19 shows no distinct deviations of the scenarios in regard of mould development.

Table 2.13: Parameters

Parameter		**1**	**14**	**15**	**16**
Location	Trondheim Bergen Oslo Kise, Hedmark Kristiansand Kristiansund Mo i Rana Tromsø	x	x	x	x
Moisture load	Low Medium High	x	x	x	x
Roof height	450 mm 350 mm 250 mm	x	x	x	x
Top insulation	0 mm 50 mm 100 mm	x	x	x	x
Beam (Spruce)	I K	x	x	x	x
Insulation	Mineral wool Wood fibre	x	x	x	x
Internal lining	$s_d = 0.2$m $s_d = 1$m	x	x	x	x
Moisture content	18 % in beam 20 % in wooden sheathing 18 % in wooden sheathing 15 % in wooden sheathing 15 % in beam	x x	x x	x x	x x
Date of closing	**1st of October** **1st of January** **1st of April** **1st of July**	**x**	**x**	**x**	**x**
SVB	AirGuard Smart Majrex	x	x	x	x
Inclination	0 ° 30 ° 45 ° 90°	x	x	x	x
Orientation	North				

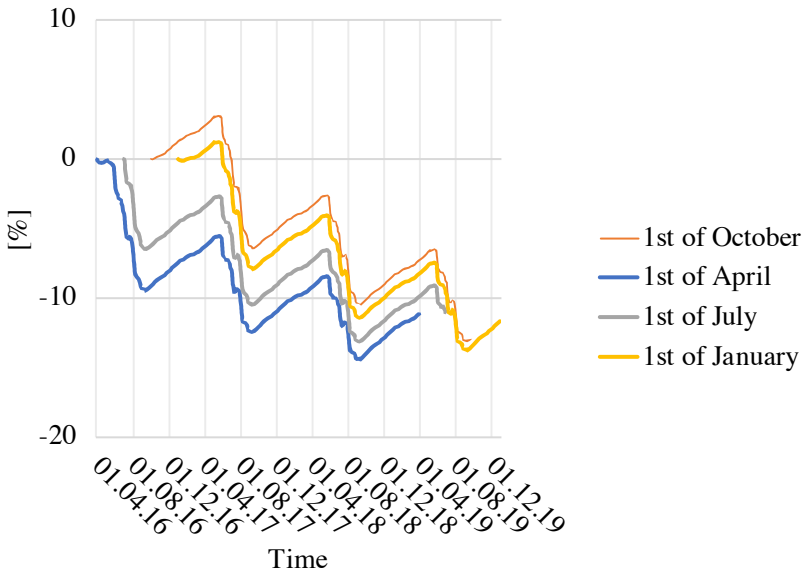

Figure 2.16: Percentage of change of the total moisture content in the roof assembly

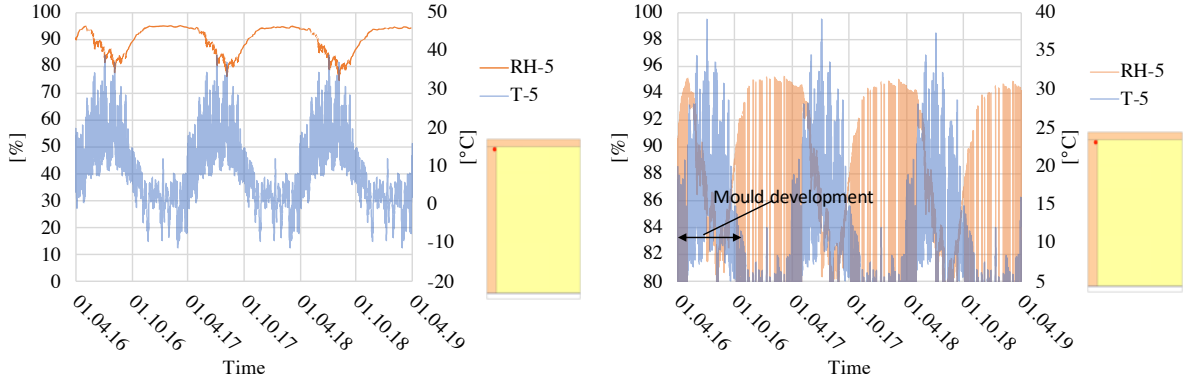

(a) RH and Temperature **(b)** RH $>$ 80% and T $>$ 5°C

Figure 2.17: Scenario: 1st of April. RH and temperature for point 5

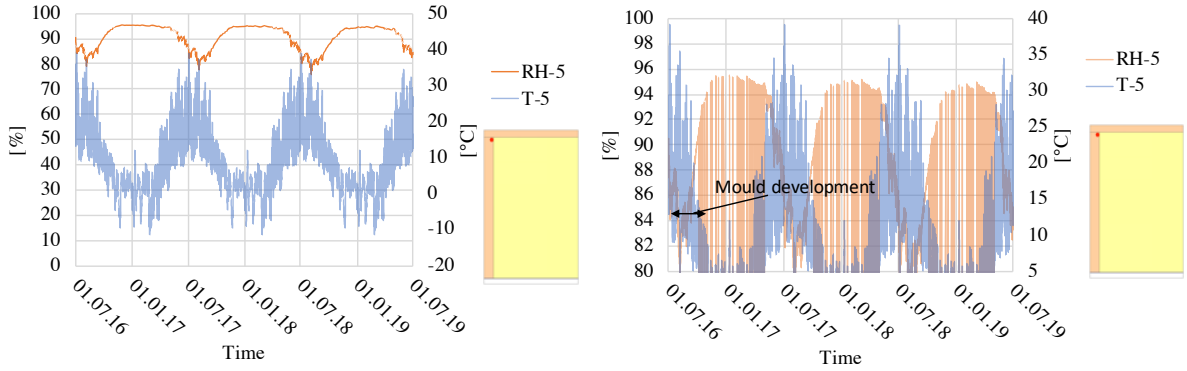

(a) RH and Temperature **(b)** RH $>$ 80% and T $>$ 5°C

Figure 2.18: Scenario: 1st of July. RH and temperature for point 5

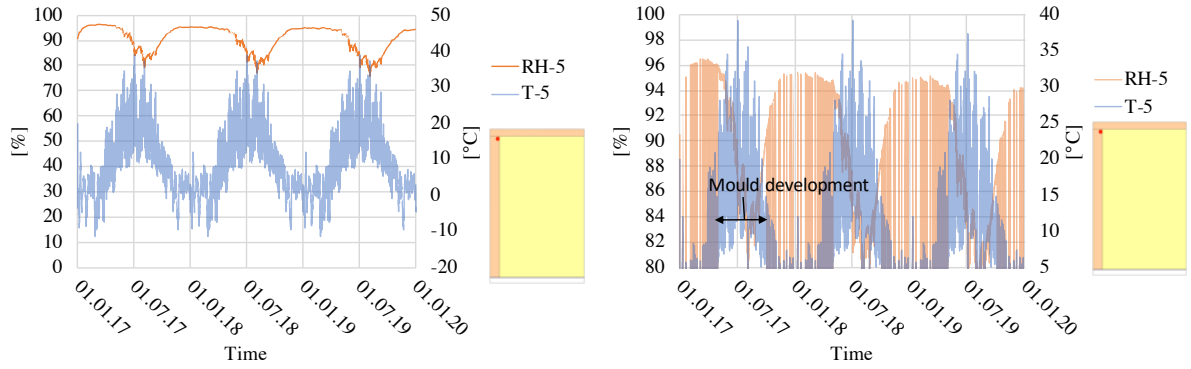

(a) RH and Temperature **(b)** RH $>$ 80% and T $>$ 5°C

Figure 2.19: Scenario: 1st of January. RH and temperature for point 5

2.2.6 The effect of insulating materials

Table 2.14 shows the parameters used for these scenarios. The effect of insulation materials is investigated in order to identify how it affects the drying potential and moisture distribution. There is no drying potential for the scenario with wood fibre insulation, as shown in figure 2.21. However, figure 2.20 shows that it reduces the moisture content in critical areas. Figures 2.22 and 2.23 show the temperature and RH of the top beam close to the insulation.

Table 2.14: Parameters

Parameter		**1**	**10**
Location	Trondheim	x	x
	Bergen		
	Oslo		
	Kise, Hedmark		
	Kristiansand		
	Kristiansund		
	Mo i Rana		
	Tromsø		
Moisture load	Low		
	Medium	x	x
	High		
Roof height	450 mm		
	350 mm	x	x
	250 mm		
Top insulation	0 mm	x	x
	50 mm		
	100 mm		
Beam (Spruce)	I		
	K	x	x
Insulation	**Mineral wool**	**x**	
	Wood fibre		**x**
Internal lining	$s_d = 0.2$m	x	x
	$s_d = 1$m		
Moisture content	18 % in beam	x	x
	20 % in wooden sheathing	x	x
	18 % in wooden sheathing		
	15 % in wooden sheathing		
	15 % in beam		
Date of closing	1st of October	x	x
	1st of January		
	1st of April		
	1st of July		
SVB	AirGuard Smart	x	x
	Majrex		
Inclination	0 °	x	x
	30 °		
	45 °		
	90°		
Orientation	North		

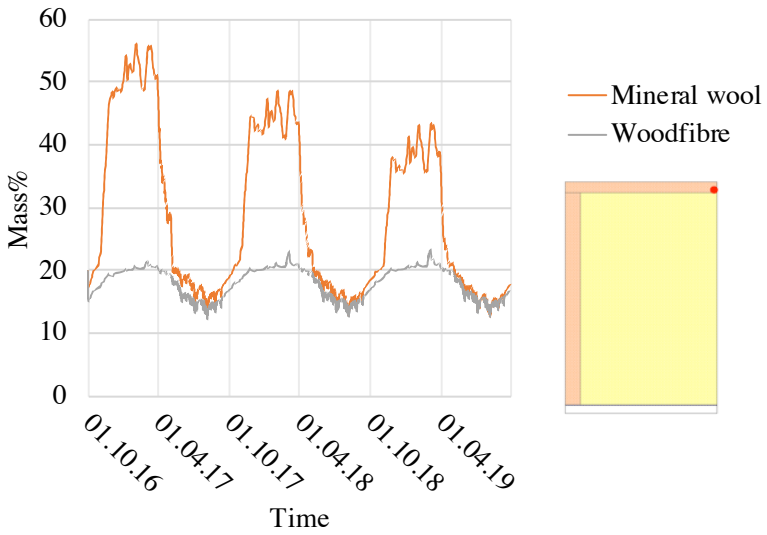

Figure 2.20: Moisture content in the roofing board towards the insulation, point 9

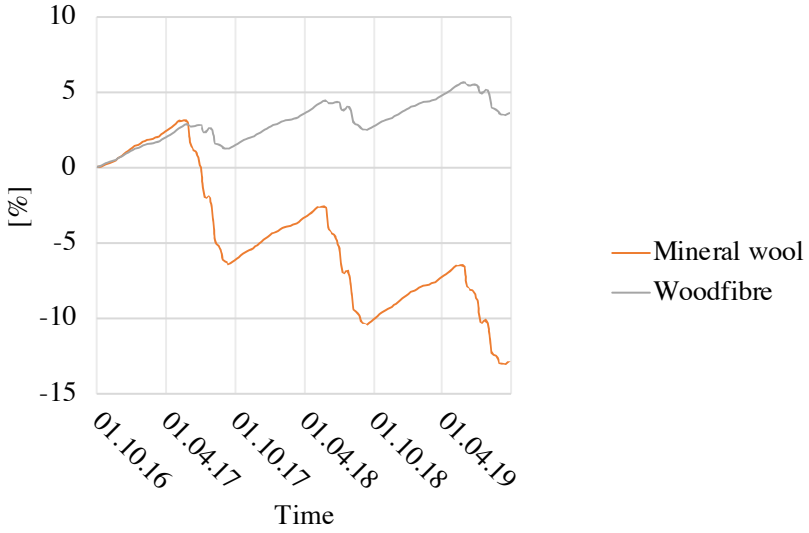

Figure 2.21: Percentage of change of the total moisture content in the roof assembly

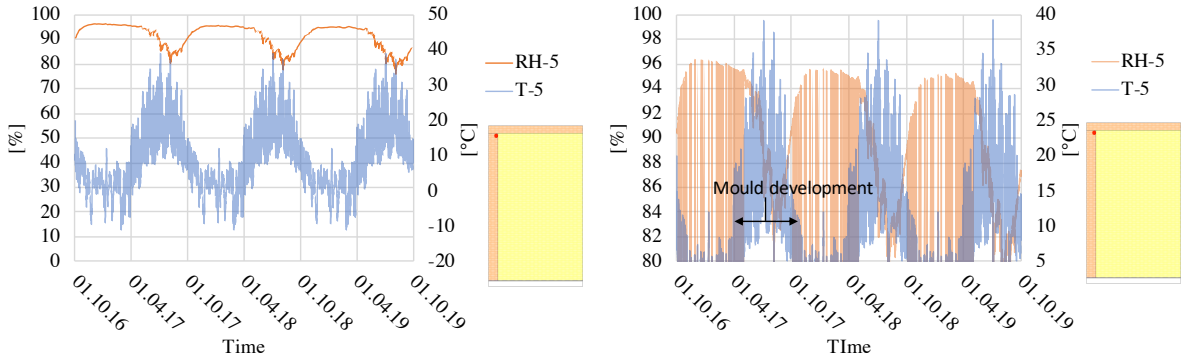

(a) RH and Temperature

(b) RH > 80% and T > 5°C

Figure 2.22: Scenario: Mineral wool. RH and temperature for point 5

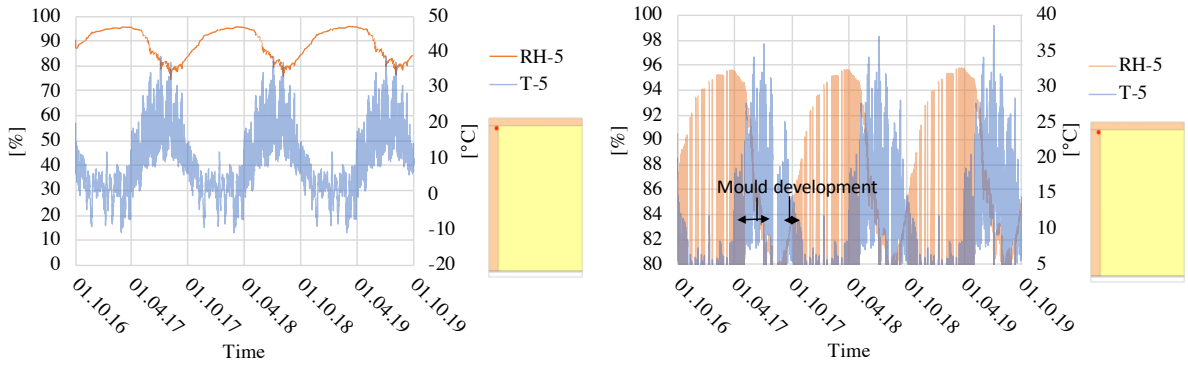

(a) RH and Temperature

(b) RH $>$ 80% and T $>$ 5°C

Figure 2.23: Scenario: Wood fibre insulation. RH and temperature for point 5

2.2.7 The effect of internal diffusion resistance

Table 2.15 shows the parameters used for these scenarios. Figure 2.24 shows that the drying potential decreases by having a high internal resistance. However, figures 2.25 and 2.26 show no significant deviation in RH between the two scenarios in monitor point 5.

Table 2.15: Parameters

Parameter		**1**	**11**
Location	Trondheim Bergen Oslo Kise, Hedmark Kristiansand Kristiansund Mo i Rana Tromsø	x	x
Moisture load	Low Medium High	x	x
Roof height	450 mm 350 mm 250 mm	x	x
Top insulation	0 mm 50 mm 100 mm	x	x
Beam (Spruce)	I K	x	x
Insulation	Mineral wool Wood fibre	x	x
Internal lining	$\mathbf{s_d = 0.2m}$ $\mathbf{s_d = 1m}$	**x**	**x**
Moisture content	18 % in beam 20 % in wooden sheathing 18 % in wooden sheathing 15 % in wooden sheathing 15 % in beam	x x	x x
Date of closing	1st of October 1st of January 1st of April 1st of July	x	x
SVB	AirGuard Smart Majrex	x	x
Inclination	0 ° 30 ° 45 ° 90°	x	x
Orientation	North		

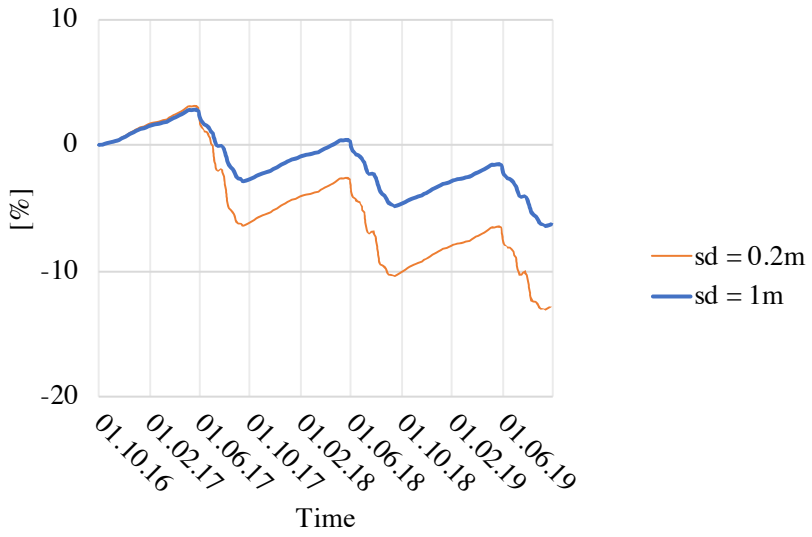

Figure 2.24: Percentage of change of the total moisture content in the roof assembly

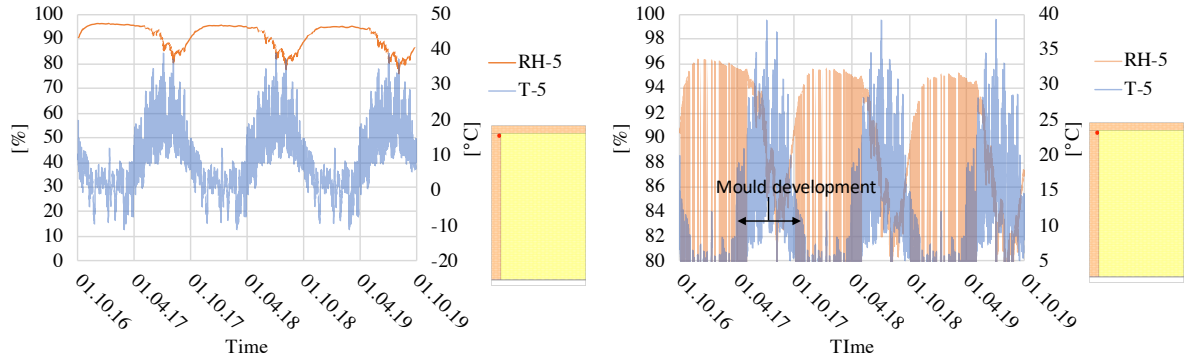

(a) RH and Temperature **(b)** RH > 80% and T > 5°C

Figure 2.25: Scenario: Internal vapour diffusion resistance s_d = 0.2m. RH and temperature for point 5

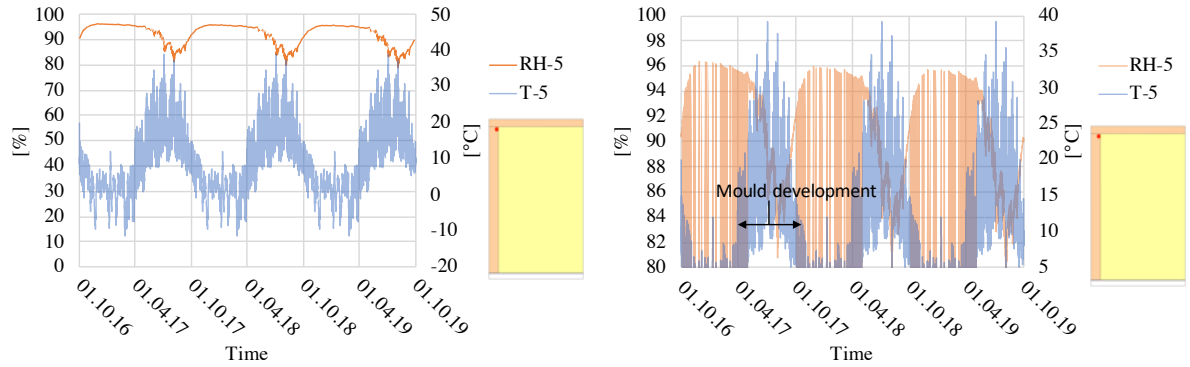

(a) RH and Temperature **(b)** RH > 80% and T > 5°C

Figure 2.26: Scenario: Internal vapour diffusion resistance s_d = 1m. RH and temperature for point 5

2.2.8 The effect of insulation height

Table 2.16 shows the parameters used for these scenarios. The height of the insulation materials affects the fluctuations of the moisture distribution, as shown in figure 2.27. The drying potential is higher for lower insulation heights. This can also be seen in figures 2.28 and 2.29, that show the temperature and RH of the top beam close to the insulation.

Table 2.16: Parameters

Parameter		**1**	**5**	**6**
Location	Trondheim Bergen Oslo Kise, Hedmark Kristiansand Kristiansund Mo i Rana Tromsø	x	x	x
Moisture load	Low Medium High	x	x	x
Roof height	**450 mm** **350 mm** **250 mm**	**x**	**x**	**x**
Top insulation	0 mm 50 mm 100 mm	x	x	x
Beam (Spruce)	I K	x	x	x
Insulation	Mineral wool Wood fibre	x	x	x
Internal lining	s_d = 0.2m s_d = 1m	x	x	x
Moisture content	18 % in beam 20 % in wooden sheathing 18 % in wooden sheathing 15 % in wooden sheathing 15 % in beam	x x	x x	x x
Date of closing	1st of October 1st of January 1st of April 1st of July	x	x	x
SVB	AirGuard Smart Majrex	x	x	x
Inclination	0 ° 30 ° 45 ° 90°	x	x	x
Orientation	North			

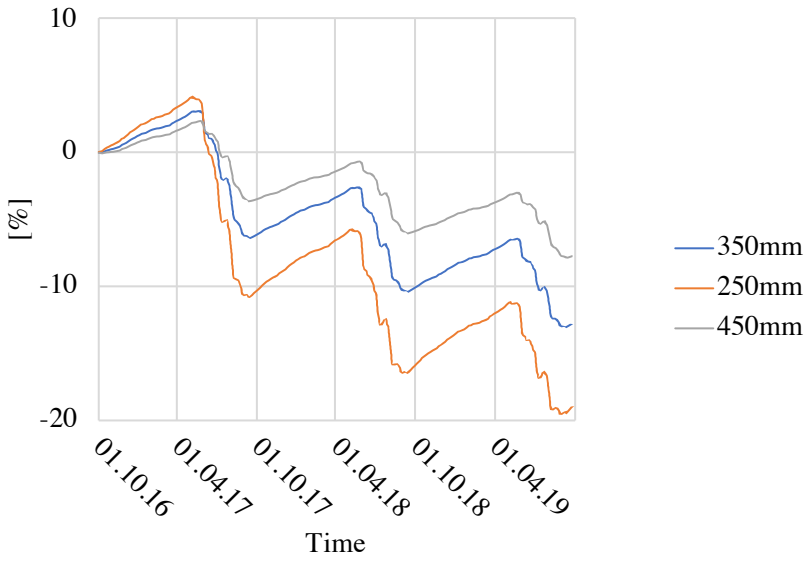

Figure 2.27: Percentage of change of the total moisture content in the roof assembly

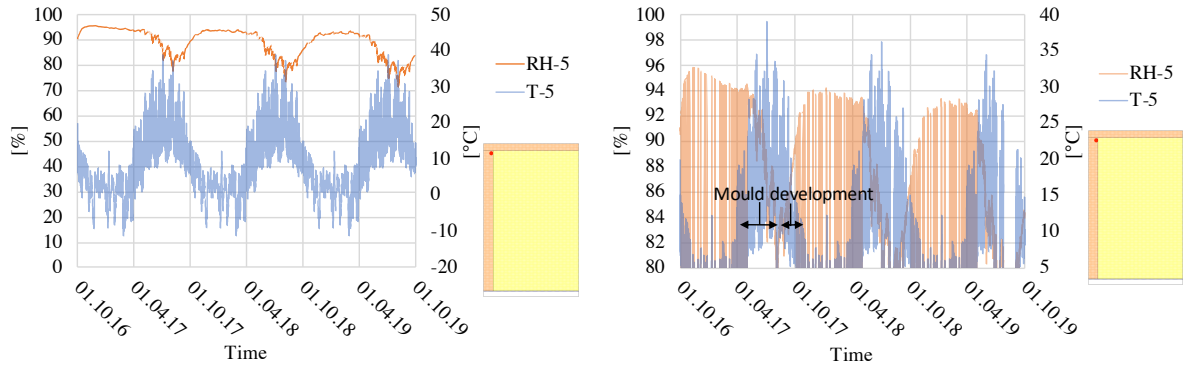

(a) RH and Temperature **(b)** RH $>$ 80% and T $>$ 5°C

Figure 2.28: Scenario: 250mm insulation height. RH and temperature for point 5

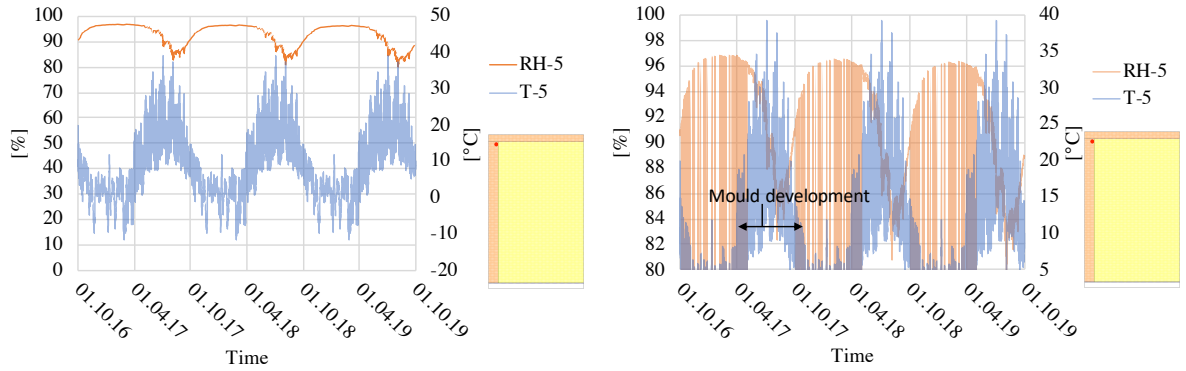

(a) RH and Temperature **(b)** RH $>$ 80% and T $>$ 5°C

Figure 2.29: Scenario: 450mm insulation height. RH and temperature for point 5

2.2.9 The effect of various smart vapour barriers (SVB)

Table 2.17 shows the parameters used for these scenarios. Various SVBs have different range of s_d values. The effect of this is investigated in order to identify the importance of the choice of SVB. Figure 2.30 shows that AirGuard Smart has the highest drying potential. However, figures 2.31 and 2.32 show no significant deviation of RH at the top beam close to the insulation.

Table 2.17: Parameters

Parameter		**1**	**17**
Location	Trondheim Bergen Oslo Kise, Hedmark Kristiansand Kristiansund Mo i Rana Tromsø	x	x
Moisture load	Low Medium High	x	x
Roof height	450 mm 350 mm 250 mm	x	x
Top insulation	0 mm 50 mm 100 mm	x	x
Beam (Spruce)	I K	x	x
Insulation	Mineral wool Wood fibre	x	x
Internal lining	s_d = 0.2m s_d = 1m	x	x
Moisture content	18 % in beam 20 % in wooden sheathing 18 % in wooden sheathing 15 % in wooden sheathing 15 % in beam	x x	x x
Date of closing	1st of October 1st of January 1st of April 1st of July	x	x
SVB	**AirGuard Smart** **Majrex**	**x**	 **x**
Inclination	0 ° 30 ° 45 ° 90°	x	x
Orientation	North		

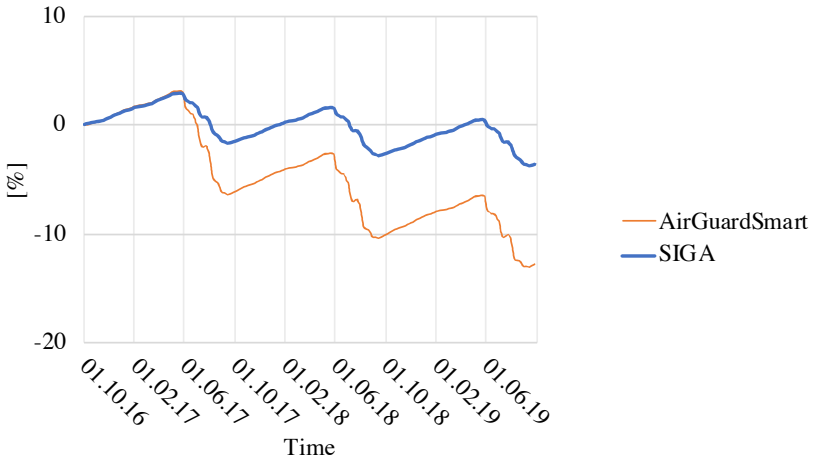

Figure 2.30: Percentage of change of the total moisture content in the roof assembly

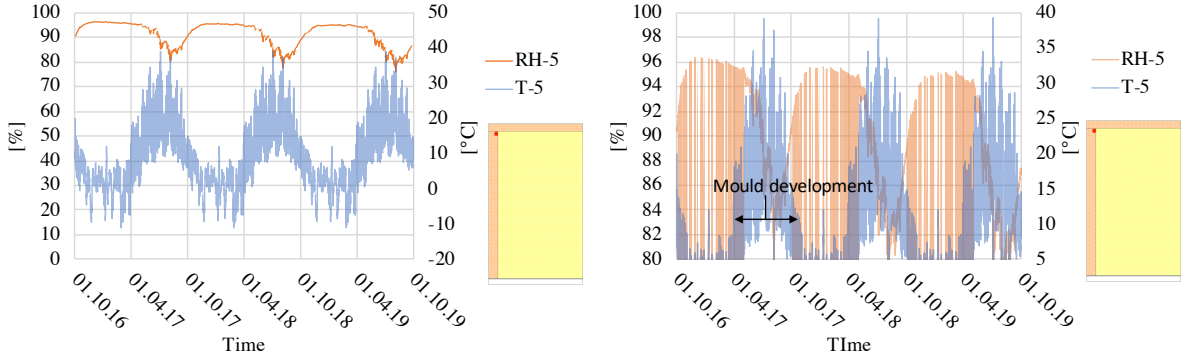

(a) RH and Temperature **(b)** RH $>$ 80% and T $>$ 5°C

Figure 2.31: Scenario: AirGuard Smart. RH and temperature for point 5

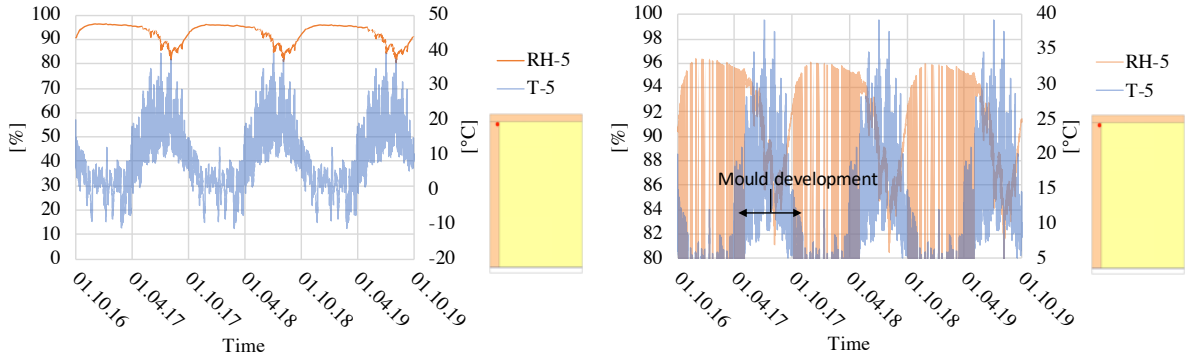

(a) RH and Temperature **(b)** RH $>$ 80% and T $>$ 5°C

Figure 2.32: Scenario: Majrex . RH and temperature for point 5

2.2.10 The effect of various beams

Table 2.18 shows the parameters used for these scenarios. The effect of various beams is investigated in order to identify possible differences in regard to mould growth. A construction with I-beams has higher fluctuations of total moisture content compared to a construction with solid-wood beams, as shown in figure 2.33. Figures 2.35 and 2.34 show the temperature and RH of the top beam close to the insulation, and it is possible to identify higher RH for the construction with solid-wood beam.

Table 2.18: Parameters

Parameter		**1**	**9**
Location	Trondheim Bergen Oslo Kise, Hedmark Kristiansand Kristiansund Mo i Rana Tromsø	x	x
Moisture load	Low Medium High	x	x
Roof height	450 mm 350 mm 250 mm	x	x
Top insulation	0 mm 50 mm 100 mm	x	x
Beam (Spruce)	I **K**	**x**	**x**
Insulation	Mineral wool Wood fibre	x	x
Internal lining	s_d = 0.2m s_d = 1m	x	x
Moisture content	18 % in beam 20 % in wooden sheathing 18 % in wooden sheathing 15 % in wooden sheathing 15 % in beam	x x	x x
Date of closing	1st of October 1st of January 1st of April 1st of July	x	x
SVB	AirGuard Smart Majrex	x	x
Inclination	0 ° 30 ° 45 ° 90°	x	x
Orientation	North		

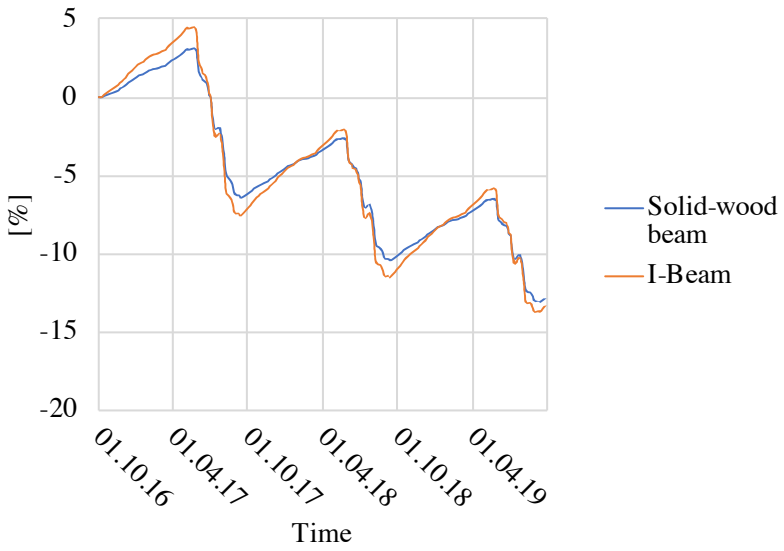

Figure 2.33: Percentage of change of the total moisture content in the roof assembly

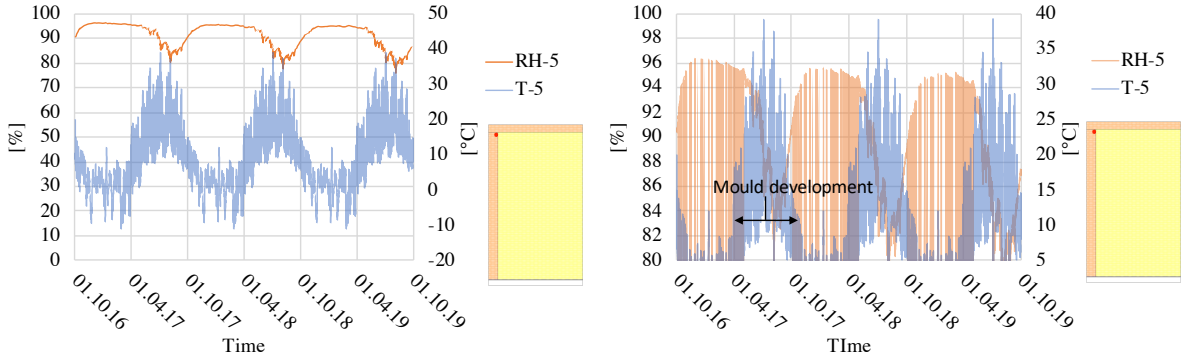

(a) RH and Temperature **(b)** RH $>$ 80% and T $>$ 5°C

Figure 2.34: Scenario: Solid-wood beam. RH and temperature for point 5

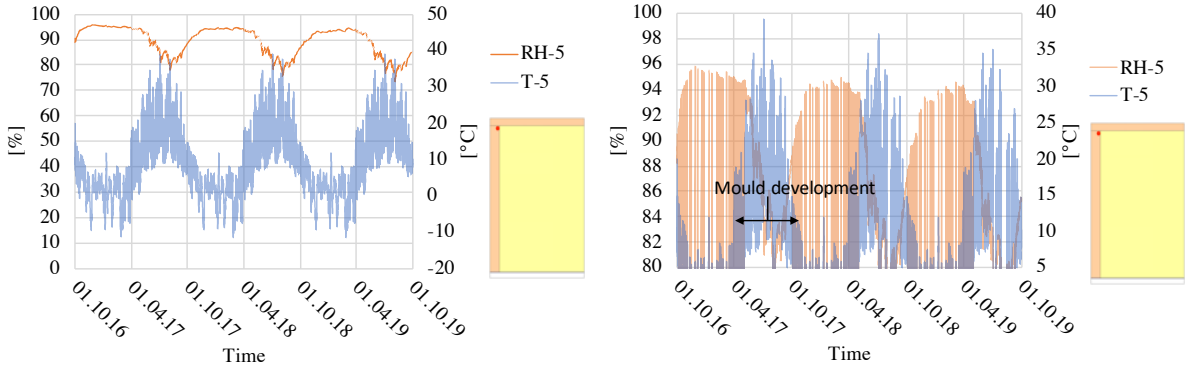

(a) RH and Temperature **(b)** RH $>$ 80% and T $>$ 5°C

Figure 2.35: Scenario: I-beam. RH and temperature for point 5

2.2.11 Changing reference model

Due to numerical problems when simulating cold climates, the reference model needed to be updated in order to decrease the moisture content in the roof assembly. Therefore, in the following results, low moisture load is used instead of medium moisture load, and 18 weight% in both the wooden sheathing and the beam is used instead of 18 weight% in the beam and 20 weight% in the wooden sheathing, as shown in table 2.19. Figure 2.37 shows that the new reference model has a higher drying potential. Therefore, the wooden sheathing does not reach as high moisture content as the old reference model.

Table 2.19: Parameters

Parameter		**1**	**2**
Location	**Trondheim**	**x**	**x**
	Bergen		**x**
	Oslo		**x**
	Kise, Hedmark		**x**
	Kristiansand		**x**
	Kristiansund		**x**
	Mo i Rana		**x**
	Tromsø		**x**
Moisture load	**Low**		**x**
	Medium	x	
	High		
Roof height	450 mm		
	350 mm	x	x
	250 mm		
Top insulation	0 mm	x	x
	50 mm		
	100 mm		
Beam (Spruce)	I		
	K	x	x
Insulation	Mineral wool	x	x
	Wood fibre		
Internal lining	s_d = 0.2m	x	x
	s_d = 1m		
Moisture content	**18 % in beam**	x	**x**
	20 % in wooden sheathing	x	
	18 % in wooden sheathing		**x**
	15 % in wooden sheathing		
	15 % in beam		
Date of closing	1st of October	x	x
	1st of January		
	1st of April		
	1st of July		
SVB	AirGuard Smart	x	x
	Majrex		
Inclination	0 °	x	x
	30 °		
	45 °		
	90°		
Orientation	North		

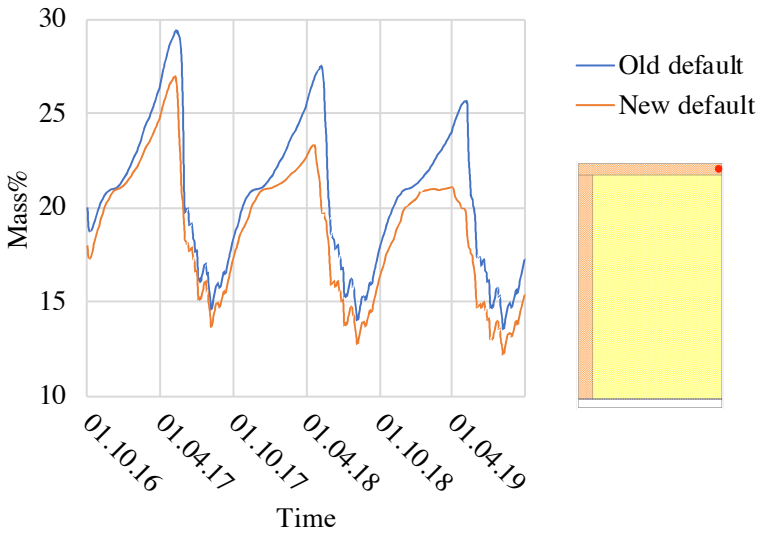

Figure 2.36: Moisture content in the wooden sheathing

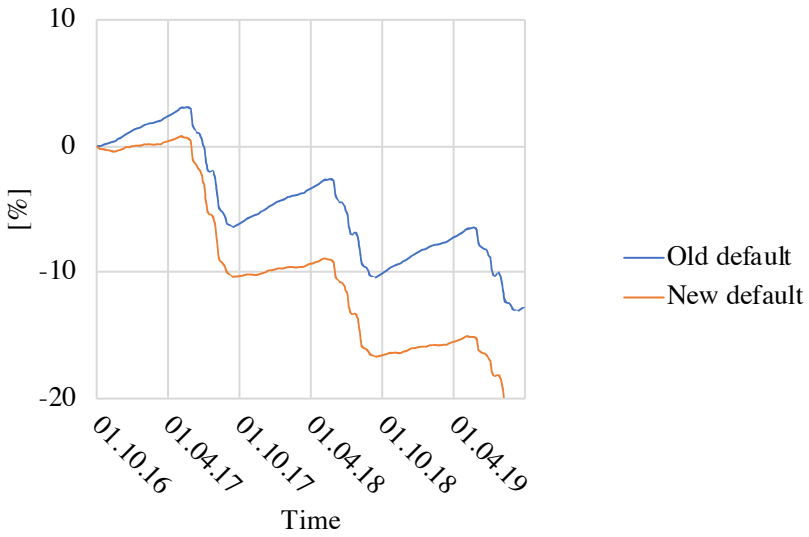

Figure 2.37: Percentage of change of the total moisture content in the roof assembly

2.2.12 The effect of external climate

Table 2.19 shows the parameters used for these scenarios. The effect of location is important to investigate because of different climates. It is possible to identify that constructions in locations at higher latitudes have a lower drying potential. Figures 2.38 and 2.39 shows that Kristiansund and Tromsø are the scenarios with the least drying potential. Figures 2.40, 2.41, 2.42, 2.43, 2.44, 2.45, 2.46 and 2.47 confirm that the risk of mould decreases with latitudes.

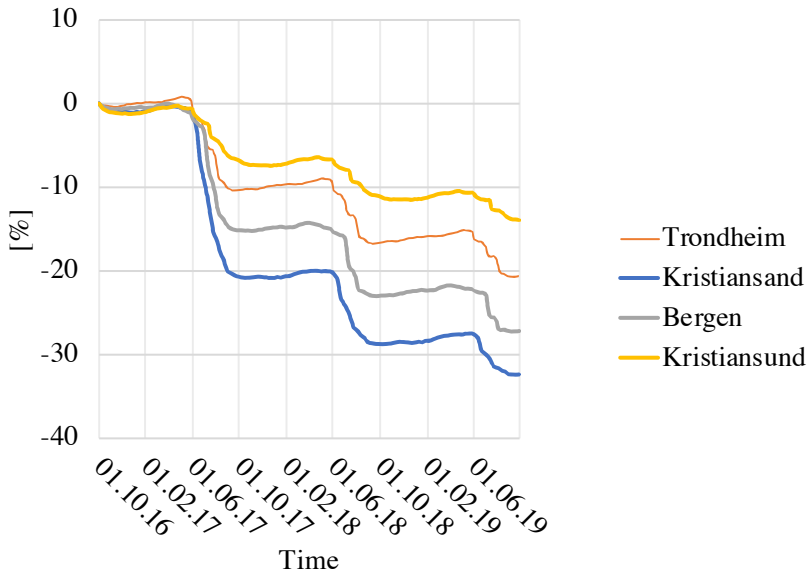

Figure 2.38: Percentage of change of the total moisture content in the roof assembly

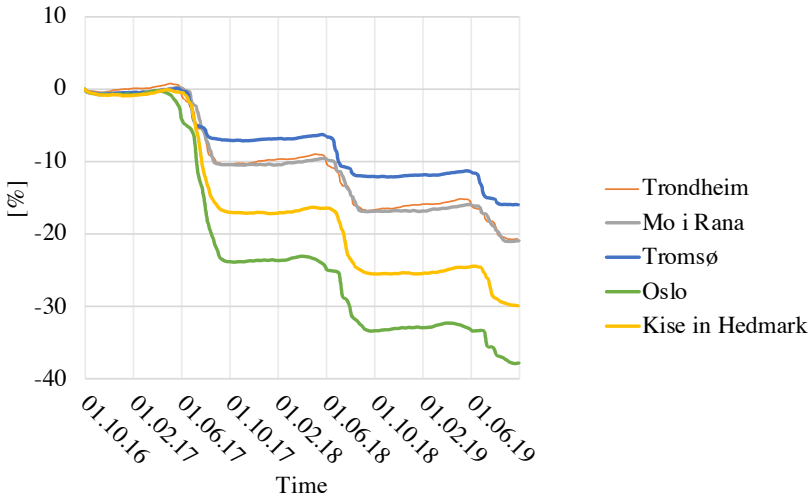

Figure 2.39: Percentage of change of the total moisture content in the roof assembly

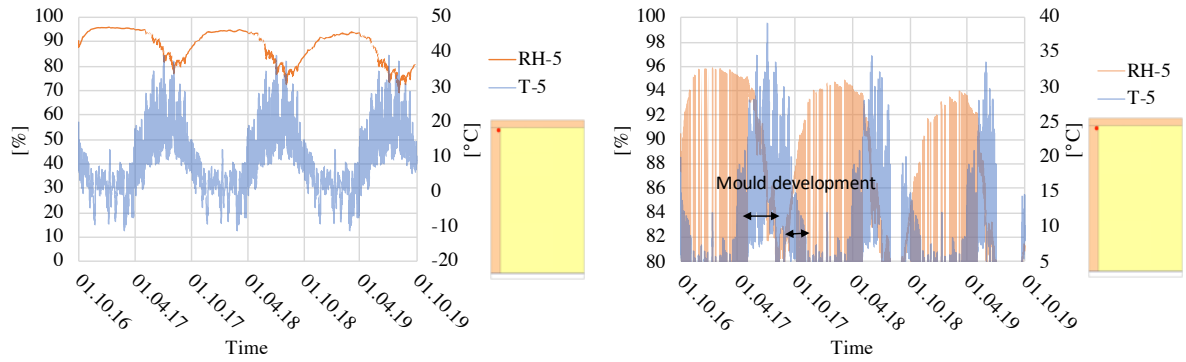

(a) RH and Temperature **(b)** RH > 80% and T > 5°C

Figure 2.40: Scenario: Trondheim. RH and temperature for point 5

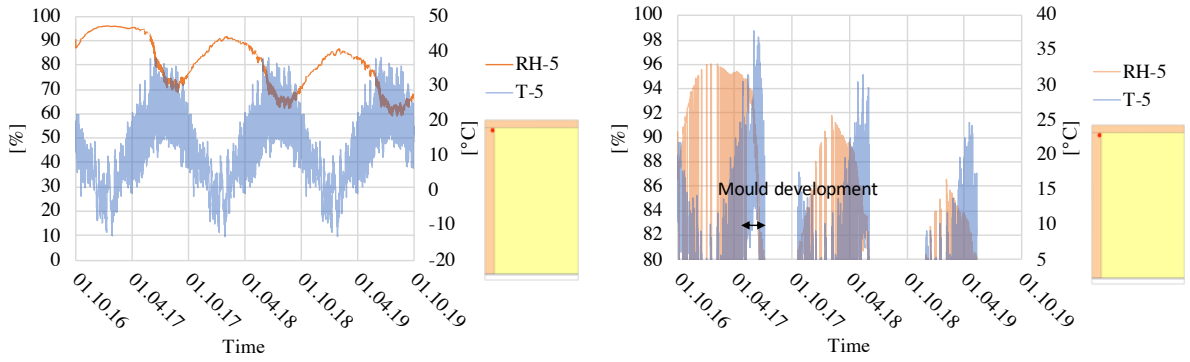

(a) RH and Temperature **(b)** RH $>$ 80% and T $>$ 5°C

Figure 2.41: Scenario: Kristiansand. RH and temperature for point 5

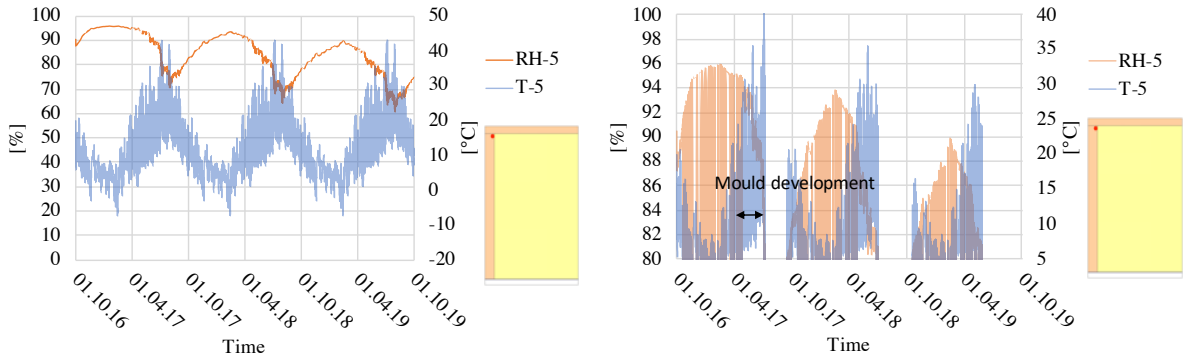

(a) RH and Temperature **(b)** RH $>$ 80% and T $>$ 5°C

Figure 2.42: Scenario: Bergen. RH and temperature for point 5

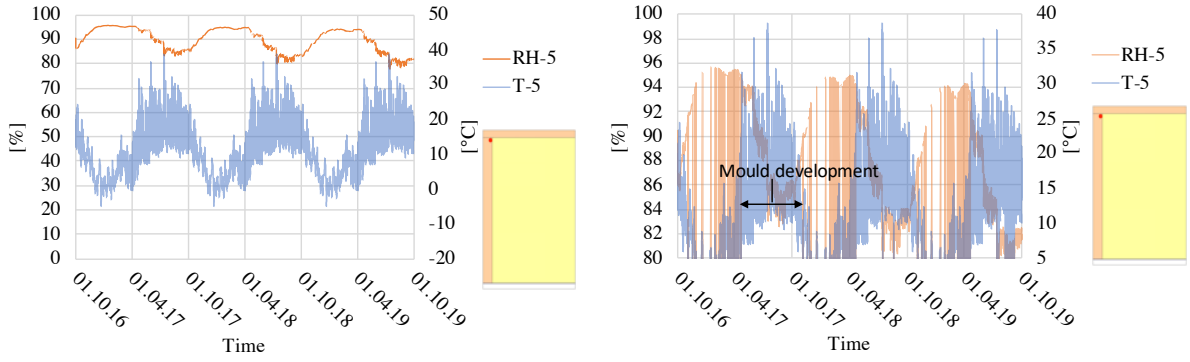

(a) RH and Temperature **(b)** RH $>$ 80% and T $>$ 5°C

Figure 2.43: Scenario: Kristiansund. RH and temperature for point 5

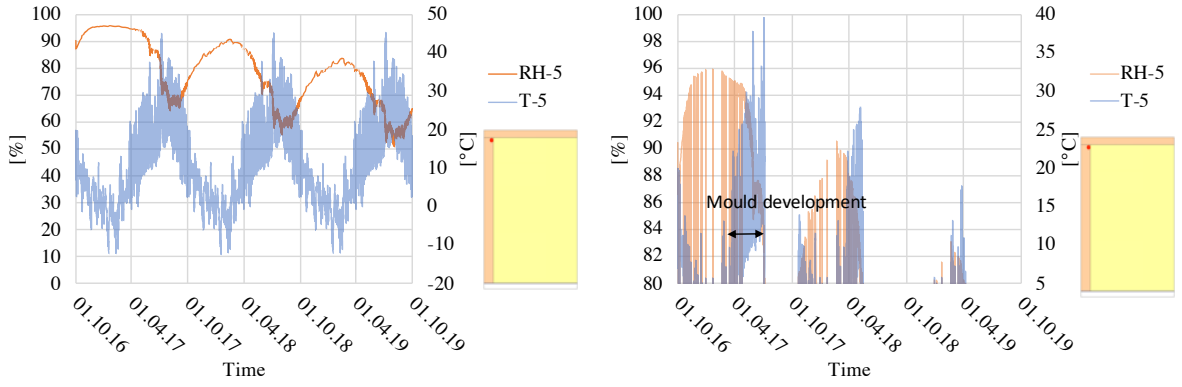

(a) RH and Temperature **(b)** RH $>$ 80% and T $>$ 5°C

Figure 2.44: Scenario: Oslo. RH and temperature for point 5

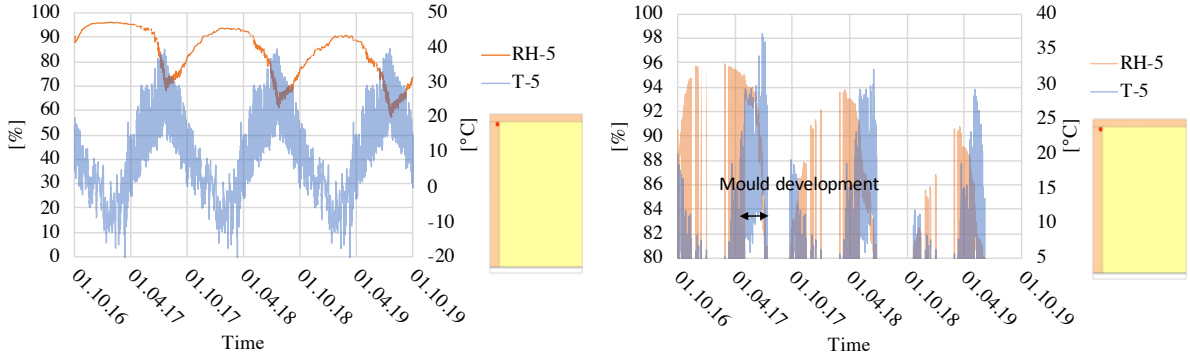

(a) RH and Temperature **(b)** RH $>$ 80% and T $>$ 5°C

Figure 2.45: Scenario: Kise in Hedmark. RH and temperature for point 5

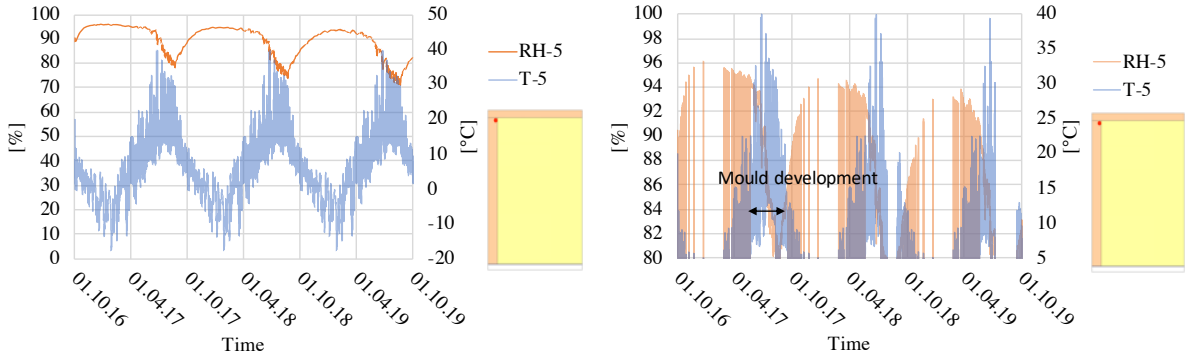

(a) RH and Temperature **(b)** RH $>$ 80% and T $>$ 5°C

Figure 2.46: Scenario: Mo i Rana. RH and temperature for point 5

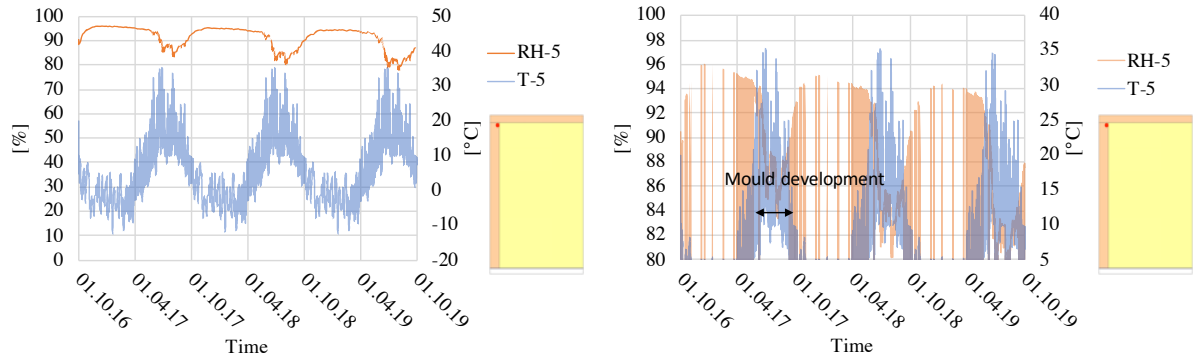

(a) RH and Temperature

(b) RH $>$ 80% and T $>$ 5℃

Figure 2.47: Scenario: Tromso RH and temperature for point 5

2.2.13 The effect of inclination towards north

Table 2.20 shows the parameters used for these scenarios. Inclination towards the north demonstrates a shading effect and figure 2.48 shows that the drying potential decreases with increasing inclination. Having an inclination of 45° towards north creates no drying potential. Figures 2.49, 2.50 and 2.51 show that the seasonal fluctuations of RH are lower with higher inclination.

Table 2.20: Parameters

Parameter		**1**	**18**	**19**	**20**
Location	Trondheim Bergen Oslo Kise, Hedmark Kristiansand Kristiansund Mo i Rana Tromsø	x	x	x	x
Moisture load	Low Medium High	x	x	x	x
Roof height	450 mm 350 mm 250 mm	x	x	x	x
Top insulation	0 mm 50 mm 100 mm	x	x	x	x
Beam (Spruce)	I K	x	x	x	x
Insulation	Mineral wool Wood fibre	x	x	x	x
Internal lining	$s_d = 0.2$m $s_d = 1$m	x	x	x	x
Moisture content	18 % in beam 20 % in wooden sheathing 18 % in wooden sheathing 15 % in wooden sheathing 15 % in beam	x x	x x	x x	x x
Date of closing	1st of October 1st of January 1st of April 1st of July	x	x	x	x
SVB	AirGuard Smart Majrex	x	x	x	x
Inclination	**0 °** **30 °** **45 °** **90°**	**x**	**x**	**x**	**x**
Orientation	**North**		x	x	x

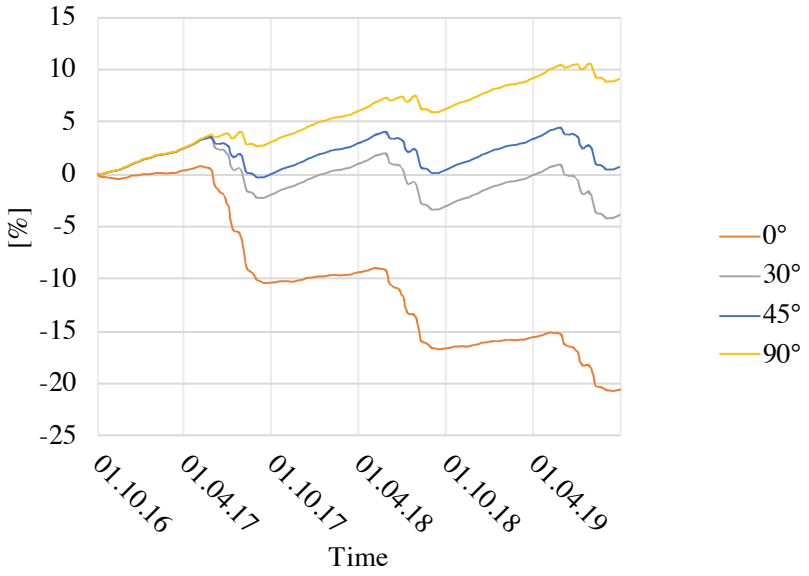

Figure 2.48: Percentage of change of the total moisture content in the roof assembly

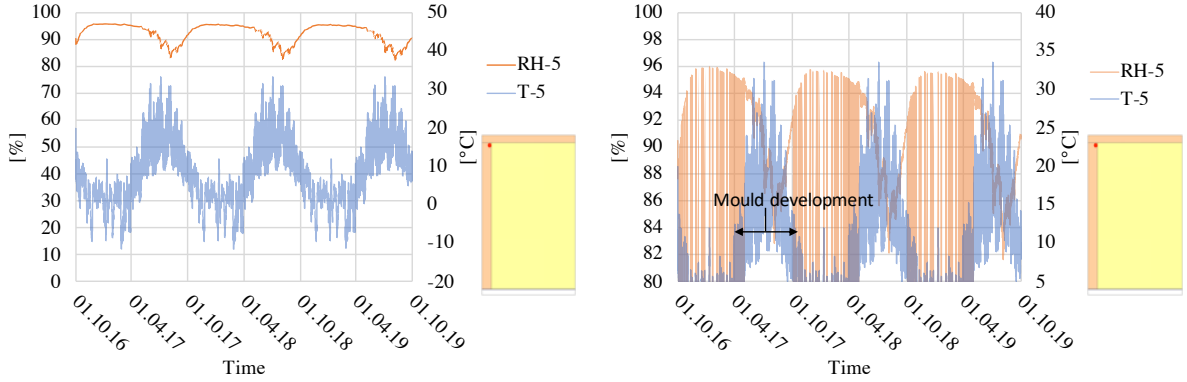

(a) RH and Temperature **(b)** RH $>$ 80% and T $>$ 5°C

Figure 2.49: Scenario: 30° inclination. RH and temperature for point 5

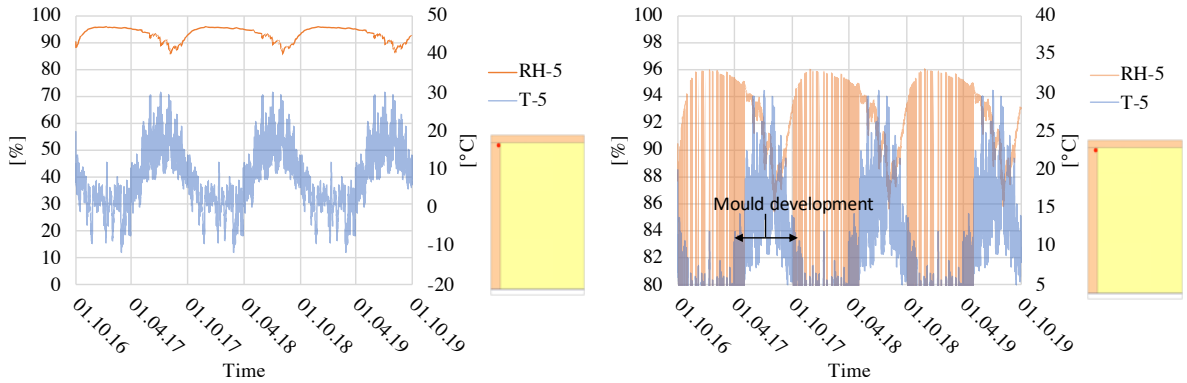

(a) RH and Temperature **(b)** RH $>$ 80% and T $>$ 5°C

Figure 2.50: Scenario: 45° inclination. RH and temperature for point 5

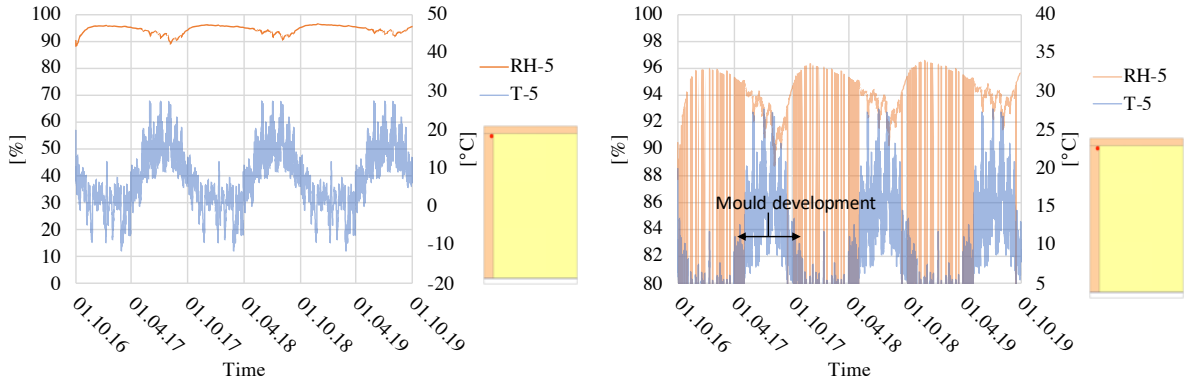

(a) RH and Temperature

(b) RH $>$ 80% and T $>$ 5°C

Figure 2.51: Scenario: 90° inclination: RH and temperature for point 5

2.2.14 Hours of potential mould growth

Figures 2.52 and 2.53 presents how the different parameters affect the robustness of a construction. The figures represent the sum of hours where the conditions are suitable for mould growth. There are in total 26300 hours calculated over three years. Notice that the scenarios with insulation above the wooden sheathing have fewer hours where the conditions are above 90% RH and temperature higher than 5°C compared to the reference case. In addition, the scenarios where the drying potential is limited, such as high moisture load, inclination towards north and wood fibre insulation have more hours where RH is higher than 90%.

This is a simplified presentation with the number of hours where RH and temperature are above a set limit. This does not, however, represent the possibility of mould development, because it does not consider the length of the period where the conditions are suitable for mould growth. Therefore, figures 2.52 and 2.53 should be evaluated in combination with the figures representing RH and temperature for each scenario above.

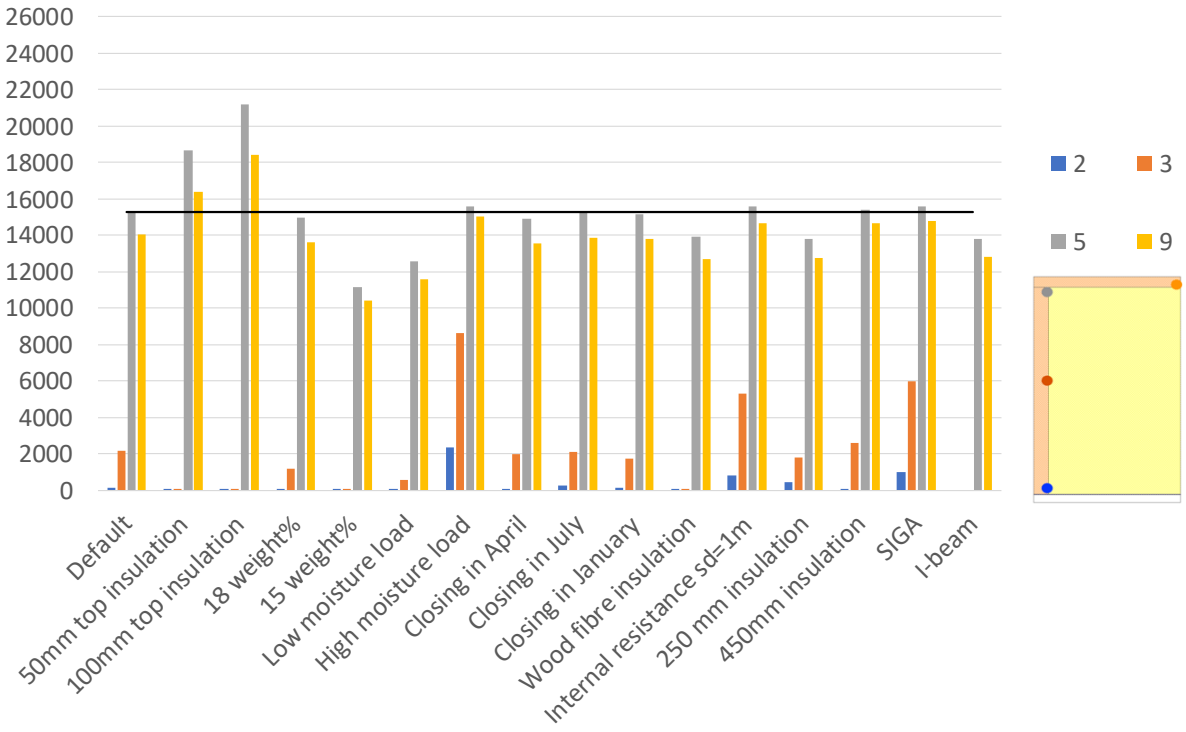

(a) RH > 80% and T > 5°C

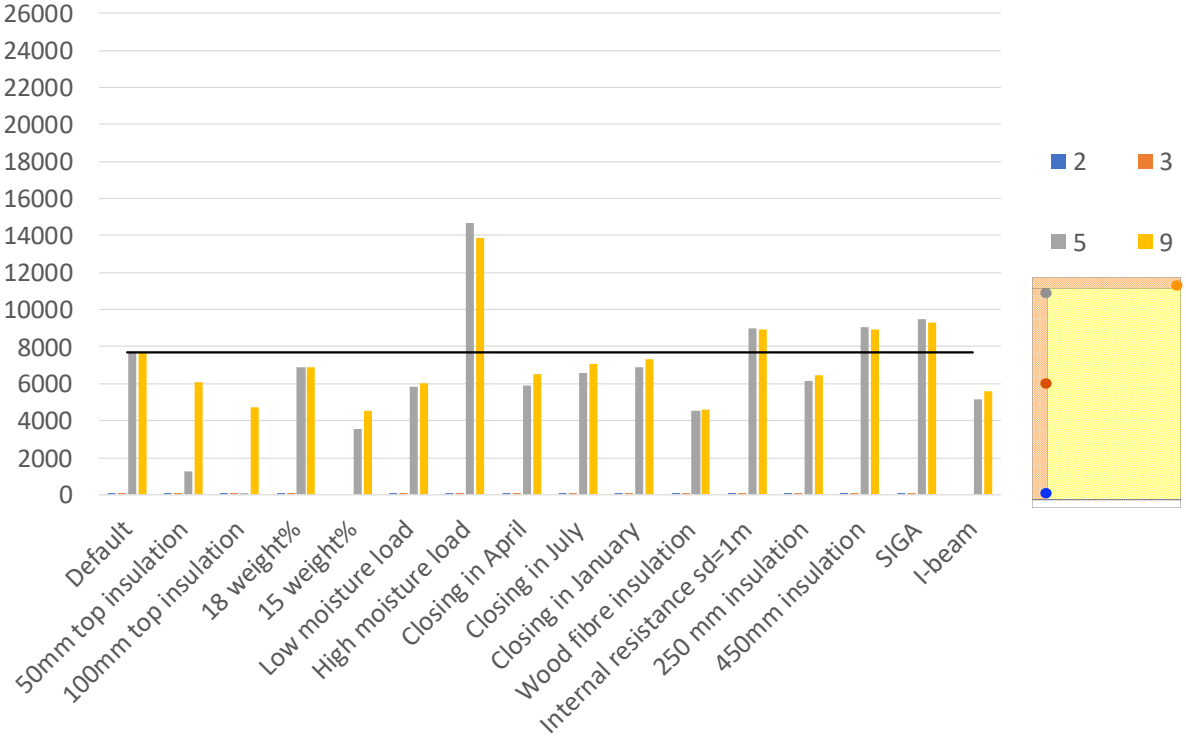

(b) RH > 90% and T > 5°C

Figure 2.52: Total amount of hours for potential of mould growth in the points, 2, 3, 5 and 9

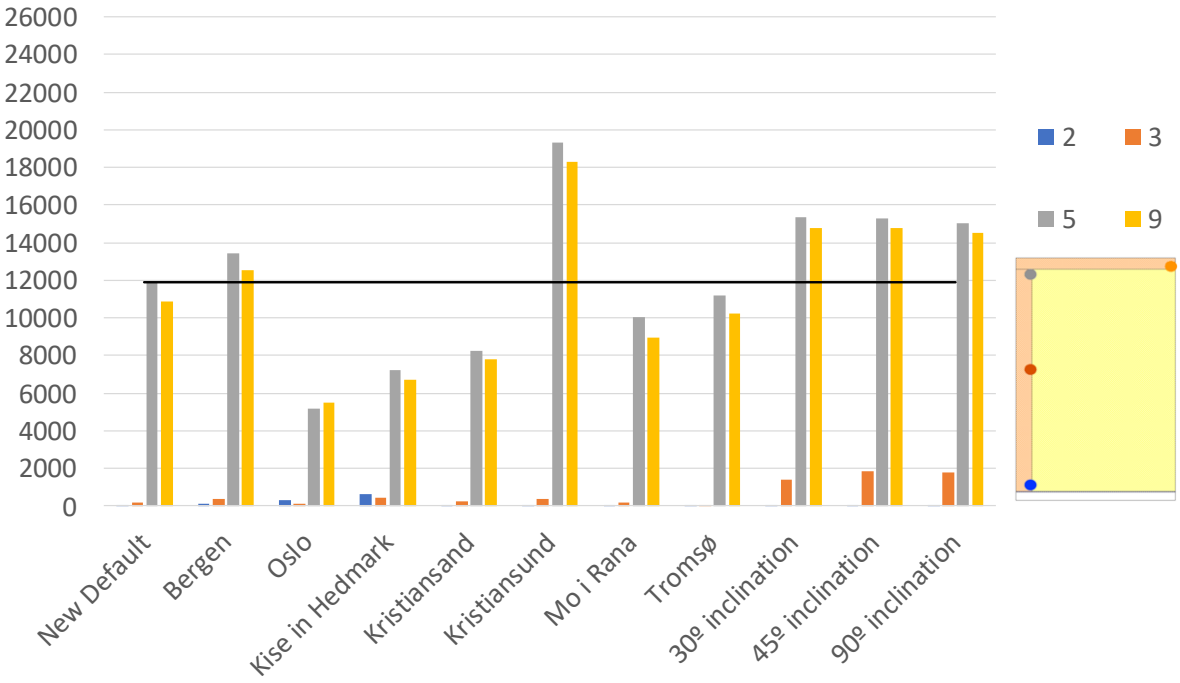

(a) RH > 80% and T > 5°C

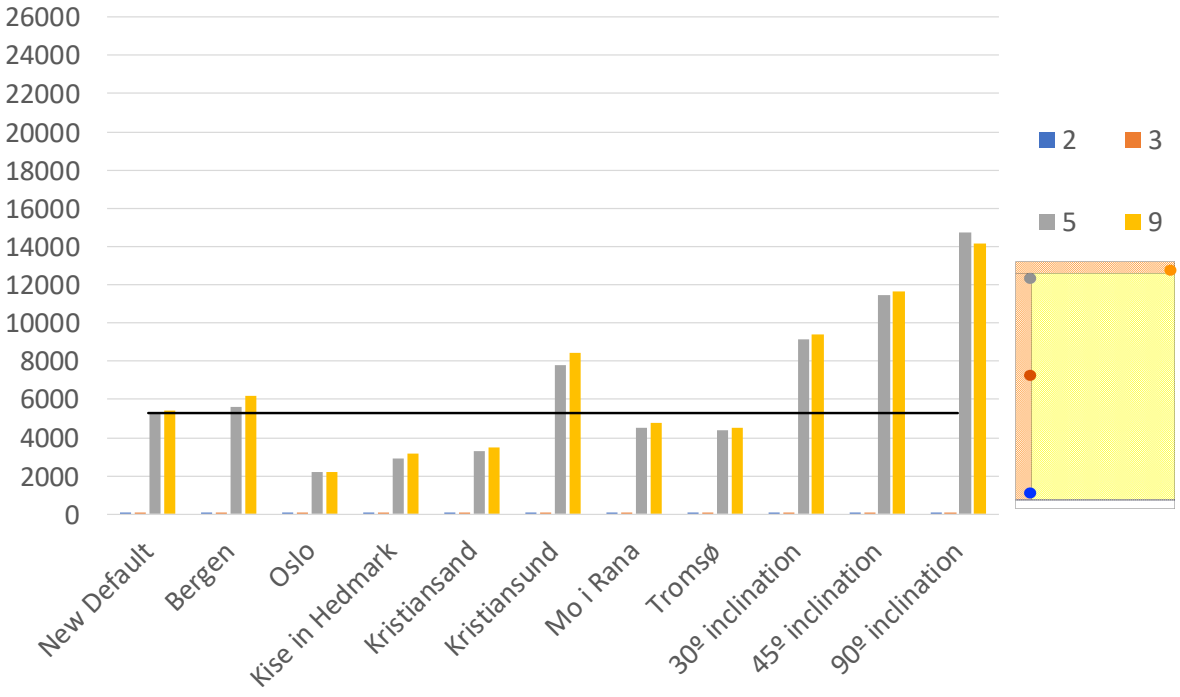

(b) RH > 90% and T > 5°C

Figure 2.53: Total amount of hours for potential of mould growth in the points, 2, 3, 5 and 9

2.2.15 Uncertainties

There are various uncertainties in the calculations. An area of interest in the simulated model is chosen where the data is extracted. These areas can differ from each other when

models have different geometry and grid sizes such as the construction with I-beams, different height and sloped insulation. It is therefore important to carefully choose areas that are of similar size and location in the model. Results extracted from critical areas can differ because WUFI calculates the mean value over the area chosen. Hence, the results can have small differences in mean moisture contents, RH and temperature if the chosen area is not matching. The scenarios where this can happen are I-beam, different insulation heights and top insulation.

In numerical calculations, convergence failures can occur, which means that the convergence criterion is not reached. Grid sizes, climates and material properties are examples of what can cause convergence failures. In order to decrease these failures to an adequate level, the grids have been modified. In addition, material properties such as the moisture storage function for "spruce transverse II" was edited from 97% RH so the function was continuously increasing to 600kg/m3 without a break in the curve. Convergence failures can disturb the calculation and cause high leaps in the moisture contents. An adequate level of convergence failures can be assumed to be 10 and below.

Mineral wool in WUFI is given a default sorption curve designed by WUFI. It allows capillary condensation of water for high values of RH. Capillary condensation is water vapour that has been transported in to the pore system and condenses. For mineral wool, this is not a realistic scenario, and will therefore create a higher initial moisture content than what is theoretically possible. The default curve has been used to avoid numerical issues during the calculation, (Wufi, 2019[b]). Despite the unrealistic property of mineral wool, it is decided not to change the sorption curve because of numerical problems. This decision is based on calculations with a user-defined sorption curve created in a previous master thesis, (Stellander, M., 2012). Read more about these results in appendix A.2.

Due to the moisture storage curve of mineral wool, the total moisture content in the model will be higher. It is calculated that 4% of the total initial water content in the default model is from the mineral wool and the percentage increases to 5.5% when changing the initial moisture content of the wooden sheathing to 18 weight%. This can cause a higher risk of mould due to higher initial moisture levels in the construction. In addition, the scenarios where top insulation is used, there is no vapour tight membrane dividing the top insulation and the wooden sheathing. Due to the standardised sorption curve, this allows moisture to travel from the wooden sheathing to the insulation placed on top.

After the calculations of all the scenarios and extracting the data needed from the analysis, it was discovered that the length of the model is 250mm long. This means that the beams are placed with cc50cm. Normally cc60cm is used in buildings. A roof assembly with lower centre distance will have higher initial moisture content, but also have more materials to distribute the moisture in. Appendix A.3 shows the results of RH in the most critical areas of the construction. The results show no significant differences. Therefore, it is decided to continue with a centre distance 50cm in the discussion.

Normally, a building is not heated and includes internal moisture load when a construction is closed. On the contrary, the construction has an external layer, a roofing membrane, that prevents rain from falling on the wooden materials. In this study, heating and moisture load initiate when the calculation starts. In fact, it is assumed that the construction is finalised and inhabited when the calculation starts. Therefore, the results regarding closing the construction will differ from reality. In reality, the wooden elements that have high initial moisture content when installing the roofing membrane, should be allowed to dry before installing the insulation and the vapour barrier.

It is also important to consider how the results can differ from reality. For example, the properties of wooden materials vary within the materials and depend on their moisture history and density variations. Other materials that are fabricated can vary depending on the producer. Therefore, it is important to consider every material independently. In reality, various damages due to human mistakes during a construction process can cause moisture problems. A common result of this for a roof construction is leakage. A roof can also have drying possibilities through the eaves and the ridge of the construction. This is not considered in these calculations.

2.3 Discussion

Drying potential

General observations in the reference model

The seasonal fluctuations of moisture content in figure 2.3 shows how the roof assembly accumulates moisture in winter and dries in summer. These trends are shown in all models investigated. Figure 2.4 shows how the moisture is distributed in the wooden elements according to the season. The AirGuard Smart has $s_d = 3.3 - 13$m for RH $= 62.5 - 37.5\%$. RH of the internal air varies between 40% and 50% during winter, according to the user-defined moisture supply curve. Therefore it creates a potential for vapour diffusion into the roof assembly due to low s_d value of the SVB. However, figure 2.3 shows a drying potential of the roof assembly, because the drying rate in summer is higher than the accumulation of moisture in winter.

Figure 2.4b shows the moisture distribution in the wooden sheathing. Notice the difference of moisture content in monitor point 9 and 12. The results indicate that there is condensation on the surface of the wooden sheathing towards the insulating material. It should be noted that the area selected for point 9 is around 2.5mm and can be assumed to be the surface of the wooden sheathing towards the insulating material. The high moisture content in this area can also be a result of the moisture content in the mineral wool as described in chapter 2.2.15. 4% of the total initial moisture content in the roof assembly is in the mineral wool and during the winter season, the moisture travels towards the wooden sheathing. Hence, the surface of the wooden sheathing will have a rapid increase in moisture content and slowly distribute it.

The rapid decrease in moisture content in point 9 during spring is caused by a direction change in the vapour pressure gradient, where the moisture travels towards the internal air, as described in chapter 1.2.3. During summer, some of the moisture travels through the SVB and dries towards the internal air. The moisture in point 9 in winter decreases with 10% over three years which is a result of this. However, it can be expected that the distribution of moisture in the wooden materials is more uniform due to capillary suction. Another explanation of the behaviour of point 9 can be numerical issues in the calculations. Figure A.1 in appendix A.1 shows the moisture content in different areas and in different sizes of the wooden sheathing. Because of the high leaps of moisture content near the surface of the wooden sheathing, these numbers should be used carefully.

The effect of sun exposure
It is expected that constructions that allow high surface temperatures on the wooden sheathing dry at a higher rate than constructions that prevent the sun to heat up the same surface. Constructions that have insulation on top and/or are inclined towards North are examples that prevent solar heating on the surface of the wooden sheathing. In addition, the latitude of the location and the corresponding altitude of the sun are expected to impact the drying potential due to the amount of solar exposure, as described in chapter 1.3.5 and 2.1.4.

Figure 2.6 verifies what is expected; the drying potential decreases with insulation on top. It is clear from the figure that the moisture fluctuations are higher for the scenario with no insulation on top. This is because the surface temperature of the wooden sheathing is lower in winter due to direct exposure to the external air. Notice that with 0mm top insulation, the accumulation of moisture in winter is higher compared to the scenarios with 50 and 100mm insulation above the wooden sheathing. This might be due to lower temperatures in the roof assembly leading to a higher RH close to the SVB. This makes the SVB more vapour permeable allowing more moisture to travel into the construction. However, the drying rate in summer is higher than the accumulation in winter which increases the drying potential. Having 100mm insulation on top creates lower seasonal temperature differences due to its insulating effect. This results in less seasonal moisture fluctuations.

Due to the altitude of the sun in Trondheim, an inclination higher than 50° towards North leads to no direct solar radiation on the roofing surface during a year. Simulating different inclinations demonstrates the shading effect. This means that the scenario with 90° is shaded all year round, while the scenarios with 45° and 30° inclination are partially shaded. Figure 2.48 shows that the water accumulation in the roof with 90° inclination is higher than the drying potential in summer. Hence, the surface temperature of the roof assembly studied when it is totally shaded and located in Trondheim is not high enough for a sufficient drying potential. In addition, a roof with 45° inclination has no drying potential, while the roof with 30° inclination has a small drying potential. Hence, a roof with 30° inclination towards North can be sufficient if other parameters that improve the

roofs robustness is used.

Figures 2.38 and 2.39 verify that the drying potential is increasing for locations at lower latitudes. However, notice that the drying potential of Kristiansund is lower compared to the drying potential of Trondheim, even though they are located at equal latitudes. This might be due to a higher cloud index for Kristiansund compared to Trondheim. This means that the roofing surface in Kristiansund is less exposed to the sun, as described in table 2.8. The same trend is shown for Trondheim and Mo i Rana, where Mo i Rana is located at higher latitudes but has a lower cloud index compared to Trondheim. This is a possible explanation why the drying potential is similar for the two cities.

Internal conditions
The internal climate impacts the drying potential in a different way. As described in chapter 1.3.5; the diffusion resistance of an SVB for high RH is low and therefore allows moisture to accumulate in the roof assembly. As expected, the results in figure 2.13 shows that it is not favourable to have a high internal moisture load and verifies the findings in the study described in chapter 1.3.5. In fact, for a high internal moisture load, accumulation of moisture during winter is higher than the drying rate in summer. This can result in rot and decay problems, as described in table 1.1. Hence, it should not be recommended to use SVB for rooms with high moisture load. However, the moisture loads used in the analysis are conservative values. The study described in chapter 2.1.4, suggests to use a high moisture load for bathrooms and laundry rooms, but it can be suggested that a medium moisture load can be adequate if the rooms are well ventilated. Furthermore, the moisture loads in these rooms are not constantly high, because the activities that create high moisture loads happens sporadically, such as showering. Therefore, it can be assumed that the internal lining works as a buffer during the short periods where the moisture load is high.

Initial conditions
The total moisture content in the roof assembly is lower when the construction is closed in April or July compared to October or January, as shown in figure 2.16. This is because the drying period starts at the beginning of the calculation if it initiates in the fall. Hence, the scenario where the construction is closed in April has the highest drying potential because it has a longer drying period when the calculation starts. However, these results do not resemble real scenarios of closing, as discussed in chapter 2.2.15, because the results demonstrate that the building is inhabited.

Initial moisture content varies depending on the roof assembly and if it has been exposed to rain before closing. According to figure 2.9, there is nothing that indicates that the roof assembly with 15 weight% is drying. Hence, the results show that the roof assembly seeks an equilibrium state with the surroundings. Figure 2.10 shows that the beam has an average of around 12 weight% moisture content, while the wooden sheathing has an average of around 18 weight% moisture content in equilibrium. However, if the conditions are changed, such as climates and material properties, the equilibrium state

will be different.

Type of constructions and the choice of materials
In a study described in chapter 1.3.3, it is shown that an internal diffusion resistance equal to 0,135m has insignificant effects. However, figure 2.24 shows that a higher internal diffusion resistance will disturb the drying potential negatively. The high diffusion resistance, s_d = 1m, prevents moisture to dry towards the internal air during summer. This is because the diffusion resistance is higher than the diffusion resistance of the SVB with minimum s_d = 0.2m. Notice that the scale of figure 2.24, shows that the difference in percentage of change is around 5%, but increasing for every year. Hence, materials used for the internal surface should be considered when using an SVB due to the increasing difference.

Regarding the choice of SVB, it is clear from figure 2.30, that an SVB with higher range of s_d values is more favourable. The figure shows that the moisture dries at a higher rate for AirGuard Smart compared to Majrex. This is because the diffusion resistance for high RH is higher for Majrex compared to AirGuard Smart, which reduces the drying rate in summer. In addition, it could be assumed that there would be a higher moisture accumulation during winter when using Majrex. This is, however, not possible to identify. Hence, the lower s_d values for high RH are what differentiate the two materials. This scenario is similar to the scenario with internal resistance, s_d = 1m, as discussed above. Figure 2.52 shows that the monitor points 3 and 2 have a higher amount of hours where the condition is suitable for mould growth compared to the reference scenario. This is probably a result of the high internal vapour diffusion resistance that prevents the moisture from travelling towards the internal air.

According to figure 2.20, wood fibre insulation is absorbing the water in the critical areas of the construction. This verifies studies discussed in chapter 1.3.2. Due to the hygroscopic effect of the wood fibre insulation, the moisture is absorbed and stored in the insulation material. This is why the moisture content is not decreasing in the roof assembly, as shown in figure 2.21. On the contrary, the figure shows that the roof assembly with an SVB and wood fibre insulation increases the moisture content. This might be because the wood fibre insulation has a higher moisture capacity for high RH and therefore is not drying sufficiently when the external surface temperature increases.

Figure 2.27 shows that a roof with 250mm height has a higher drying rate than for taller roof assemblies. A possible explanation is that the vapour pressure gradient is increasing with decreasing thickness. Additionally, the figure B.1i in appendix B shows that the moisture content in the wooden sheathing is lower for the roof assembly with I-beams compared to the roof assembly with all wooden beams. This is probably due to the higher initial moisture content in a roof assembly with all wooden beams. Figure 2.33 shows that the roof assembly has approximately the same drying potential. However, the roof assembly with I-beams has a higher accumulation rate in winter and drying rate in summer. This might be due to more surfaces of the beam that can potentially dry and

accumulate moisture.

Mould development

In general, most of the scenarios are at risk of mould. As shown in figure 2.52, most of the scenarios have suitable conditions for mould growth for half of the total hours over three years. The figure shows that the parameters that have the possibility to increase the robustness are initial moisture content, moisture load and external climate.

The results and the analysis are based on that mould develop when the conditions are above the critical value over a period of time. However, figure 1.3 in chapter 1.2.2 shows that if the conditions are 5℃ and 83% RH, the period needed for mould to develop is around 6 months. This period is decreasing with higher temperatures and RH. Figure 2.53, which presents the sum of total hours where the conditions are above 5℃ and RH higher than 90%, shows which of the scenarios that have the highest risk of mould. It can be seen from figure 1.3 that for these conditions mould development needs 2 months to develop and this period decreases significantly for higher temperatures.

Reference model

As shown in figure 2.5, there are periods where conditions are suitable for mould growth. The figure shows that the first period is during the first summer where the conditions are stable above the critical limit for around 5 months. The period starts at the beginning of April and lasts until October where RH varies between 94% and 80%. The temperature varies from 10 to 40℃ within this period. Based on figure 1.3 in chapter 1.2.2, mould develop after around 1 months for conditions with 88% RH and 20℃. Hence, the construction is at risk of mould. After mould first has been developed, the growth continues every time the conditions are suitable.

The effect of sun exposure

Figures 2.49, 2.50 and 2.51 show that RH increase with inclination. Therefore, a higher risk of mould in roof assemblies that are being shaded is identified. However, the amount of hours above the critical limit is more or less equal for all scenarios with an inclination towards north, but higher inclination creates higher RH as shown in figure 2.53. Hence, the surface temperature of inclined roofs towards north is not high enough to decrease the RH sufficiently in the summer and further, reduce the risk of mould.

Figure 2.52 shows that having insulation on top increases the number of hours suitable for mould growth. However, it also reduces the amount of hours with RH above 90%. As shown in figure 2.7 and 2.8, the wooden elements are not reaching high enough temperatures to reduce RH below the critical value. In addition, the temperature is higher during winter and creates a potential of mould growth also here. RH is lower for the constructions with insulation above the wooden sheathing. Based on the theory described in chapter 1.2.2, mould development decreases when the conditions are closer to the critical limit. Figure 2.8, construction with 100mm insulation above the wooden sheathing, shows that RH is fluctuating around 82% RH and temperature around 15℃ over a time period of 5-6 months. Based on figure 1.3, it will take around 17 weeks(around 4-5 months) for mould

to develop for these conditions. Notice that RH is decreasing with 2%, which is probably due to moisture distribution in the roof assembly. The standardised sorption curve or mineral wool in WUFI allows the mineral wool to accumulate some water. Because a vapour tight membrane has not been placed between the wooden sheathing and the top insulation, some of the moisture in the wooden sheathing can be distributed into the top insulation.

In general, locations at lower latitudes have a lower risk of mould. However, Kristiansund is the most critical city in this analysis in terms of mould development. Even though Tromsø has a similar drying potential, the period of possible mould development is longer. This is probably because the summer season is longer in Kristiansund. This is possible to see in figure 2.43, and 2.47, where the temperature is above 0°C in April while in Tromsø this happens much later. This can also be identified by comparing the climate of Bergen and Trondheim. As shown in figure 2.53, the construction located in Bergen has more hours of possible mould growth compared to the scenario in Trondheim. However, figures 2.40 and 2.42 show that the temperature in winter and in autumn is higher in Bergen which is why the sum of hours is higher. However, the conditions in winter are not stable, and can not represent possible mould development. Hence, the robustness of a roof in different climates is not only depending on solar altitude, but also on external temperatures and cloud index.

Internal conditions
As mentioned, high internal moisture load can result in rot and decay. This is verified in figure 2.15, where it is clear that the period with suitable conditions for mould growth is increasing each year. As shown in figure 2.52, the hours of possible mould growth for the lower beam is also high. This verifies that the roof assembly is accumulating moisture because of high RH. However, as shown in figure 2.14, periods with suitable conditions for mould growth is decreasing every year when having low internal moisture supply. Hence, the risk of mould will decrease significantly by assuring well ventilation of the building.

Initial conditions
Figure 2.11 shows that the risk of mould seem identical to the reference scenario, probably because the initial moisture content is not changing much; from 20 weight% to 18 weight% in the wooden sheathing. Figure 2.12 shows that there is a risk of mould for the scenario with 15 weight% around the same period as the reference scenario. However, as shown in figure 2.52, the risk of mould decreases significantly for the scenario with 15 weight%. Furthermore, based on figure 1.3 in chapter 1.2.2, it seems that the mould does not have time to develop if the initial moisture content in the wooden elements is low.

Figures 2.17, 2.18 and 2.19 show that there are no distinct deviations between the scenarios of when the construction is being closed. Hence, the initial drying possibility of a roof assembly closed in April and June, is not effective regarding the risk of mould. Furthermore, it is important to consider the initial moisture content of the materials used

in the roof assembly, and manage the materials so they are not exposed to rain. A way to decrease the initial moisture content is by using prefabricated modules which are ready to be installed quickly.

Type of constructions and the choice of materials
For the roof assembly with higher internal diffusion resistance, the risk of mould is similar to the reference model. The same is for the roof assembly with Majrex. This might be because of the small difference in moisture content in the scenarios. However, notice that these scenarios have a higher number of hours with RH above 90%, as shown in figure 2.52, including higher RH close to SVB. A possible explanation is that the internal resistance is preventing moisture to dry in summer.

Using wood fibre insulation decreased the moisture content in the critical area. Figure 2.23 also verifies that the period of possible mould development in the critical area is shorter compared to the reference case. However, the critical areas are at risk of mould because the period of mould development increases every year due to the accumulation of moisture in the roof assembly.

Figures 2.28 and 2.29 indi that the period when the conditions are suitable for mould growth is longer for taller roofs. The periods of possible mould development of the roof with 450mm insulation are similar to the reference model. However, figure 2.52 shows that RH is higher in the top of the roof assembly for the construction with 450mm insulation height. The temperatures in figures 2.28 and 2.29 show no significant difference. Higher drying potential of a roof with 250mm insulation is identified in the figures, where the RH of this roof is decreasing every year and so does the period of mould development. However, because mould has time to develop during the first summer, the roof should be carefully considered in combination with other initial parameters that can reduce the risk of mould.

In a roof assembly using I-beams, figure 2.35 indicates that there is a shorter period where mould can develop during the first summer compared to a roof assembly using solid-beams. This is probably due to a smaller total initial moisture content when using I-beams. The trend is similar; the period is decreasing for every year.

Chapter 3: Field measurements

Two pilot projects managed by Klima2050 with SVB are investigated. They are located at different latitudes with two different climates. A pilot project can increase knowledge of developing solutions and materials.

3.1 Methodology

3.1.1 Measuring devices

The constructions are built with sensors of type S-16, measuring moisture in the wooden elements, as described in table 3.1. The devices are wireless and communicate with a gate-way that is located inside the building. As shown in figure 3.1, the sensors are small boxes, approximately 55cm^2 ($5,7*3,8*2,5\text{cm}$), that measure the temperature and RH in the insulation, and Wood Moisture Equivalent (%WME) in the timber structure. %WME is the moisture content in a specific wooden material that the sensors are calibrated with. The sensors used in these projects are calibrated with the wooden material Douglas fir (Omnisense, 2018). Properties of wooden materials vary depending on type. Therefore, the moisture content of various wooden material can differ from %WME reported by the sensors. The moisture content is calculated by measuring the electric resistance between two electrodes that are placed in the material studied (SINTEF byggforsk, 2015).

Table 3.1: Measuring devices used in the project delivered by OmniSense (Omnisense, 2018)

Device	**Description**
Gate away	A modem that collects data from the sensors and sends it through internet to servers outside of the construction
S-16 sensor	Wireless sensors installed in the beam which measure temperature, surrounding RH and moisture content (%WME). Accuracy: ±0.3℃ /±2.0%RH)
S-2 sensor	Wireless sensor with two plugins. Used to monitor the surrounding RH and temperature. Accuracy: ±0.3℃ /±2.0%RH
A-1 HumiSense™ Temperature and Humidity Probe	Cable for S-2 sensors for measuring ambient RH and temperature. Accuracy: ±0.3℃ /±2.0%RH

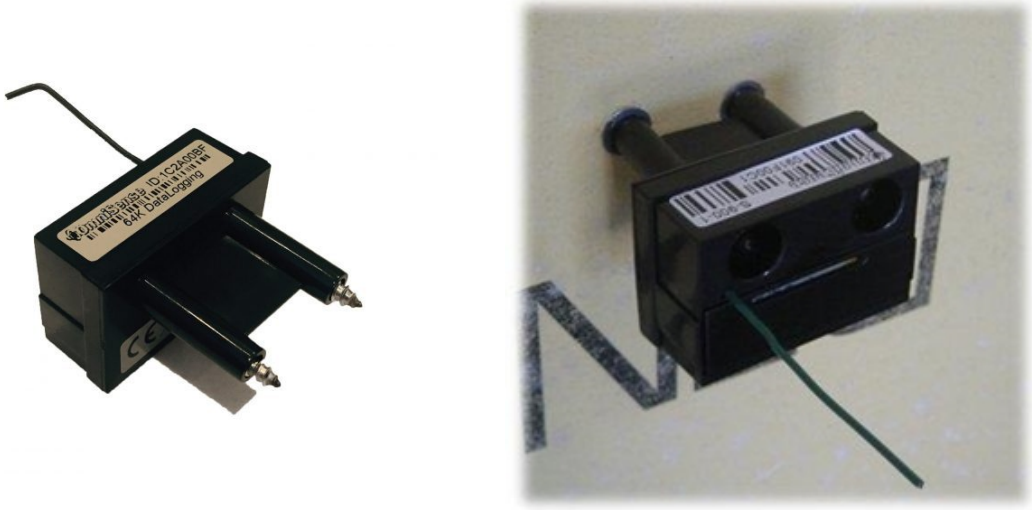

Figure 3.1: Sensor S-16 installed in the wooden elements to measure the %WME, ambient RH and temperature (*Finesterra - OmniSense S-16 sensor* 2019) (left), (Omnisense, 2018) (right)

Handling measurement data

The electric resistance in the timber depends on the temperature (Standard Norge, 2014). However, the sensors are locally calculating the moisture content adjusted to temperature, and there is no need for temperature adjustments. Since the moisture content measured is given for Douglas fir, the results have been adjusted with the formulae 3.1 given by the producer in order to reach the results of Norwegian spruce.

$$\begin{aligned}\%\mathrm{MC}_{\mathrm{spruce}} = &-0.504256 + 1.1386808 * \%\mathrm{MC}_{\mathrm{pine}} + 0.0111586 * (\%\mathrm{MC}_{\mathrm{pine}} - 16.5)^2 \\ &- 0.0010783 * (\%\mathrm{MC}_{\mathrm{pine}} - 16.5)^3\end{aligned} \tag{3.1}$$

Uncertainty range of the measurements varies according to the moisture content. Equation 3.2, shows that the uncertainties increase for higher moisture contents, %MC. The standard limits the measuring range from 8 weight% to 28 weight%. Beyond these limits, the measurement uncertainty will be substantial. However, comparing with the critical conditions in regard to mould growth, the uncertainties should not be considered (Standard Norge, 2014).

$$\pm\text{uncertainty} = 0.1 * \%\mathrm{MC} \tag{3.2}$$

Positioning

The measuring devices are located both on the cold and warm side of the construction, as shown in the figures 3.4 and 3.7. They are placed in such a way that they measure moisture content in the middle of the beam and are placed 1 cm above the SVB and 1

cm beneath the wooden sheathing.

It is important to consider how the devices are placed. The conductivity is measured at where the conductance is the highest. This means that if the surface of the wooden elements are wet and non isolated electrodes are used, the results will show the moisture content of the surface. The sensors used in this project are isolated and will therefore not be affected by this. RH and temperature are measured inside the box, while moisture content is measured in the timber. The area of where the box is placed has reduced insulation, which impacts the measured temperature and RH.

Lund Vest
One sensor measuring the internal climate is located in the ventilated air cavity in the suspended ceiling. The other is located on the internal wall in a storage room on the second floor 1.2 m above the floor, as shown in figure 3.2. The sensors measuring the moisture content in the wooden beams are placed as shown in figures 3.3 and 3.4.

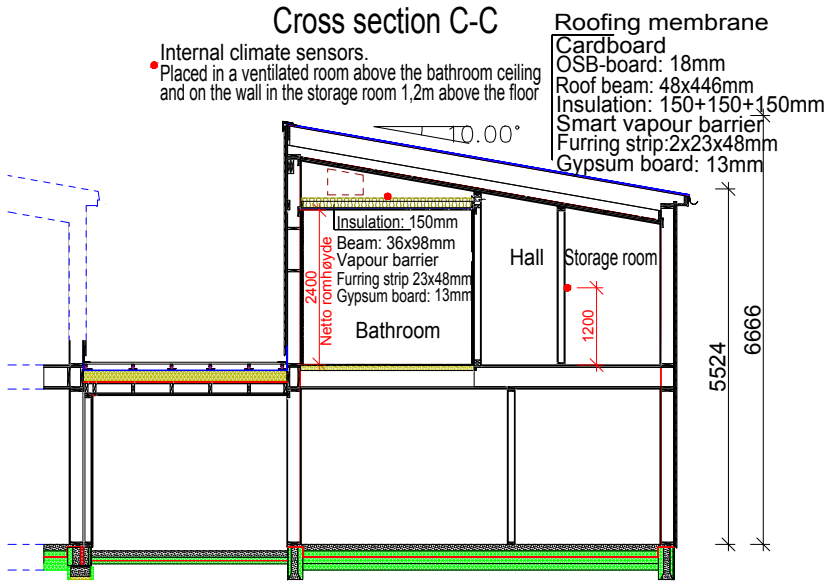

(a) Cross section

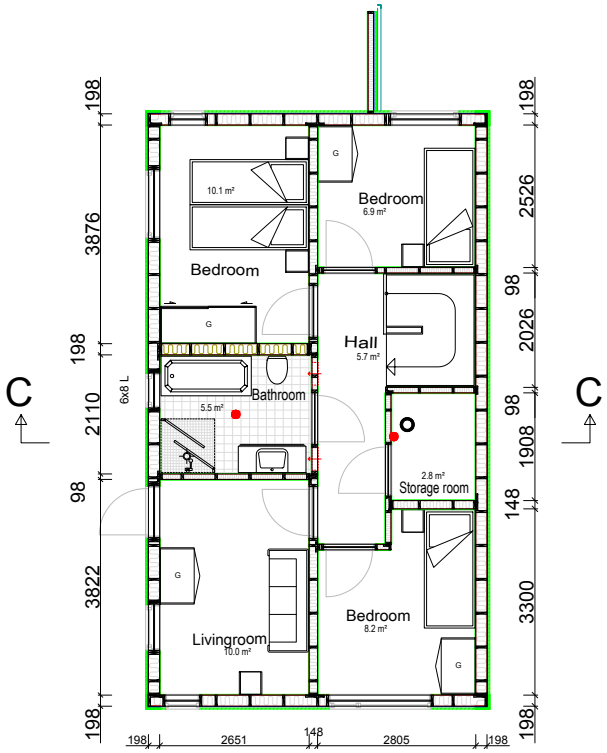

(b) Floor plan

Figure 3.2: Red dots indicate the positioning of the sensors measuring internal climate in the project in Lund Vest (Gullbrekken, L. and Elvebakk, K., 2018)

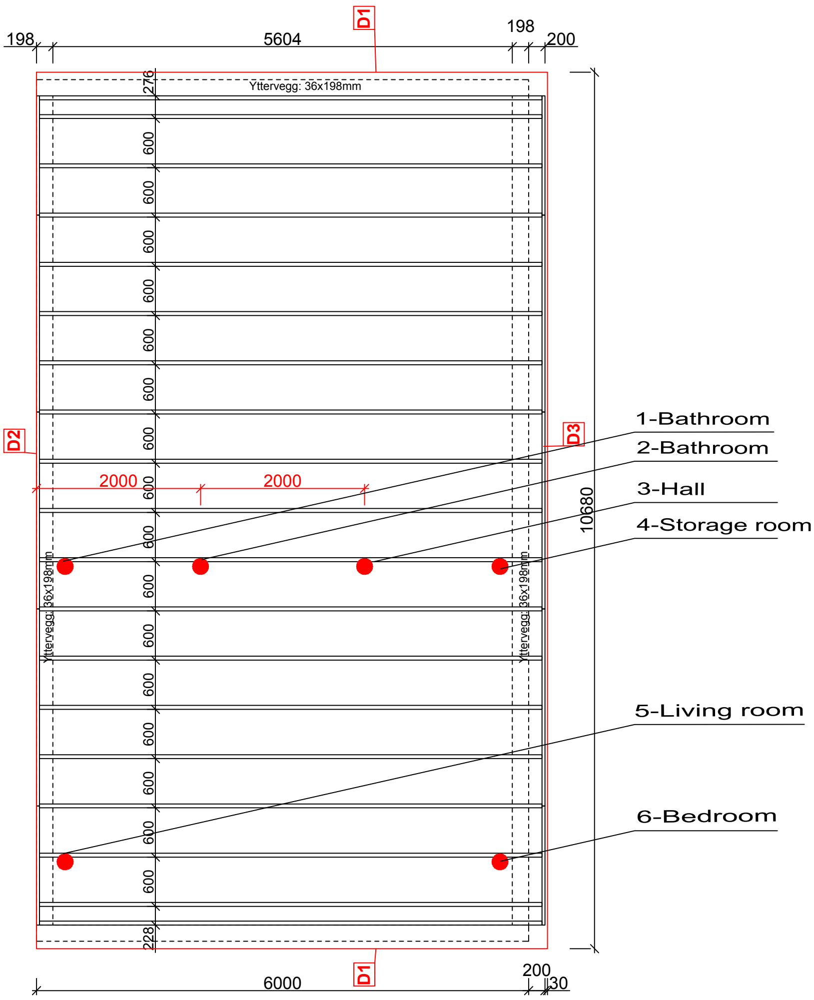

Figure 3.3: Roof plan. Red dots indicate the positioning of the sensors (Gullbrekken, L. and Elvebakk, K., 2018)

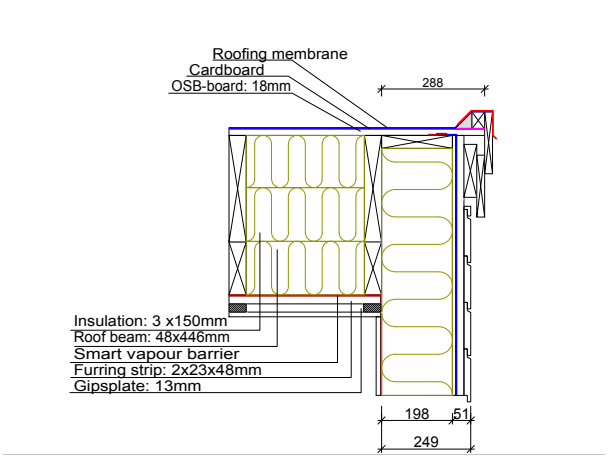

(a) D1: Cross section of the roof

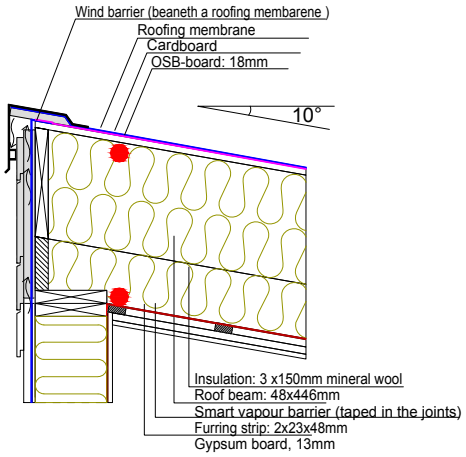

(b) D2: Cross section of the ridge

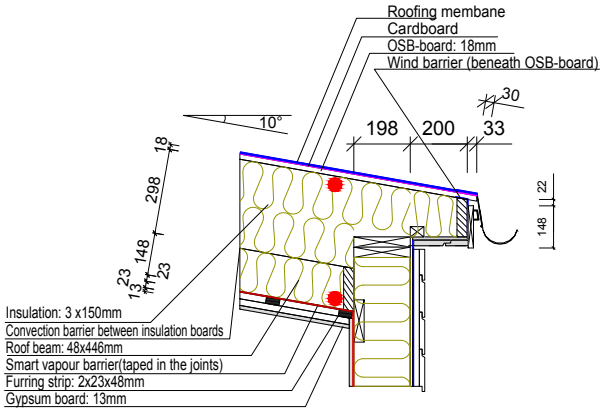

(c) D3: Cross section of the eave

Figure 3.4: Roof assembly: Red dots indicate the positioning of the sensors (Gullbrekken, L. and Elvebakk, K., 2018)

Longyearbyen

The sensors measuring the internal climate are located in the bathroom above the suspended ceiling and in the bedroom closet, as shown in figure 3.6. The sensors measuring the moisture content in the wooden beams are placed as shown in figures 3.5 and 3.7.

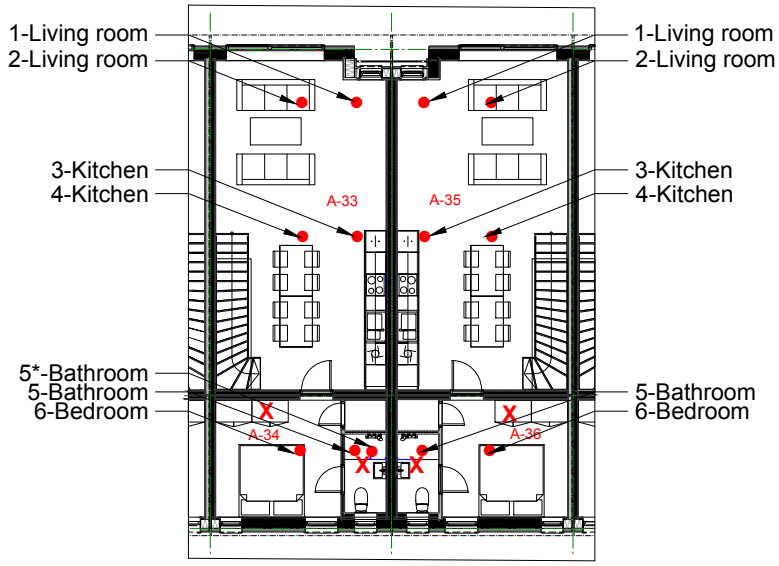

Figure 3.5: Floor plan. Red dots indicate the positioning of the sensors measuring moisture content in the wooden elements, red crosses indicates positioning of sensors measuring the internal climate (Kvande, T., Gullbrekken, L., and Geving, S., 2018)

(a) Bathroom **(b)** Bedroom

Figure 3.6: Placement of the internal climate sensors (Kvande, T., Gullbrekken, L., and Geving, S., 2018)

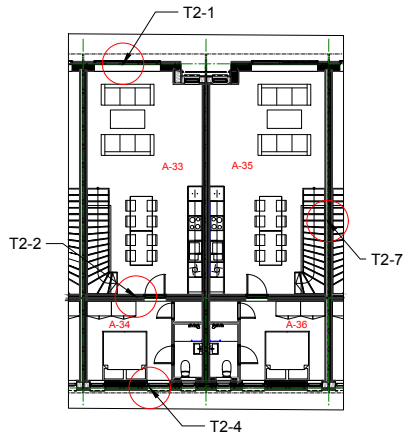

(a) Floor plan

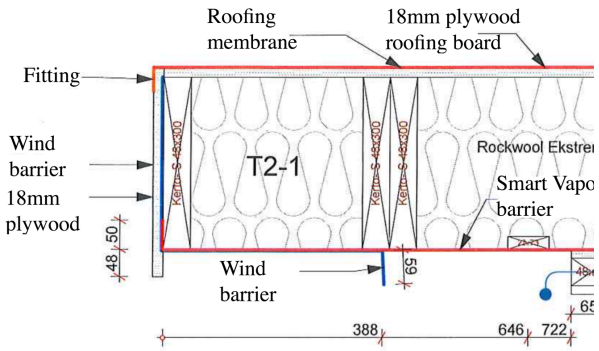

(b) The eave of the module A33/35

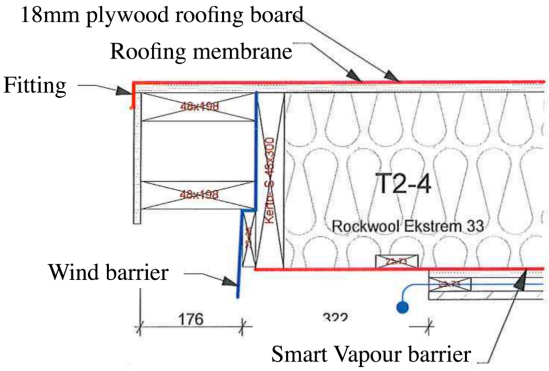

(c) The eave of the module A34/36

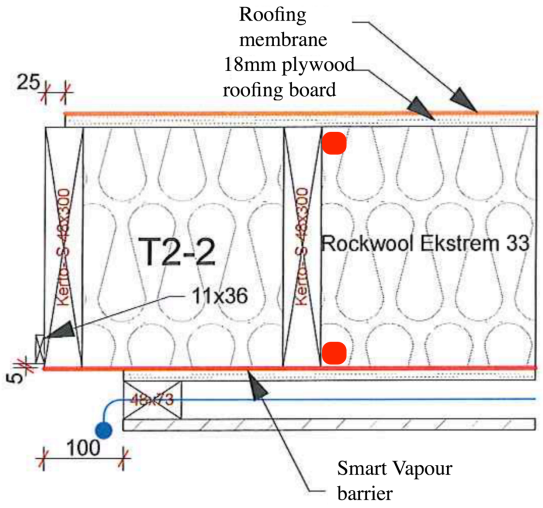

(d) Connection of module A35/33 towards the module A34/36

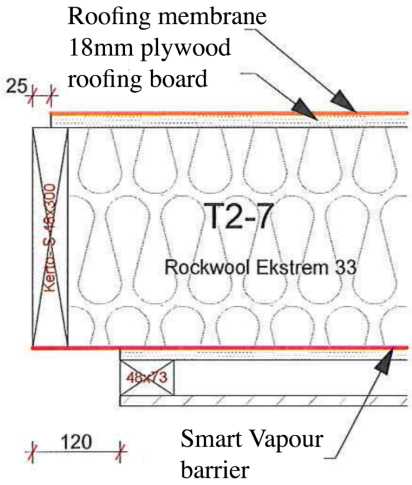

(e) Connection towards the neighbouring house in module A33/35

Figure 3.7: Detailed drawings of the roof assembly. Red dots indicate the positioning of the sensors for project in Longyerbyen (Kvande, T., Gullbrekken, L., and Geving, S., 2018)

3.1.2 Constructions

Table 3.2 describes the comparison of the two projects. In this study, it is assumed that the SVB are installed continuously with taped joints without perforation. The measured moisture content in the timber framing is aiming to be below 15 weight% during the building process for both projects. Therefore, the sensors were installed in the factory where the elements were produced, so it is possible to identify if the dry conditions for the materials were obtained. The analysis period initiates when the building is ready for occupation, from 18th of December to 24th of April.

Lund Vest
The pilot project located in Lund vest in Spydeberg commune in Norway is constructed by Bakke bygg. It is constructed with prefabricated elements of walls, floors and roofs. Before the elements are transported to the construction site, the elements are covered and protected against rain. Furthermore, the construction is closed before the insulation and the SVB are installed. Roof inclination is created by installing the structure in tilted position, and it has a roof inclination towards the south-east.

Longyearbyen
The pilot project located in Longyearbyen in Svalbard, Norway, is constructed by Statsbygg in collaboration with Skanska Husfrabrikken delivering building modules. The construction is made up of modules. The modules are produced in dry conditions by Skanska Husfabrikk. They are transported in controlled conditions by boat before installation. Each house is built up by two modules, where A33 and A35 include the kitchen and living room, while A34 and A36 include the bedroom and bathroom.

As for the construction in Lund Vest, the roof inclination is reached by installing the structure in tilted position. The beams are not parallel with the inclination. This reduces the drying possibility through the eaves.

Gypsum board has low vapour diffusion resistance, while wooden panels have a diffusion resistance approximately equal to 0.7m. However, in the project in Longyearbyen where wooden panels are used, it is assumed that perforation in the wooden panels due to down-lights can create a sufficient drying potential. In the bathroom where PE-foil is used, the PE-foil is installed beneath the SVB in order to maintain the continuity of the SVB.

Table 3.2: Comparison of the pilot projects (Kvande, T., Gullbrekken, L., and Geving, S., 2018), (Gullbrekken, L. and Elvebakk, K., 2018)

	Longyearbyen, Statsbygg	**Lund Vest, Bakke Bygg**
Climate	Arctic	Oceanic, temperate and continental climate
Latitude	78° north	59° north
Highest solar altitude	35°	52°
Type of house	Row house	Chained house
Number of floors	2 and 3	3
Roof slope	Beams installed with 3° slope	Beams installed with 10° slope
Roof drainage system	Lead the water beyond the eave with no gutter nor downspout	External
Other drying possibilities	Modules with wood framing on the length of the building, this limits drying possibilities towards perimeter	Drying possibility through the eaves
Ventilation	Balanced ventilation	Balanced ventilation
Date of closing the construction	First half of august	First half of august
Ready for occupation	19.12.2018	19.12.2018
Roofing membrane	Black two layered asphalt membrane	Black two layered asphalt membrane
Wooden sheathing	18mm plywood	18mm OSB
Wood framing	Kerto S 48x300mm	Solid-wood beam 48x446mm
Insulation	Rockwool extreme 33	Mineral wool
Vapour barrier*	Isola DuPont AirGuard Smart	Isola DuPont AirGuard Smart
Internal lining	16mm gypsum board, 48mm air cavity and 14mm wooden panels	2x23mm air cavity and 13mm gypsum board
* Both projects use AirGuard Smart in at least one bathroom. For the project located in Svalbard, only one bathroom has been equipped with AirGuard Smart.		

3.1.3 Climate

The two projects are located at different latitudes and therefore will be exposed to different climates. External temperature and solar altitude are the most distinctive differences between the two areas. The highest solar altitude on the 18th of December is 3° and -13° in Lund Vest and Longyearbyen respectively. On the 24th of April, the highest solar

altitude has increased to 42° and 24° in Lund Vest and Longyearbyen respectively.

Indoor
It is important to consider and evaluate the internal climate when using an SVB because the vapour permeable resistance decreases with high RH. This is why it should be used carefully in rooms with high moisture load such as bathrooms. At least one bathroom is equipped with SVB in each of the pilot projects. The sensors measuring the internal climate are placed where they are not impacted by the external weather such as solar heating, see figures 3.2 and 3.5.

Outdoor
Solar exposure is essential for the drying process of a roof. Increasing latitudes decrease the direct solar radiation on the roof. This is why it is assumed that the project in Svalbard will have a lower drying potential than the project in Lund Vest. External climate sensors are placed where they are not exposed to direct sunlight and rain to measure the RH and temperature of the surrounding air.

3.1.4 WUFI model

Input and material properties
The material properties used in the WUFI calculation are based on the material data from the projects and are described in table 3.4. Additional input data are given in table 3.5. The initial conditions given in table 3.6 are defined by the measurements, where the initial values of moisture content resemble the measured conditions on the 19th of December 00.00. The temperature is set equal to 20°C because it is assumed that it will adjust according to the climate file when the simulation initiates.

Isola DuPont™AirGuard Smart
AirGuard Smart is used in both projects. Table 3.3 shows measured values of s_d for RH on two sides of the membrane (SINTEF certification, 2018). WUFI does not allow the material to be direction dependent, and therefore a simplified water vapour diffusion curve is used in the calculations. The values used are highlighted in table 3.3 and they are based on the average of RH on both sides of the SVB.

Table 3.3: s_d values for Isola DuPont™AirGuard Smart (SINTEF certification, 2018)

s_d [m]	μ [-]	RH side 1 [%]	RH side 2 [%]	RHaverage [%]
100	**100000**	0	**2**5	**13**
48	**48000**	33	50	**42**
14	14000	0	75	43
12	12000	11	76	43
8	**8000**	33	76	**54**
3	3000	25	75	50
1.4	**1400**	50	75	**63**
0.36	360	12	94	53
0.18	**180**	50	94	**72**
0.03	**30**	95	100	**98**

Air cavity

Air layers must be used with the thickness they are provided with by the WUFI database. When simulating non-ventilated air layers, convection is not included. WUFI has created a standard air layer material with varying thickness (Wufi, 2019[a]). Similar to the material of mineral wool, a standardised WUFI sorption curve is given for these.

Table 3.4: Material data

Material	Material in WUFI	Water vapour diffusion resistance factor [-]	Moisture storage function [kg/m³]
Wooden sheathing			
18mm plywood	Plywood high[1]	383-42 (20-70 % RH)	36.6-103.8-354 (49-90-100 % RH)
18mm OSB	Oriented Strand Board (density 595 kg/m2)[2] 165	61-95-814 (30-80-100 % RH)	
Beam			
Kerto S 48x300mm	Scandinavian spruce transverse direction II[3]	108-27 (30-70 % RH)	11.1-81.9 (10-97 % RH)
All wood 48x446mm	Scandinavian spruce transverse direction II[3]	108-27 (30-70 % RH)	11.1-81.9 (10-97 % RH)
Insulation			
Mineral wool	Mineral Wool[4]	1.3	0.07-0.16-7 (40-90-99 % RH)
Smart Vapour barrier			
AirGuard Smart	Isover Varo Xtra Safe[5]	10000-180-30 (13-72-100 % RH)	0
Internal Lining			
Gypsum board	Gypsum board[7]	8.3	4-11 (50-95% RH)
Wooden panels 14mm	Scandinavian spruce transverse direction II[3]	108-27 (30-70 % RH)	11.1-81.9 (10-97 % RH)

[1] North America Database
[2] Frainhofer-IBP - Holzkirchen, Germany
[3] SNTNU Norwegian University of Science and Technology - Trondheim, Norway
[4] Fraunhofer-IBP - Holzkirchen, Germany, changing density according to (Glava, 2018[b]) and the moisture storage is user defined as described in appendix A.2
[5] Fraunhofer-IBP - Holzkirchen, Germany, changing vapour diffusion resistance factor (SINTEF certification, 2018)
[6] Lund, Sweden

Table 3.5: Additional input data

Coefficients	Unit	Value	Marks
External			
Heat transfer coefficient	[W/m^{2}K]	25	Roof
s_d value	[m]	300	Bituminous felt with PVC
Short-wave radiation absorptivity	[-]	0.7	User defined
Long-wave radiation emissivity	[-]	0.9	Standard value
Adhering fraction of Rain	[-]	0	No absorption
Internal			
Heat transfer coefficient	[W/m^{2}K]	8	Indoor surface
s_d value	[m]	0	No coating

Table 3.6: Initial conditions

Materials used in WUFI	RH[%]	WC [kg/m^3]	T [℃]
Lund Vest			
Wooden sheathing	80	63	20
Solid-wood beam - top	43	63	20
Solid-wood beam - buttom	39	57	20
Mineral wool	70	0.1	20
Longyearbyen			
Wooden sheathing	45	34	20
Solid-wood beam - top	55	36	20
Solid-wood beam - buttom	55	36	20
Wooden panels	23	20.5	20
Mineral wool	70	0.1	20

Climate

In order to evaluate the material properties with WUFI, the internal and external climates should be similar to the real climates the construction has been exposed to. Therefore, a KLI file has been developed for each of the climates with real measurements from sensors located in the pilot projects. The sensors measuring the internal and external climates are S-2 and A-1 cables. However, the measurements of external climates are not suitable to use for the calculations in WUFI, because they do not consider the effect of radiation. Therefore, a correlation of the temperature 1cm below the wooden sheathing and the temperature at the surface is calculated with WUFI, using the climate file of Oslo in the WUFI database, and a climate file given by the simulation program, IDA Indoor Climate and Energy (IDA ICE), for Longyearbyen. The correlation and the corresponding function is given in appendix C. In the KLI file, the measured internal temperature and RH for specified rooms are used in addition to the calculated surface temperature. The calculated surface temperature is set to be the external temperature and no additional solar radiation is added.

3.2 Results

The results show the measurements in the period from where the buildings were ready for occupation, from 18th of December until the 24th of April. Appendix D.1 shows the moisture content during the building process measured in order to identify a dry building process. Notice that the supplier of the measuring devices has set the lower limit for moisture content equal to 9.4 weight% for Norwegian spruce. Therefore, moisture contents below this point are reported as 9.4 weight%.

3.2.1 Lund Vest

Figure 3.8 shows the moisture content in the points 1-6 measured 1cm beneath the wooden sheathing and 1cm above the SVB, while the figures 3.9 and 3.10 present the measured RH and temperature at the same points. Notice that the internal climate is measured in the storage room, 1.2cm above the floor, and in the bathroom, in an air cavity above the internal lining. Therefore, the WUFI calculations presented in figures 3.12 and 3.13 are based on the measured internal climate in the storage room as shown in figure 3.11a.

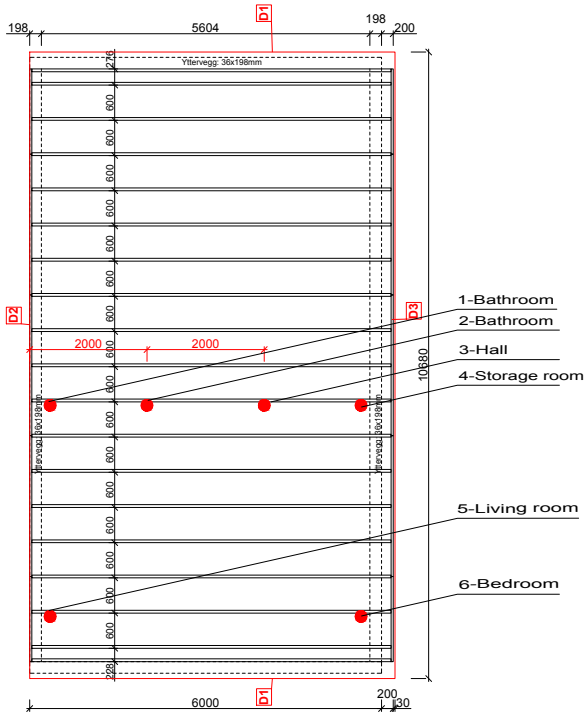

(a) Roof plan

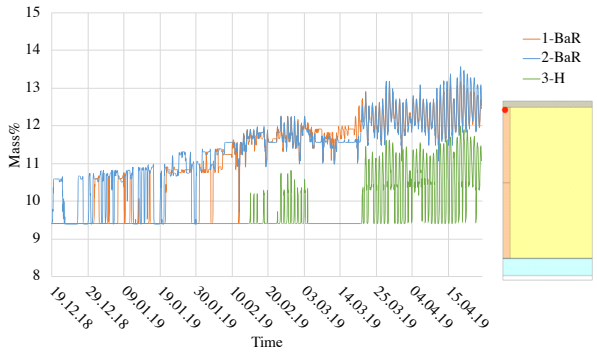

(b) Sensors 1-3, 1cm beneath the wooden sheathing

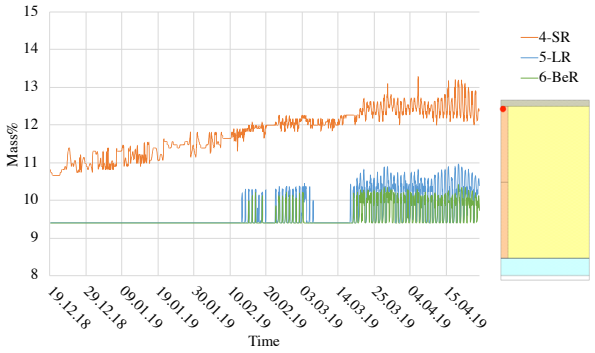

(c) Sensors 4-6, 1cm beneath the wooden sheathing

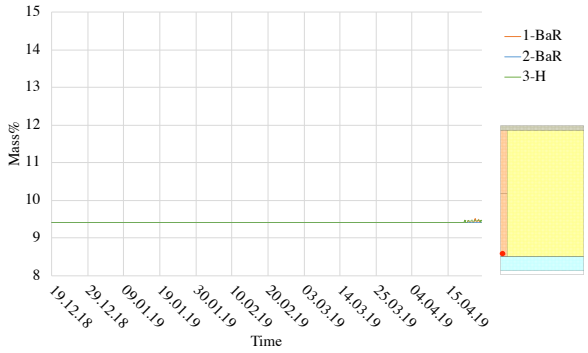

(d) Sensors 1-3, 1cm Above the SVB

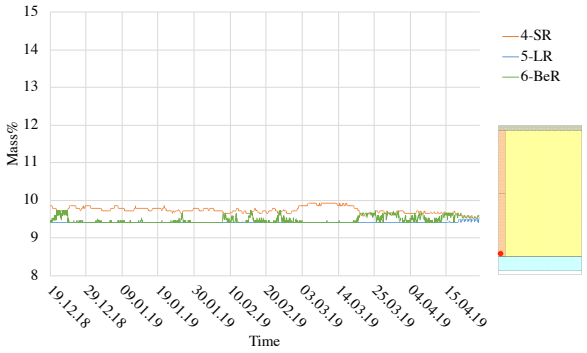

(e) Sensors 4-6, 1cm above the SVB

Figure 3.8: Moisture content measured by sensors 1-6 in the project in Lund Vest

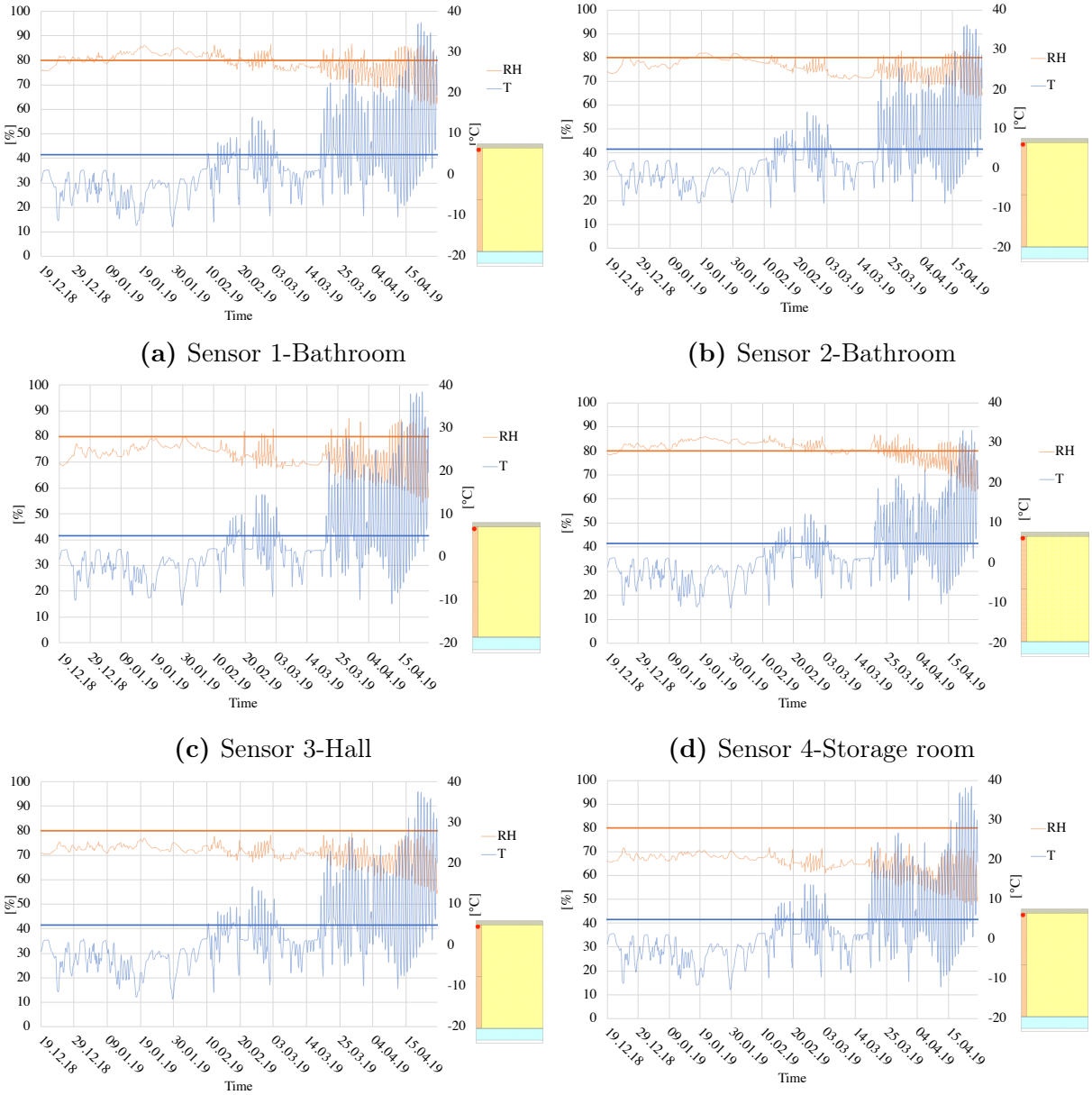

(a) Sensor 1-Bathroom

(b) Sensor 2-Bathroom

(c) Sensor 3-Hall

(d) Sensor 4-Storage room

(e) Sensor 5-Living room

(f) Sensor 6-Bedroom

Figure 3.9: RH-T for each sensor in the project in Lund Vest, measured 1cm beneath the wooden sheathing

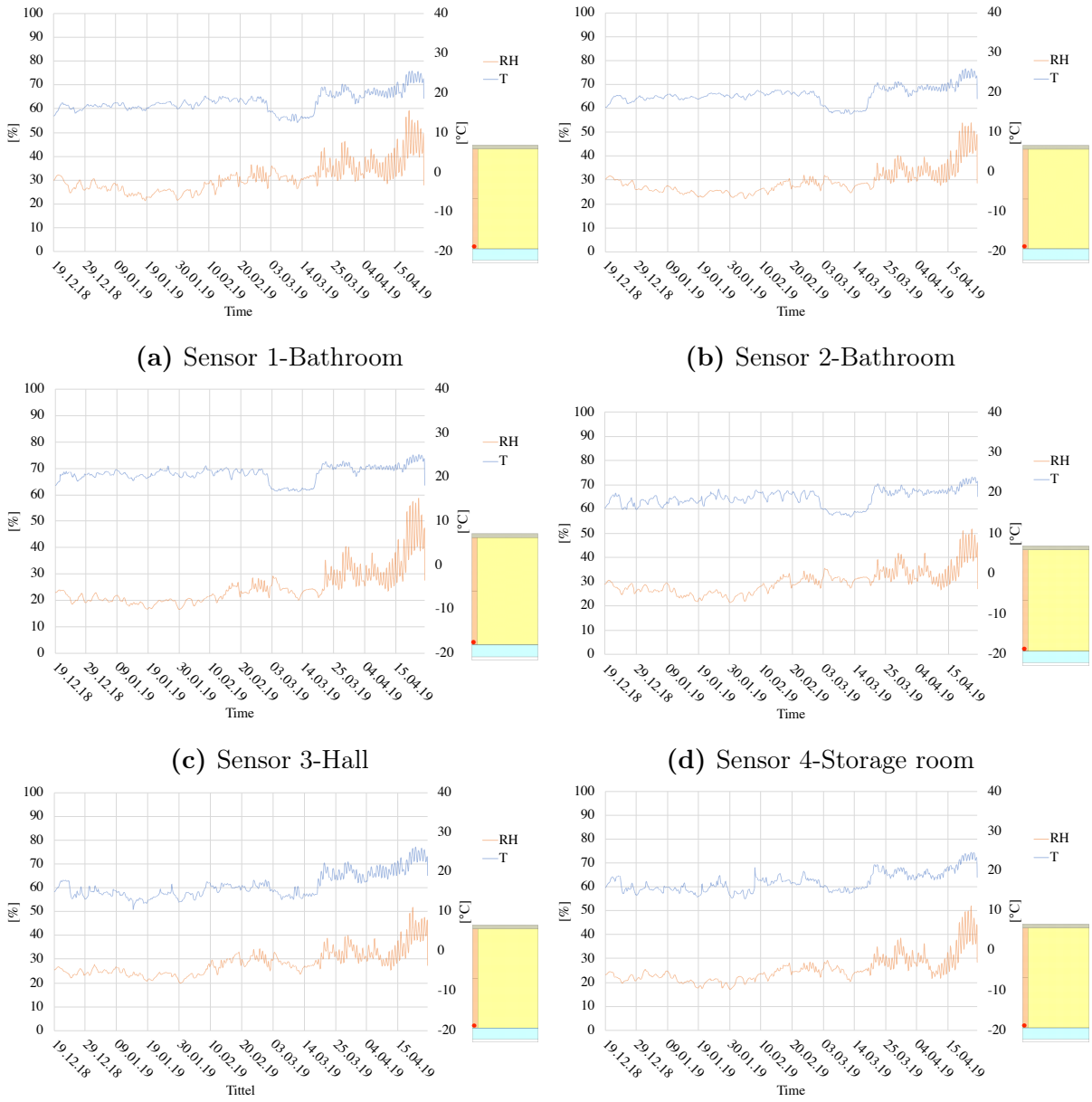

(a) Sensor 1-Bathroom

(b) Sensor 2-Bathroom

(c) Sensor 3-Hall

(d) Sensor 4-Storage room

(e) Sensor 5-Living room

(f) Sensor 6-Bedroom

Figure 3.10: RH-T for each sensor in the project in Lund Vest, measured 1cm above the SVB

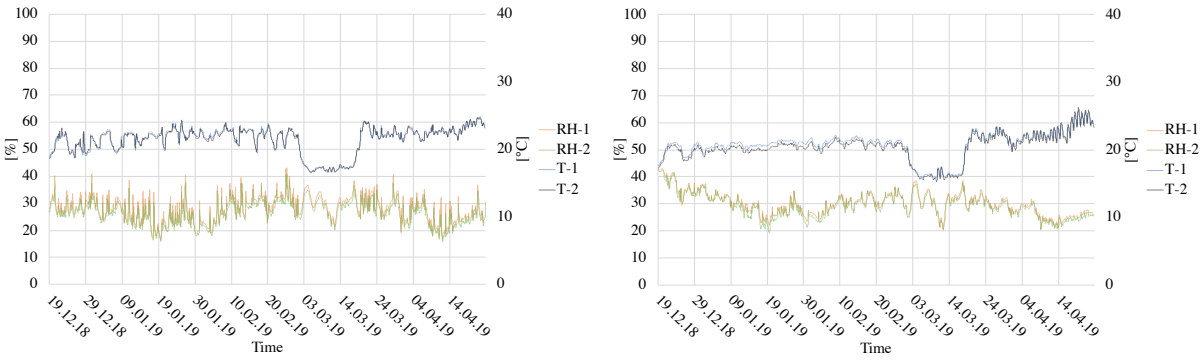

(a) Storage room **(b)** Bathroom

Figure 3.11: Internal climate

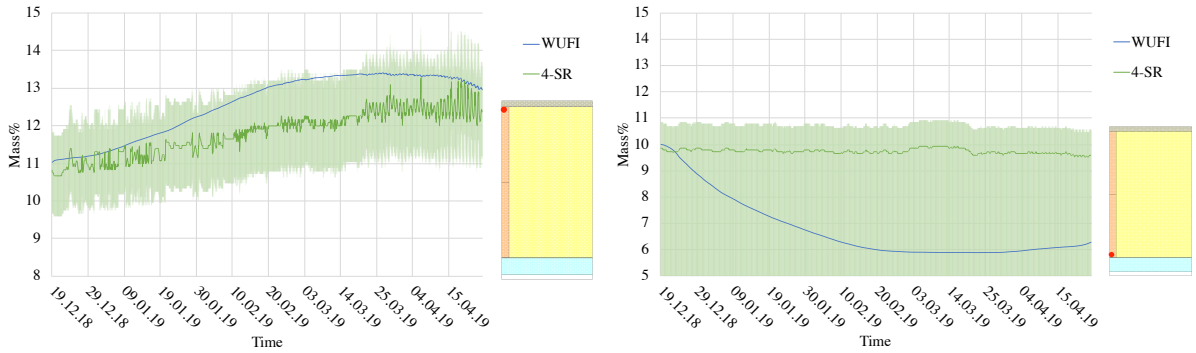

(a) 1cm beneath the wooden sheathing **(b)** 1cm above the SVB

Figure 3.12: WUFI calculation and real measurements for sensor 4 (storage room) including uncertainties calculated by the standard

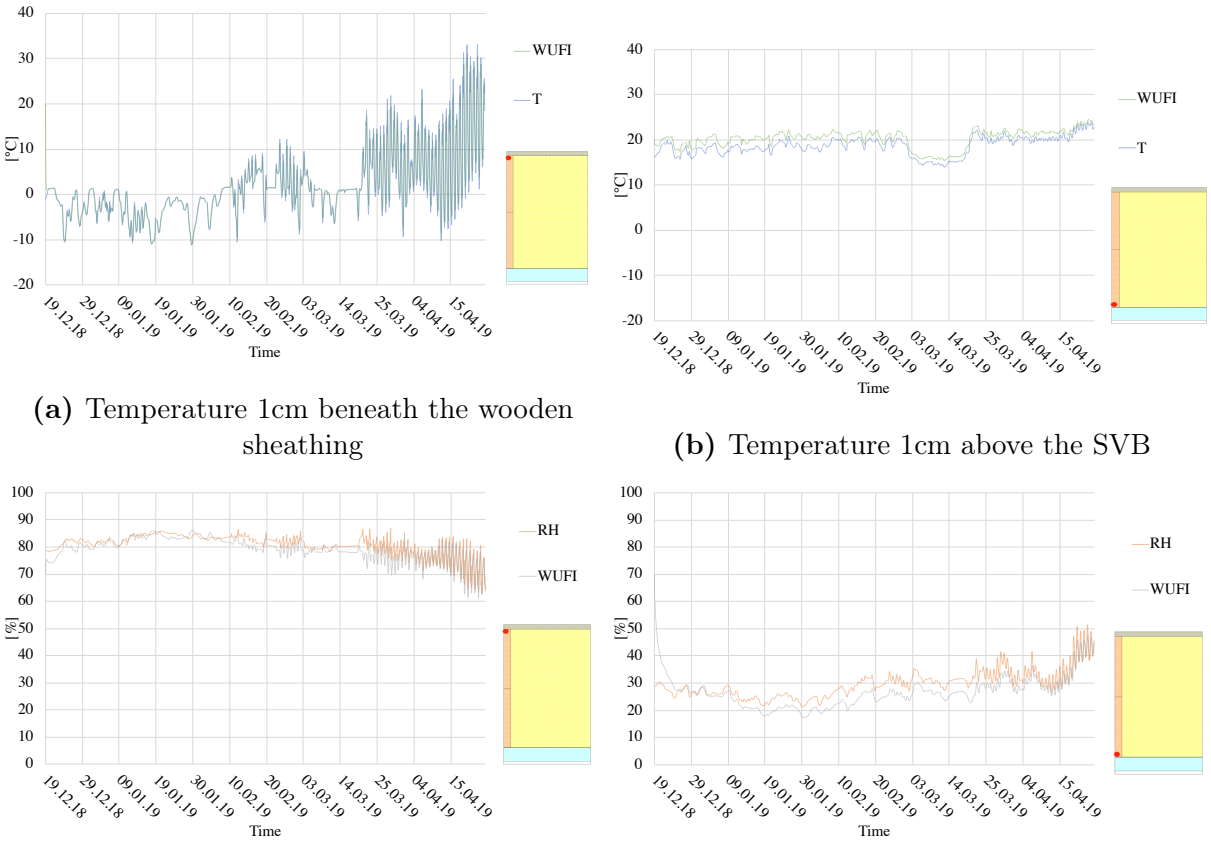

(a) Temperature 1cm beneath the wooden sheathing

(b) Temperature 1cm above the SVB

(c) RH 1cm beneath the wooden sheathing

(d) RH 1cm above the SVB

Figure 3.13: WUFI calculation and real measurements for sensor 4 (storage room)

3.2.2 Longyearbyen-A33/34

Figure 3.17 shows the moisture content in the points 1-6 measured 1cm beneath the wooden sheathing and 1cm above the SVB, while figure 3.15 and 3.16 present the measured RH and temperature at the same points in building A33/34. These measurements are similar with the measurements of the house A35/36 that are presented in Appendix D.1.1 Notice that the internal climate is measured in the bedroom closet, and in the bathroom in the air cavity above the internal lining. Therefore, the WUFI calculations presented in figures 3.17 and 3.18 are based on the measured internal climate in the bedroom as shown in figure 3.19a.

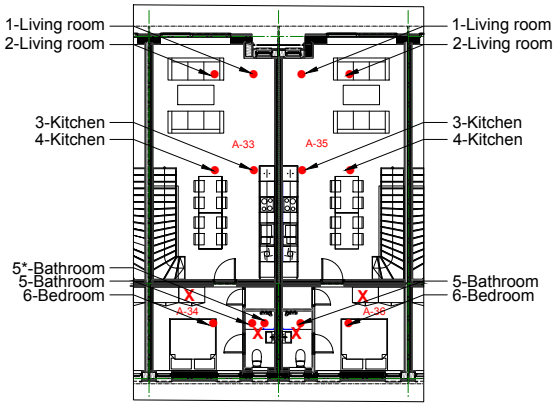

(a) Floor plan

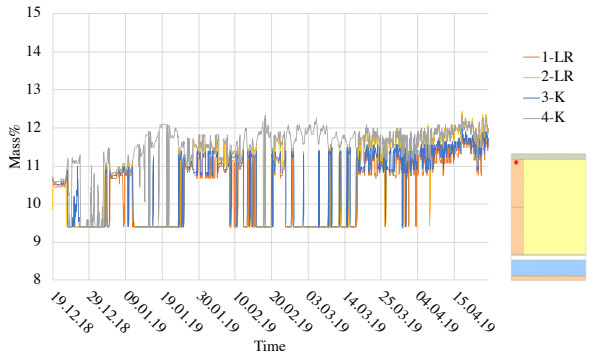

(b) Sensors 1-4 (A33), 1cm beneath the wooden sheathing

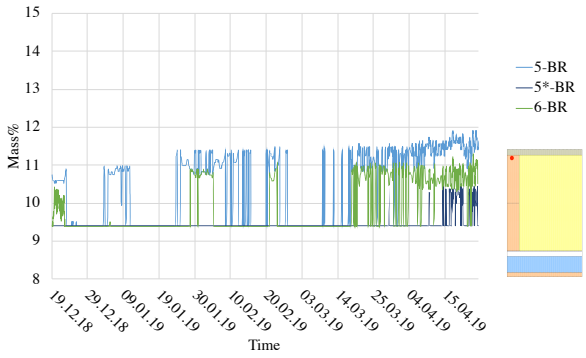

(c) Sensors 5-6 (A34), 1cm beneath the wooden sheathing

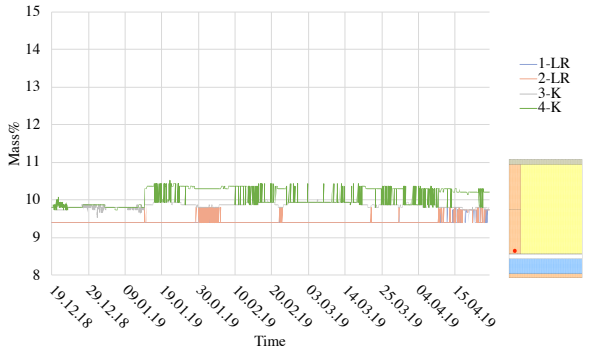

(d) Sensors 1-4 (A33), 1cm above the SVB

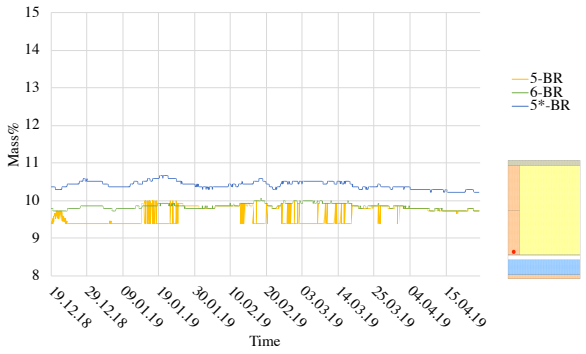

(e) Sensors 5-6 (A34), 1cm above the SVB

Figure 3.14: Moisture content measured by sensors 1-6 in the project in Longyearbyen house A33/34

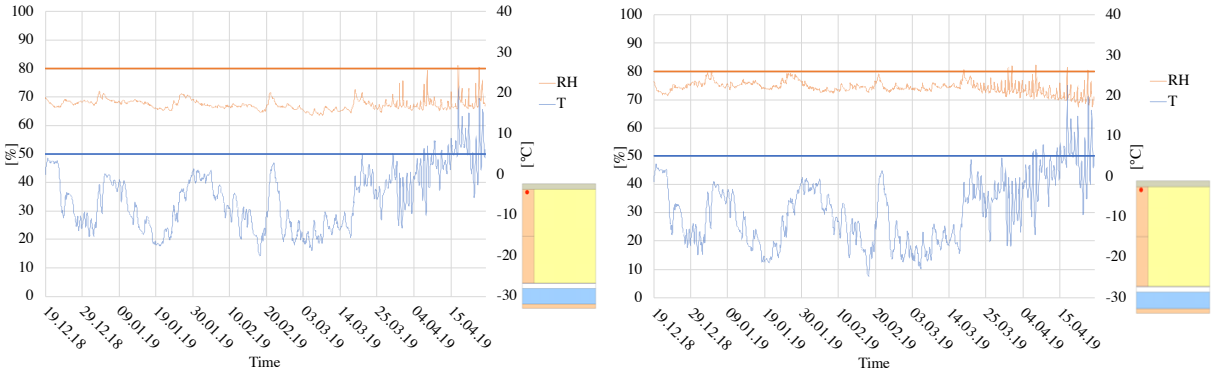

(a) Sensor 1-Living room

(b) Sensor 2-Living room

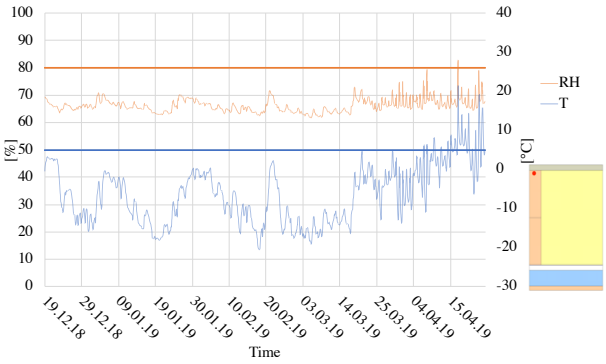

(c) Sensor 3-Kitchen

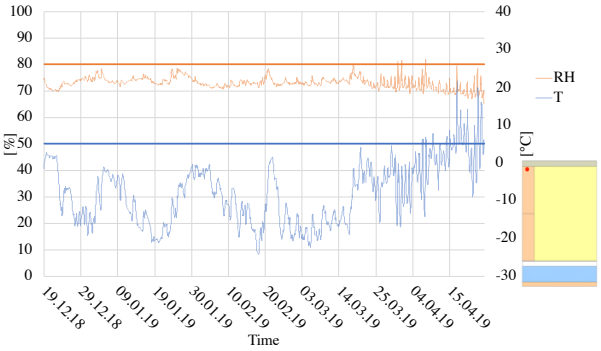

(d) Sensor 4-Kitchen

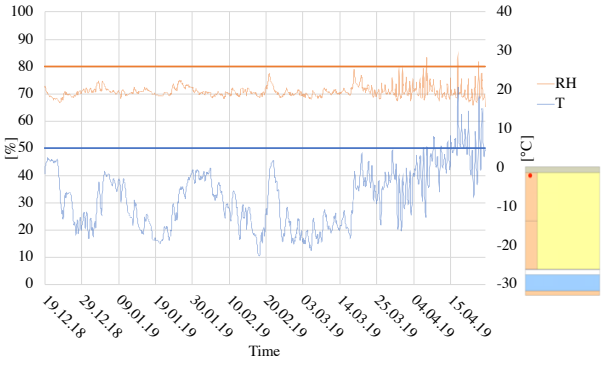

(e) Sensor 5-Bathroom

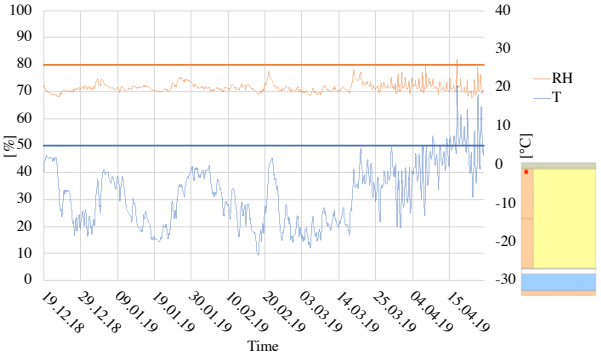

(f) Sensor 5*-Bathroom

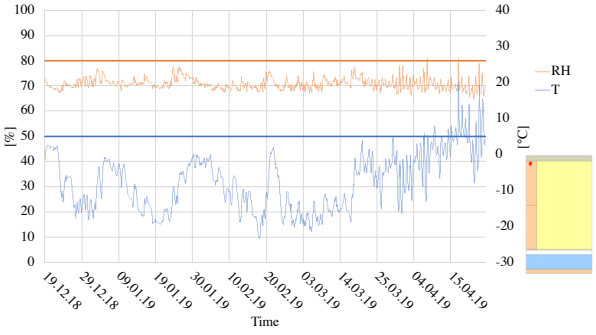

(g) Sensor 6-Bedroom

Figure 3.15: RH-T for each sensor in the project in Longyearbyen A33/34, measured 1cm beneath the wooden sheathing

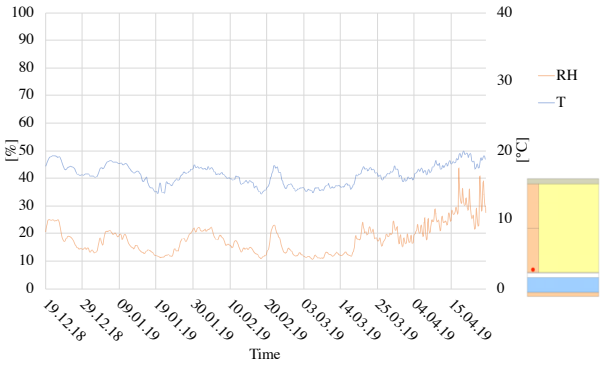

(a) Sensor 1-Living room

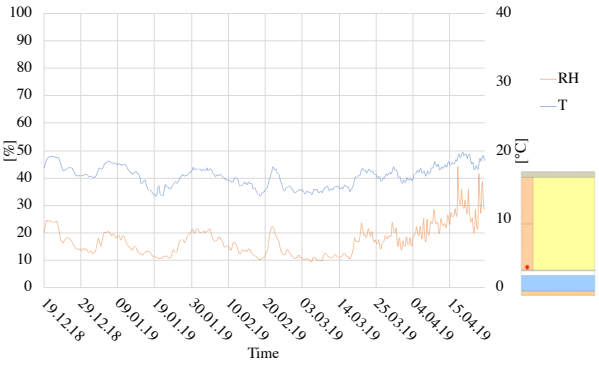

(b) Sensor 2-Living room

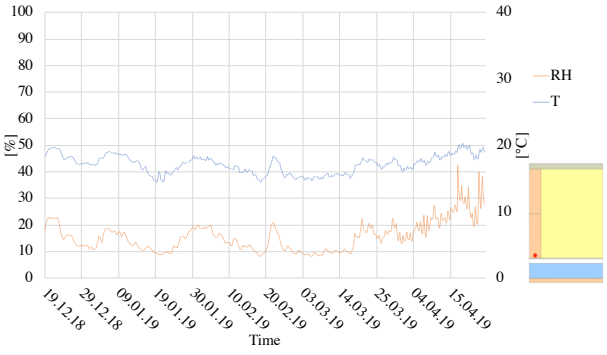

(c) Sensor 3-Kitchen

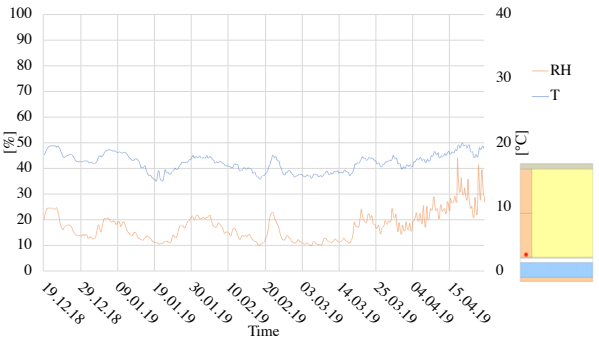

(d) Sensor 4-Kitchen

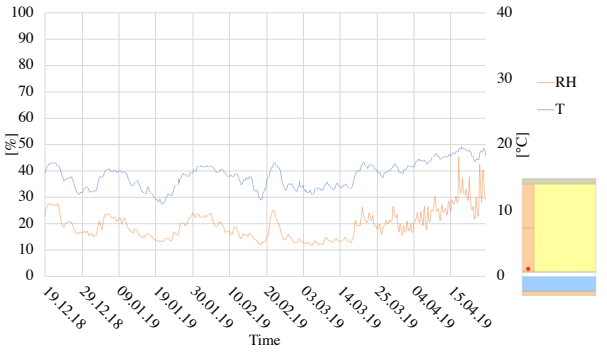

(e) Sensor 5-Bathroom

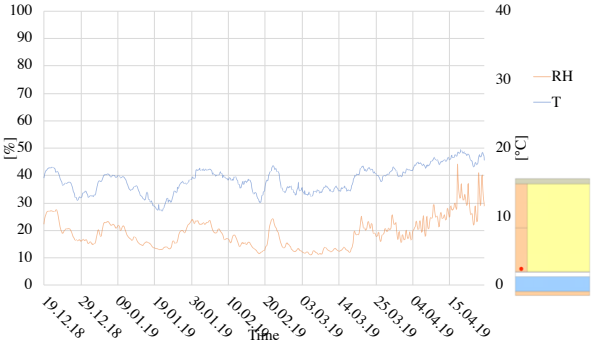

(f) Sensor 5*-Bathroom

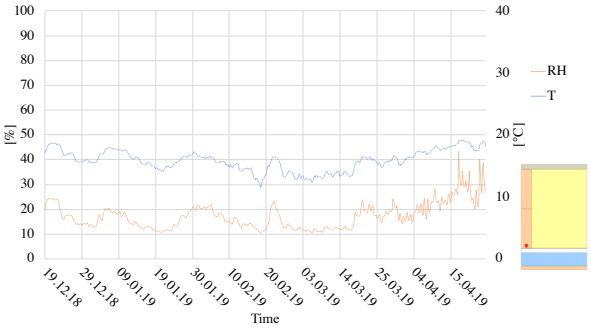

(g) Sensor 6-Bedroom

Figure 3.16: RH-T for each sensor in the project in Longyearbyen A33/34, measured 1cm above the SVB

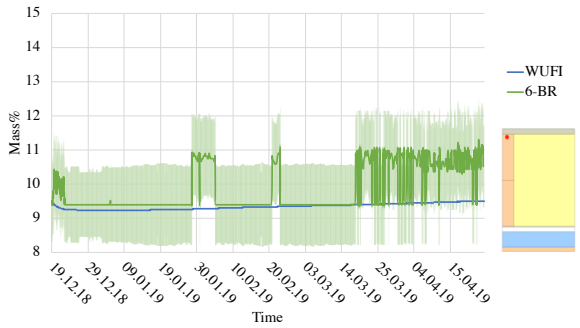

(a) 1cm beneath the wooden sheathing

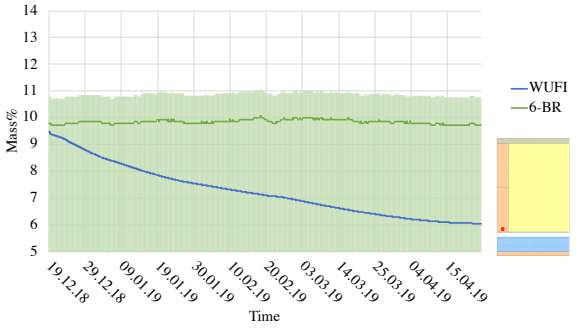

(b) 1cm above the SVB

Figure 3.17: WUFI calculation and real measurements for sensor 6 (bedroom) including uncertainties calculated by the standard

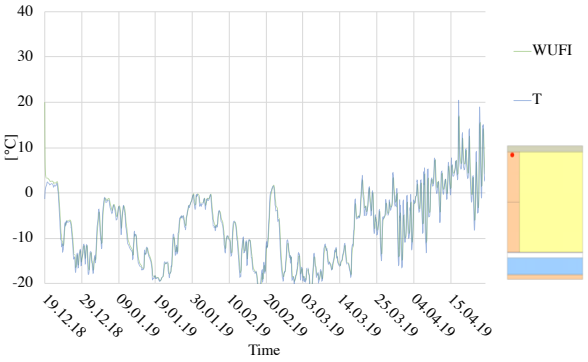

(a) Temperature 1cm beneath the wooden sheathing

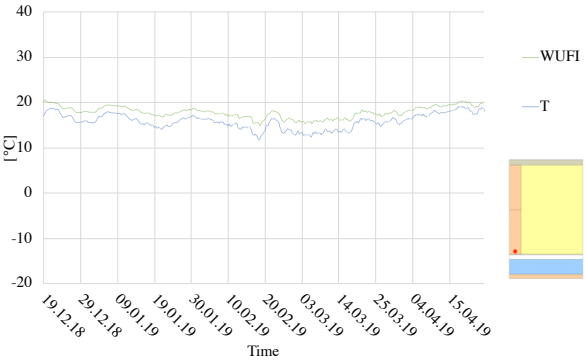

(b) Temperature 1cm above the SVB

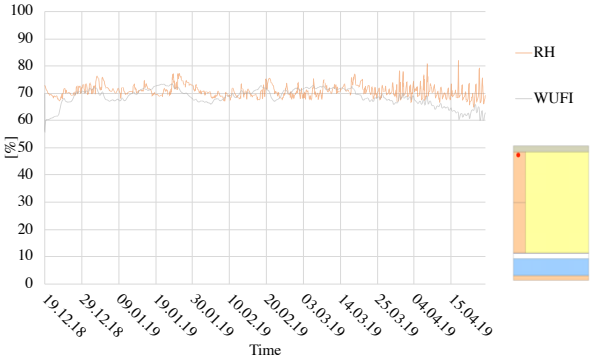

(c) RH 1cm beneath the wooden sheathing

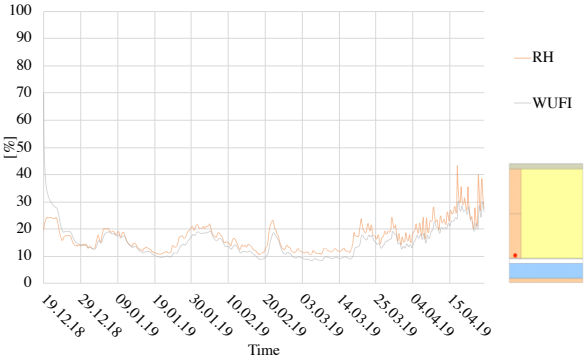

(d) RH 1cm above the SVB

Figure 3.18: WUFI calculation and real measurements for sensor 6 (bedroom)

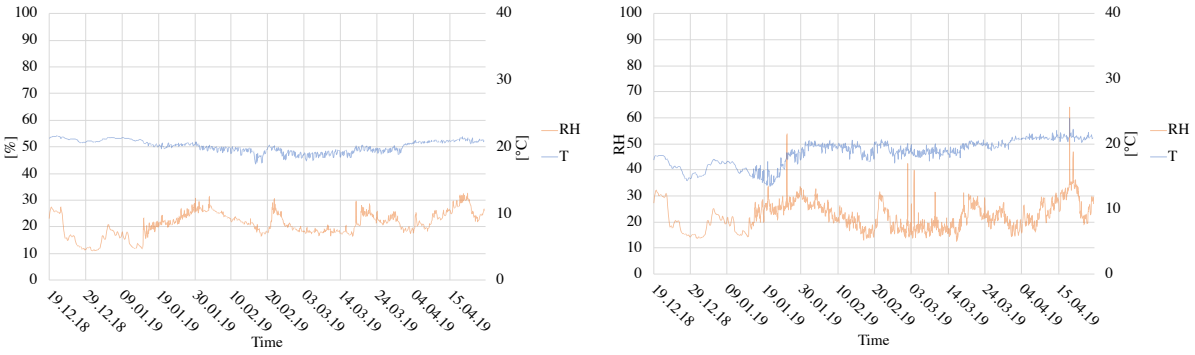

(a) Bedroom **(b)** Bathroom

Figure 3.19: Internal climate - A33/34

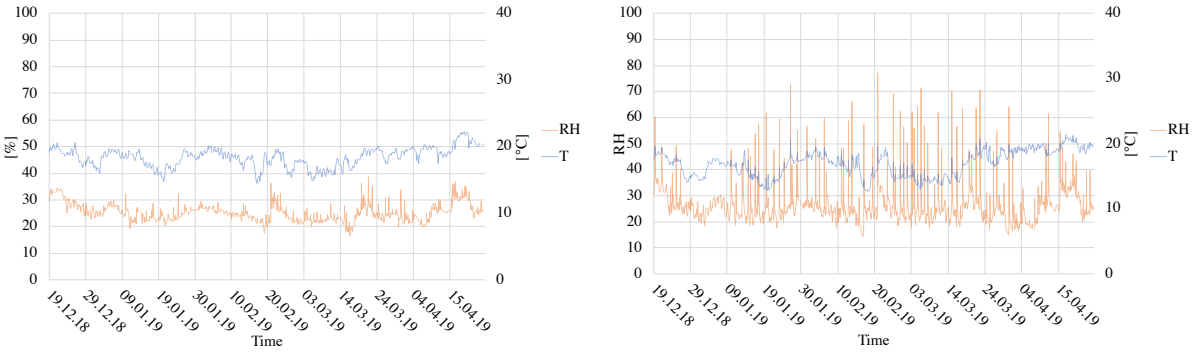

(a) Bedroom **(b)** Bathroom

Figure 3.20: Internal climate - A35/36

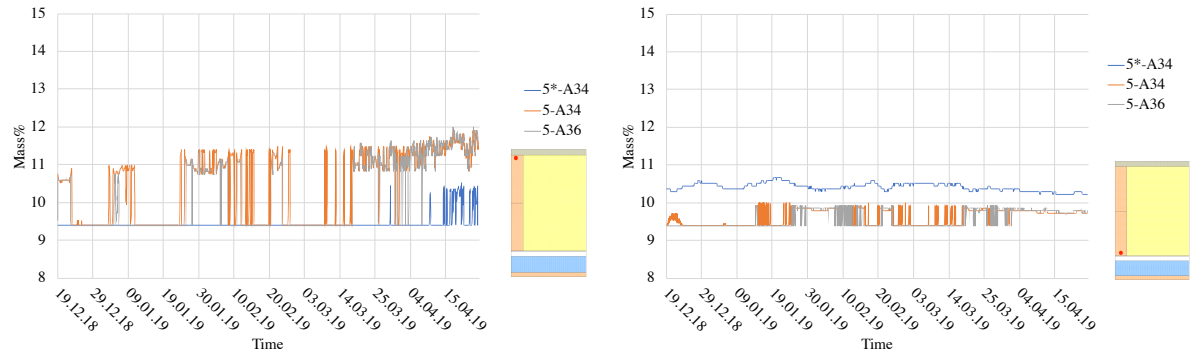

(a) 1cm beneath the wooden sheathing **(b)** 1cm above the SVB

Figure 3.21: Moisture content in the roof above the bathroom with (A33/34) and without (A35/36) the PE-foil

3.2.3 Uncertainties

Lack of measurement data

There are lacks of results showing the moisture history of the construction during the

building process. It seems like the connection of some sensors and the gate-way was blocked for some periods. This is why the results are divided into two periods; before and after the building was ready for occupation. The former is used to verify a dry building process, while the latter is used to study the drying potential of the construction.

Calculation of the external climate
The correlation is simplified and assumed to be linear, but in reality, it depends on the cloud index and solar radiation. This correlation is complex and not easy to model. Figure C.1 in appendix C, shows the correlation of the temperature at the surface of, and the temperature 1cm below, the wooden sheathing. It is clear that the amount of solar radiation is affecting the difference of the two points. Figure C.2 shows that when there is high solar radiation, the temperature of the surface increases beyond the temperature at the point 1cm below the wooden sheathing, even though the external temperature is low. The simplified model shows the mean value of the surface temperature for the corresponding temperature 1 cm below the wooden sheathing. Hence, the effect of solar radiation is reduced. This can affect the results from the WUFI calculations in a way in which the moisture content curve will have reduced daily fluctuations.

Measurement uncertainty
The electric resistance is also dependent on glue and salts in the material which needs to be considered for materials such as laminated beams (SINTEF byggforsk, 2015). In the pilot project located in Svalbard, laminated beams are used. Aiming to avoid uncertainties due to multiple glue layers, an extra solid-wood beam is placed next to the original laminated beam where the sensors are installed. The glue in a laminated beam can impact the moisture content in various ways, but there are few studies that are investigating this effect. However, it is assumed in this study that the moisture content in the laminated beams is more or less equal to the moisture content in a solid wood beam.

Extracting data: WUFI versus measurement data
When extracting data from WUFI, the area selected can differ from the area measured in the pilot projects. Because of different temperatures through the construction, the results will deviate. The dimensions of the box can also disturb the temperature and RH in the chosen area because it replaces the insulation in the point where the sensors are installed. In the WUFI calculation, the box is not considered which can result in different values of RH and temperatures, depending on if the area chosen is matching.

Material properties in WUFI
The material properties in WUFI are mostly already defined by various institutions and are based on studies. The SVB, however, has user-defined values for diffusion resistance. The material used in the pilot projects is direction dependent. The simplification of the diffusion resistance in WUFI can make the result differ in which the SVB allows more moisture to diffuse into the construction. As seen in table 3.3, the sd values for average RH 42 % and 43% are 48 and 14 respectively. The former has RH 33% on the dry side and 50% on the wet side, while the latter has RH 0% on the dry side and 75% on the

wet side. This means that in the latter scenario, the SVB is more vapour permeable than the former. The values chosen in this study are based on a winter scenario. The internal climate is quite dry and the external temperature is low which causes an upward vapour pressure gradient, as discussed in chapter 1.2.3. Therefore, the risk of vapour diffusion into the construction is high. For summer scenarios, the diffusion resistance should be updated accordingly.

3.3 Discussion

Figure D.1 in appendix D.1 shows that the building process has been in dry conditions. An overall impression of the results is that the moisture content is well below the critical value. This is a result of low initial moisture content. As shown in the parameter analysis, the initial moisture content is important in regard to robustness. According to the parameter analysis, the moisture content in the beam will increase to an average of around 12 weight%. However, the internal moisture load in the field measurements are lower than in the parameter analysis. This can lead to a lower moisture content equilibrium state of the wooden elements in the roof. The risk of mould is minimal where there are small periods for mould to develop in the construction located in Lund Vest. The conditions are not, however, stable enough for mould to have time to develop.

Notice that the RH for the sensors located near the wooden sheathing is between 60 and 80 %. This corresponds to a moisture content between 10-15 weight% as described in figure 1.2 in chapter 1.2.2. The results of the field measurements show a moisture content between 9-13 weight%. The uncertainty range for moisture content is around ±0.9-1.3, and for RH is ±%2. Hence, the measurements seem to report lower values of moisture content than the theory suggests if the wooden elements have reached equilibrium with the surroundings.

The sensors located near the SVB reports around 10-40% RH which corresponds to moisture contents between 2-8 weight% according to the theory. This is why the measurements of the moisture content of these sensors can be assumed non reliable. Measurements of moisture content below 8 weight% have high uncertainties, and should therefore not be considered in this analysis.

Lund Vest

Figure 3.8 shows that the moisture content is increasing near the wooden sheathing. This is probably because of moisture distribution in the beam, where the moisture is moving towards the wooden sheathing due to an upward vapour pressure gradient, as described in chapter 1.2.3. Sensors located near the SVB report low moisture content, where all are around the limit, 9-10 mass%. The sensors situated in the roof above the storage room and the bathroom near the wooden sheathing report higher moisture content compared to the other sensors. These sensors are also the ones having the highest values of RH,

which is a result of higher moisture content in addition to lower temperatures. However, the measured temperature of sensor 4, located above the storage room near the wooden sheathing, is lower compared to the others. This can be a result of less solar exposure, maybe because the lower roof can be partially shaded by the neighbouring house.

Figures 3.9 and 3.10 show that the risk of mould is minimal. The possible period for mould growth is from the end of March to the beginning of April including a small period in the end of February, for sensors 1 and 4. However, the period is probably not long enough for mould to develop. The figures show that RH decrease when the temperature rises. Hence, it can be assumed that the temperature increase towards the summer and therefore reduces the RH below the critical value. Figure 3.10 also shows that the RH increases at the point near the SVB in April. The reason for this is probably that the vapour pressure gradient is changing direction due to the higher surface temperature of the roof, and that the moisture is moving towards the internal air.

The storage room has a more turbulent internal climate than the bathroom, as shown in figure 3.11. This is probably because the sensor measuring the internal climate in the bathroom is located in an air cavity above the ceiling. The ceiling works as a buffer and therefore reduces the fluctuation of RH and temperature. Notice that the temperature decreases from 20℃ to 15℃ in the beginning of March. A probable explanation of this behaviour can be that the occupants of the house went away for two weeks. Furthermore, the building seems to be well ventilated because the RH is between 20% and 40%. This is especially important in rooms with high moisture load, such as bathrooms.

Based on the parameter analysis, the location of the construction is favourable. The parameter analysis shows that Oslo is one of the most favourable locations in case of drying potential of a roof with SVB. The solar altitude is 52° at the highest in summer and combined with a 10° inclination towards the south, the drying potential will increase due to higher solar exposure. The roof has 450mm insulation thickness which can reduce the drying potential according to the parameter analysis. However, this effect is probably insignificant due to the low initial moisture content, the favourable location and the inclination towards the south.

Longyearbyen

As shown in figure 3.14, the distribution of moisture content in the construction is more uniform than for the construction in Lund Vest. It is possible to identify small differences, where there are higher moisture contents in the middle of the roof. A possible reason for this is that the areas close to the outer walls have possibilities to distribute the moisture towards the perimeter of the building. The moisture content near the wooden sheathing is increasing at a low rate, which indicates a moisture distribution directed upwards. The moisture content measured matches the theoretical moisture content given by the RH, between 12 and 13 weight%. The leaps down to 9.4 weight% can be due to disruption on the signal, or that something within the material disturbs the electric resistance and decrease the conductance.

RH is mostly below the critical value, which means that the risk of mould is limited because, when the temperature rises, RH will decrease, as shown in figures 3.15, 3.16. The houses seems to be well ventilated except for the bathroom where the internal RH fluctuate from around 20% to 70%, as shown in figures 3.19 and 3.20. However, the sensors located in the bathrooms near the SVB seems not to be affected by this. The internal climate sensors are located in the air cavity of the ceiling, and therefore the wooden panels in the ceiling should work as a buffer. However, it seems that the perforation of the wooden panels due to downlights, allows the moist air to reach into the air cavity. Hence, the gypsum board in combination with the PE-foil or SVB works well even for rooms with periodically high internal moisture load.

Figure 3.21 compares the moisture content of the beam above the bathroom with PE-foil and SVB. The figure shows that the difference in measured moisture content is insignificant. Hence, the SVB can be assumed to work well for the bathrooms. However, it can be possible to notice a difference of 1-2 weight% in the measured moisture content of the roof above the bathroom in the module A34 with PE-foil. These sensors are located close to each other in the same beam. The difference can be a result of the uncertainties of the measurements or bad moisture distribution due to the laminated beams.

For the constructions in Longyearbyen, it is important to consider that the sun is on its highest 32° over the horizon, and the highest altitude of the sun during the analysis period is 24° the 24th of April. Based on the parameter analysis, constructions at higher latitudes have less drying potential due to less direct solar radiation. The temperature is increasing in the end of March in the measuring points near the wooden sheathing. This is probably a result of increasing external temperatures and increasing altitude of the sun. Moreover, RH is not decreasing significantly at the same point. However, it can be assumed that the temperature will rise even further towards the summer, which can result in a shift in the vapour pressure gradient. In addition, RH is increasing in April at the points near the SVB, which can indicate that the moisture is travelling downward. Another reason for an increasing RH in April near the SVB can also be that the SVB is open to vapour diffusion. This is, however, not probable because the internal RH is around 30%, which should not be high enough for the SVB to be vapour permeable.

Notice that the internal temperature and RH start fluctuation around the middle of January for the house A33/34, as shown in figure 3.19. A probable explanation of this behaviour can be that the building was inhabited at this time. However, this is not as distinct for the house A35/36, where the internal fluctuations are high from the beginning of the analysis period. Hence, the house might be occupied from the start.

In the parameter analysis, thin roofs resulted in higher drying potential. The roof of the construction located in Longyearbyen has 300mm insulation thickness. However, in order to increase the drying potential, it requires solar radiation. This can be improved with a higher slope towards south. In addition, the parameter analysis shows that the external temperature is a driving factor for mould development. Cold climates seem to have a

lower risk of mould because the temperature are not reaching above the critical limit for a long period. Hence, the roof construction in Longyearbyen will probably not be at risk of mould.

WUFI results

As shown in figures 3.12, 3.13, 3.17 and 3.18 the WUFI results are more or less similar to the measured values for both the pilot projects. The moisture storage curve for the sensor located near the wooden sheathing is within the uncertainty range and therefore can be assumed to be adequate. Furthermore, the figure showing the point near the SVB decreases greatly below the measurements for both the projects. However, these measurements should not be considered due to high uncertainties as described above.

As shown in figures 3.13 and 3.18, the difference in RH and temperature from the calculation and the measurements are marginal. Therefore, it can be assumed that the climate files that are calculated, resembles the real climate the construction has been exposed to. It is important to notice that the SVB is modelled with s_d values for the average RH on both sides. In reality, the s_d value depends on the direction of the vapour pressure gradient. In addition, the values used are based on that the vapour pressure gradient is upward. This means that for the summer scenarios, it is important to reconsider these values accordingly.

Chapter 4: Conclusion

The purpose of this study was to identify the robustness of a compact timber-framed roof with SVB and parameters that can increase the drying potential. Various parameters have been investigated with WUFI 2D, and two pilot projects have been analysed.

Parameter affecting the drying potential

The results of the parameter analysis indicate that the external climate and solar exposure are driving factors for the drying potential. In Norway, Oslo has the highest drying potential. Internal moisture load is essential due to lower accumulation of moisture in the roof construction during the winter season. Other parameters such as low insulation height, low diffusion resistance of the internal lining the and an SVB with high range of diffusion resistance are recommended to consider in order to increase the drying potential even further.

Risk of mould

Parameter analysis

The risk of mould in the reference construction located in Trondheim is high, but the risk can decrease by improving parameters as described above. External temperature and cloud index are also identified to impact the risk of mould. In locations with high latitudes, even though the drying potential is low, the risk of mould is not increasing due to low external temperatures and short summers. However, it is based on a simplified assumption on that mould develop if the conditions are stable above the critical limit, RH>80% and T>5℃, over a longer period of time.

Pilot projects

The upper beam of the construction in Lund Vest has small periods where the temperature and RH are fluctuating around the critical value. However, the period is not long enough for mould to develop. Despite the cold climate, the construction in Longyearbyen has RH below the critical value throughout the whole analysis period and therefore has no risk of mould development.

Robustness of the pilot projects

The project in Lund Vest is located near Oslo, which is the most favourable location based on the parameter analysis. In addition, the project has an inclined roof towards the south and drying possibilities through the perimeter which increase the drying potential. Longyearbyen has RH below the critical limit throughout the analysing period which indicates no moisture accumulation in the construction. Additionally, the project has low insulation thickness, which increases the drying potential based on the parameter analysis. However, the construction is at high latitudes and it is uncertain how it responds to the climate over time. The sun has a low altitude of 32° and the roof has little inclination.

Therefore, the solar radiation might not be high enough to increase the roof surface temperature sufficiently to create a drying potential in summer.

The moisture content in the timber structure in both pilot projects is well below the critical limit. Additionally, the internal climate for both pilot project indicates good ventilation. The parameter analysis shows that a roofs robustness increases if the wooden elements have low initial moisture contents. Therefore, the pilot projects seem to be well constructed and robust regarding moisture accumulation and mould development.

Verification of the material data in WUFI
WUFI calculations match the measurements well for RH, temperature and the moisture content in the upper beam. This shows that the material data and the procedure to calculate the external climate file are adequate.

4.1 Further work

Parameter analysis
The parameter analysis has been simulated with conservative values. There is a risk of mould in almost all scenarios. Therefore, other parameters should be investigated in order to avoid mould problems. Inclination towards south can increase the drying potential, and an optimal inclination depending on the altitude of the sun could be of interest in order to achieve a higher drying potential. Additionally, the risk of mould-analysis in this study is a simplified method where it has been assumed that mould development happens if the conditions are above the critical limit. WufiBio, a tool that calculates the risk of mould for the given conditions, can be used in order to identify the extent of mould growth.

Based on the results, the wooden elements seem to seek an equilibrium state with the surroundings with the given conditions. However, these conditions vary depending on the construction, material properties and climate. Therefore, an analysis aiming to find the equilibrium state of the wooden elements within different climates can be included in a parameter analysis. In addition, the results show that the risk of mould depends highly on temperature. Due to numerical issues, cold climates was excluded from the parameter analysis. Therefore, this should be further investigated in order to understand the coherence of temperature, solar radiation and cloud index. Furthermore, a roof assembly exposed to accumulation of snow on top could be of interest in order to identify how a roof assembly with SVB responds to Nordic winters.

Different materials can affect the drying potential in different ways. Various timber materials have different sorption curves. This can be of interest in order to understand the importance of the materials chosen. In addition, wooden panels as ceilings can work as a buffer which should be further investigated.

Field measurements

The results collected are over one winter and in order to see trends or any risks, the construction should be analysed over a longer period of time. Furthermore, the parameter analysis shows that the drying period starts in April/May. In the field study, the analysis period stops at the 24th of April. Therefore, in order to identify a drying potential of the roof assembly, the constructions should be analysed at least over one year.

The initial moisture content of the roof assembly was identified to be well below the critical value and the construction might already be in equilibrium. With a roof assembly with higher initial moisture content, the use of an SVB will be more effective. Therefore, it can be of interest to investigate how a roof assembly with SVB and moisture contents near the critical value will behave, despite the risk of mould growth.

In the project located in Svalbard, the beams used were laminated. The glue can disturb the measurements and it was therefore added a solid-wood beam where the sensors was installed. Measurements from one bathroom shows different moisture content. This can be a result of the laminated beams. Therefore, it can be of interest to investigate the effect of the laminated beams and how it distributes moisture.

Bibliography

Bergheim, E, Geving, S, and Time, B (1998). *Hygroscopic Moisture Transport in Wood*. Byggforsk, Norwegian Building Research Institute.

Bludau, C. and Künzel, H. M. (2009). "Flat Roofs in Cold Climates - CLimatic Limits for Building Flat Roods with a Permeable Vapour Retarder". In: *Proceedings of the 6th International Conference on Cold Climate HVAC*. Sisimut, Greenland.

Bludau, C., Schmidt, T., and Künzel, H. M. (2010). "Hygrothermal effects in lightweight roofs shaded by PV-elements". In: *Proceedings of Thermophysics 2010*. Valtice, Czech Republic, pp. 56–62.

Crosson, N. (2008). *Green building press: Airtightness and the 'Intelligent' membrane*. Green Building Magazine. Volume 18, no3.

Direktoratet for byggkvalitet (2014). *Byggteknisk forskrift (TEK17)*. URL: `https://dibk.no/byggereglene/byggteknisk-forskrift-tek17/` (visited on 11/14/2018).

Finesterra - OmniSense S-16 sensor (2019). URL: `https://www.finisterra.no/produkter/fukt/omnisense-s-2-sensor/` (visited on 03/17/2019).

Flyen, C. et al. (2010). *Klima- og sårbarhetsanalyse for bygninger i Norge: Utredning som grunnlag for NOU om klimatilpassing*. SINTEF Byggforsk.

Frey, N. and Geving, S. (2018). *EPD-sd values for AirGuard Smart*. Email correspondence.

Geving, S, Holme, J., and Jenssen, J.A. (2008). "Indoor air humidity in Norwegian houses". In: *Proceedings of the 8th Nordic Symposium on Building Physics*. Copenhagen, Denmark.

Geving, S., Stellander, M., and Uvsløkk, S. (2013). "Smart vapour barriers in compact wood frame roofs". In: *Thermal Performance of the Exterior Envelopes of Whole Buildings - 12th International Conference*. Florida, pp. 1–15.

Geving, S, Thorsrud, E, and Uvsøkk, S. (2013). "Smart vapour barriers in unventilated wooden roofs in a Nordic climate – laboratory study of drying effect under shaded conditions". In: *Proceedings of the 2nd Central European symposium on building physics, Contributions to building physics.* Wien, Austria, pp. 327–334.

— (2014). "The performance of unventilated wooden roofs with smart vapour barriers during winter conditions". In: *Proceedings of the 10th Nordic Symposium on Building Physics*. Lund, Sweden, pp. 207–214.

Ghazi Wakili, K. and Frank, T. (2004). "A humidity dependent vapour retarder in non-ventilated flat roofs. In situ measurements and numerical analysis". In: *Indoor and Built Environment* 13, pp. 433–441.

Glava (2018[a]). *Glava Blåseull*. Product sheet. URL: https://www.glava.no/bygg/losninger/blaseisolering/blaseisolering-med-glava/ (visited on 11/14/2018).

— (2018[b]). *Ytelseserklæring (DoC), glava blåseull innblåst i lukket hulrom*. Product sheet. URL: https://www.glava.no/bygg/losninger/blaseisolering/blaseisolering-med-glava/ (visited on 11/14/2018).

Grunewald, J. (2016). *Prüfung Berichte SIGA-Majrex (estellt durch das büro für holz(bau)physik*. Technische Universität Dresden.

Gullbrekken, L. and Elvebakk, K. (2018). *Prosjektnotat: Smart dampspserre Lund Vest, Bakke Bygg - Premisser og trefuktmålinger*. SINTEF Byggforsk.

Holme, J. and Geving, S. (2018). *Unngå byggskader - Reduser risikoen for mugg- og råtesopp*. URL: https://www.sintef.no/globalassets/upload/artikkel-03-10-byggaktuelt.pdf (visited on 11/10/2018).

Klima2050 (2018). *Smart vapour barrier pilot; Longyearbyen dwellings*. URL: http://www.klima2050.no/longyearbyen-pilot (visited on 11/30/2018).

— (2019). *What we do*. URL: http://www.klima2050.no/what-we-do (visited on 03/17/2019).

Künzel, H. M. (1995). *Simultaneous heat and moisture transport in building components*. Stuttgart: Fraunhofer IRB Verlag.

Kvande, T., Gullbrekken, L., and Geving, S. (2018). *Piltoprosjekt, Smart dampsperre Longyearbyen boliger, Statsbygg. Premisser og trefuktmåling*. Klima2050.

Langerock, C. et al. (2017). "Hygrothermal behaviour of compact roofs in wood frame constructions through on-site measurements". In: *Energy Procedia* 132, pp. 813–818.

Nusser, B. and Teibinger, M. (2013). "Effects of combined shading and air exfiltration on lightweight building elements with high outer diffusion resistance". In: *Conference: 2nd Central European Symposium on Building Physics*. Vienna, Autria.

Olsen, T. A. (2017). "Uttørking av kompakte tretak med smarte dampsperrer - Bjelkelagets betydning for fuktforholdene". MA thesis. Trondheim: NTNU.

Omnisense (2018). *Product information*. URL: https://www.omnisense.com/help/sensor1_brief.asp?fbclid=IwAR1Rp2uaBT6seUUSd4tY2LCByLhyWQPuQLS-2sg-9kRhHeNTNTrnJMcamjg (visited on 03/29/2018).

SINTEF byggforsk (2005). *Muggsopp i bygninger - Forekomst og konsekvenser for inneklimaet*. Byggdetaljer 701.401. Norges byggforskinstitutt.

— (2015). *Fuktmåling i bygninger - Instrumenter og metoder*. Byggdetaljer 474.531. Norges byggforskinstitutt.

— (2018a). *Fukt i bygninger. Teorigrunnlag*. Byggdetaljer 421.132. Norges byggforskinstitutt.

— (2018b). *Kompakte tak*. Byggdetaljer 525.207. Norges byggforskinstitutt.

SINTEF certification (2018). *Teknisk godkjenning: Isola AirGuard Smart*. nr. 20321.

Standard Norge (2014). *NS 2512:2014 - Measurement of moisture in timber structures*.

Stellander, M. (2012). "Smarte dampsperrer med uttørkingsmulighet mot innelufta". MA thesis. Trondheim: NTNU.

The Norwegian EPD Foundation (2014). *Environmental product declaration - Paroc*. URL: `https://media.glava.net/mediabank/store/11331/NEPD00266E-Paroc-Insulation--product-group-with-density--120-kg-m---1.pdf` (visited on 03/12/2019).

Thorsrud, E. (2013). "Smarte dampsperrer - betydningen av vinterforhold". MA thesis. Trondheim: NTNU.

Thue, J. V. (2016). *Bygningsfysikk grunnlag*. Trondheim: Fagbokforlaget.

Viitanen, H. et al. (2003). "Moisture conditions and biodeterioration risk of building materials and structure". In: *Proceedings of the 2nd International Symposium ILCDES 2003, Integrated Lifetime Engineering of Buildings and Civil Infrastructures*. Kuopio, pp. 151–156.

Viitanen, H. (1994). "Factors affecting the development of biodeterioration in wooden constructions". In: *Materials and Structures* 27, pp. 483–493.

Werther, N., Winter, S., and Sieder, M. (2010). "Experimental and numerical study on the hygrothermal behaviour of nonventilated wooden flat roof constructions with ecological building products". In: *World conference on timber engineering*. Riva del Garda, Italia.

Wikimedia Commons (2019). *Norgeskart*. URL: `https://no.wikipedia.org/wiki/Fil:Airports_in_Norway_map.svg#file` (visited on 02/04/2019).

Wufi (2018). *What is WUFI?* URL: `https://wufi.de/en/software/what-is-wufi/` (visited on 11/09/2018).

— (2019[a]). *Wufi wiki - Air Layers*. URL: `https://www.wufi-wiki.com/mediawiki/index.php/Details:AirLayers` (visited on 02/06/2019).

— (2019[b]). *Wufi wiki - Moisture Storage Function*. URL: `https://www.wufi-wiki.com/mediawiki/index.php/Details:MoistureStorageFunction` (visited on 02/06/2019).

Appendix A: WUFI model

A.1 Investigation of numerical issues

Figure A.1 shows how the moisture is being distributed in the wooden sheathing. The high leap in the values can be due to numerical issues. Figure A.1b shows that the moisture content decreases towards the middle of the wooden sheathing. This figure is showing different sizes of the area where 2,5mm corresponds to the surface towards the insulation, while 9mm is half of the cross section of the wooden sheathing. Figure A.1a shows the distribution of moisture in the length of the wooden sheathing.

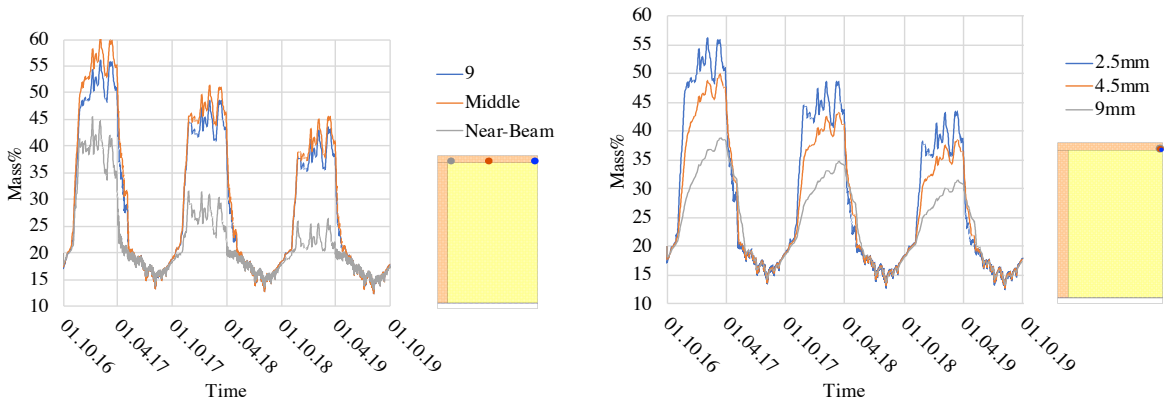

(a) Different locations in the wooden sheathing **(b)** Different areas chosen in point 9

Figure A.1: Comparing different locations and areas in the wooden sheathing to investigate possible numerical issues

A.2 Moisture storage function mineral wool

In a master thesis, a user-defined moisture storage curve is proposed based on the sorption curve of rock wool as shown in table A.1 (Stellander, M., 2012). Through a WUFI 1D calculation, Stellander, M. (2012) concludes that the user-defined sorption curve is valid for a construction with SVB, while with the use of a PE-foil numerical issues emerged.

Calculations with WUFI 2D for the default model used in the parameter analysis, show that more numerical issues emerged when using the user-defined sorption curve and the results are not considered reliable. See the results in figure A.2. As expected, the standardised moisture storage function creates higher moisture content, but due to the similarities of RH it is assumed to be accurate enough. In the field study, however, no numerical issues emerged when using the user-defined sorption curve. Therefore, this is used in order to achieve results similar to the measurements.

Table A.1: Moisture storage curve, mineral wool (Stellander, M., 2012)

RH	**Water content[kg/m^3]**		
	standard function in WUFI	**Sorption curve for rock wool**	**User defined sorption curve**
0	0	0	0
20	0.12	0.04	0.04
40	0.31	0.07	0.07
60	0.69	0.08	0.08
80	1.79	0.12	0.12
90	3.83	0.16	0.16
95	7.38	0.23	0.8
96	8.94	0.33	1.8
99	22.71	-	7.0
99.5	30.2	-	8.0
100	44.79	-	8.5

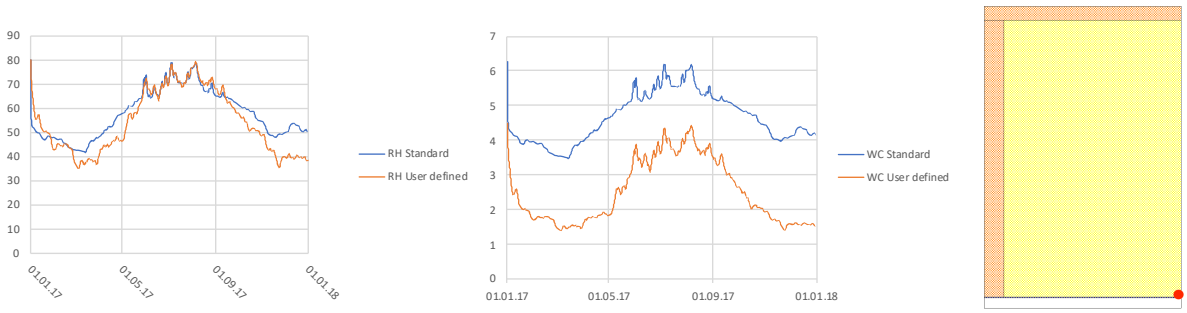

Figure A.2: RH and moisture content of the mineral wool close to the SVB

A.3 cc50cm versus cc60cm structure

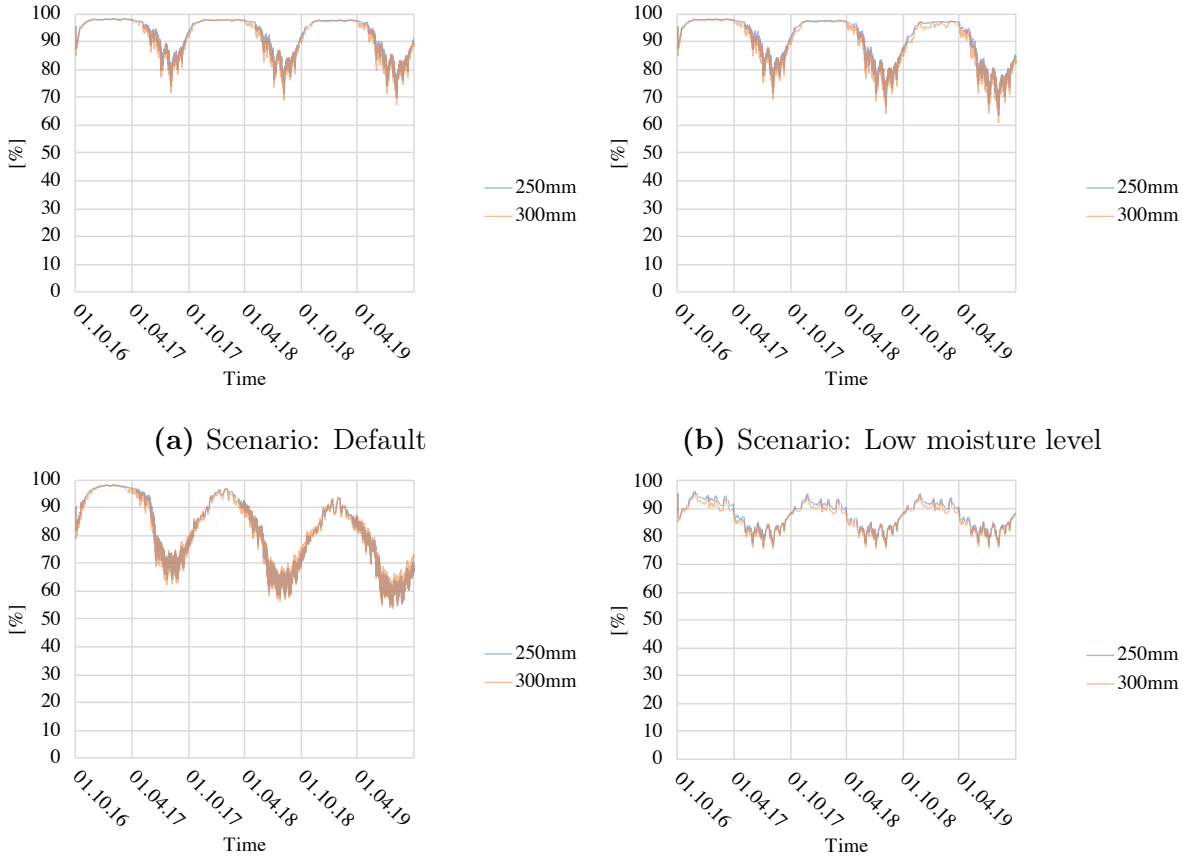

(a) Scenario: Default

(b) Scenario: Low moisture level

(c) Scenario: Kristiansand

(d) Scenario: 100mm insulation on top

Figure A.3: RH in point 9

Appendix B: Parameter analysis

B.1 Moisture content in the wooden sheathing

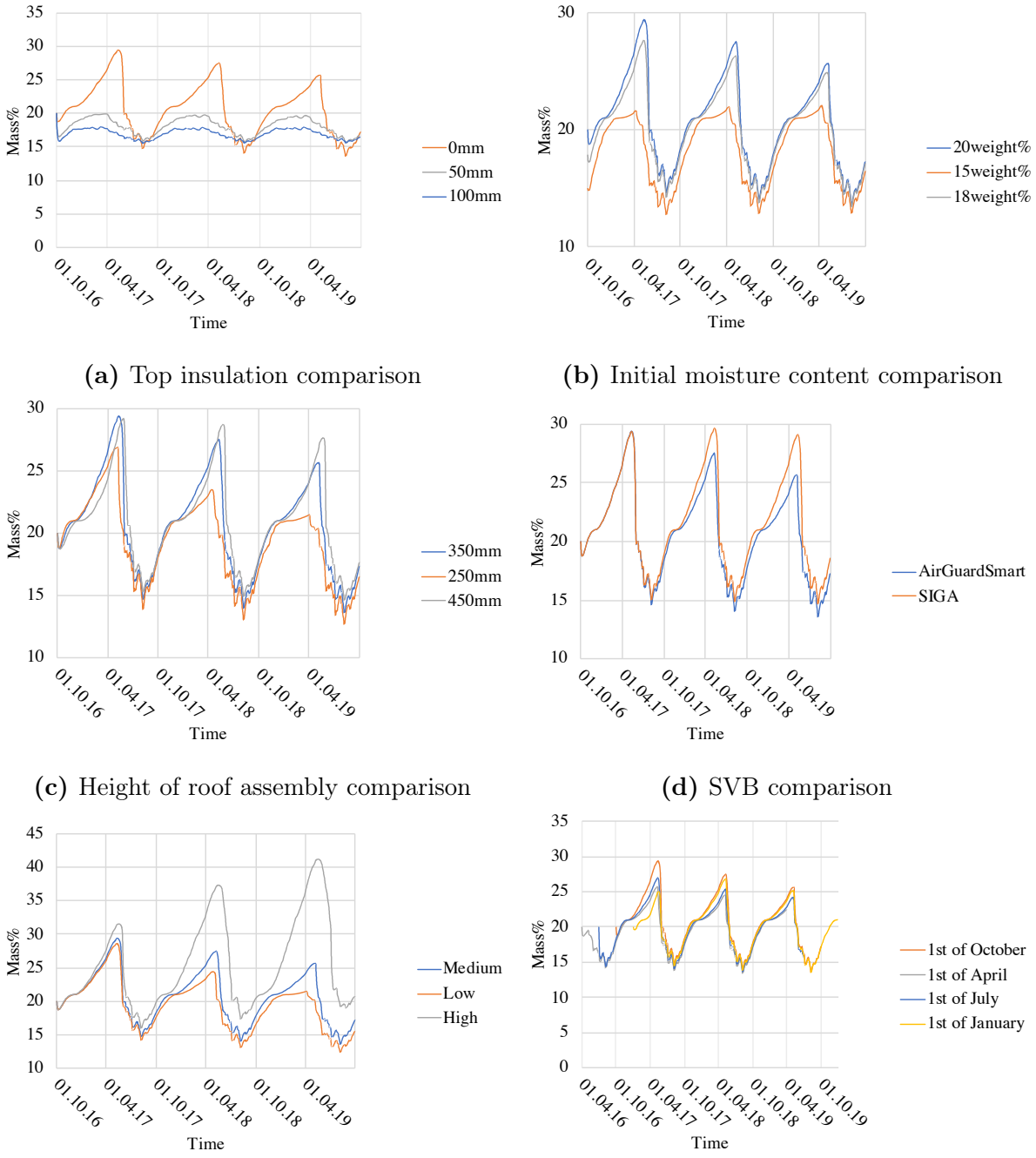

(a) Top insulation comparison

(b) Initial moisture content comparison

(c) Height of roof assembly comparison

(d) SVB comparison

(e) Internal moisture load comparison

(f) Closing of the construction comparison

Figure B.1: Moisture content in the middle of the wooden sheathing, monitor point 12

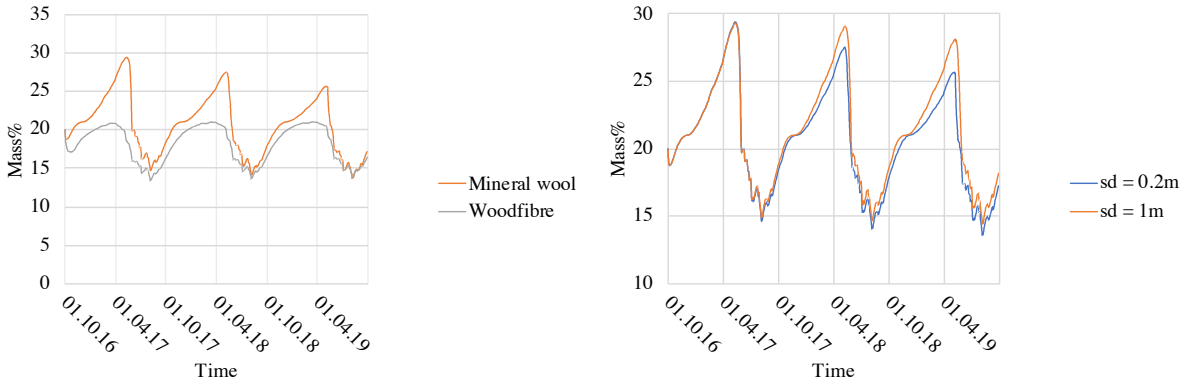

(g) Comparing insulating materials

(h) Internal diffusion resistance comparison

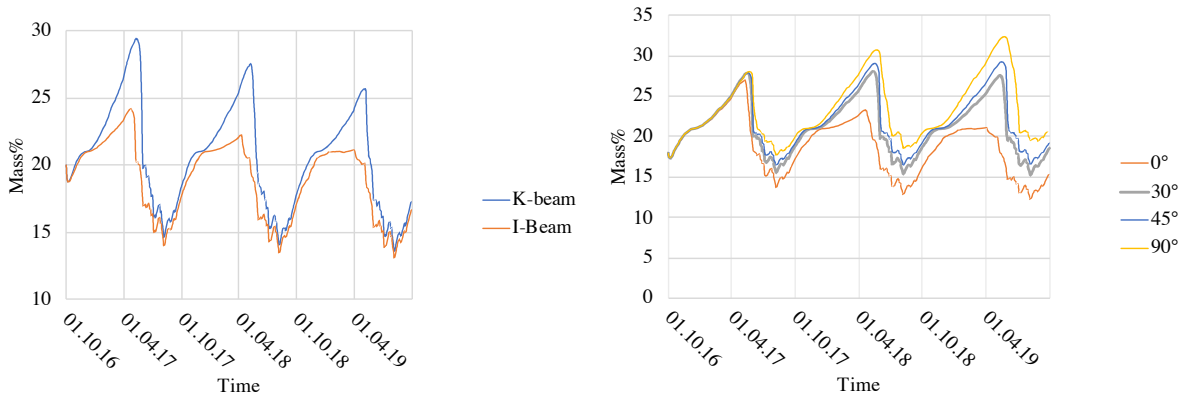

(i) Type of beam comparison

(j) Inclination comparison

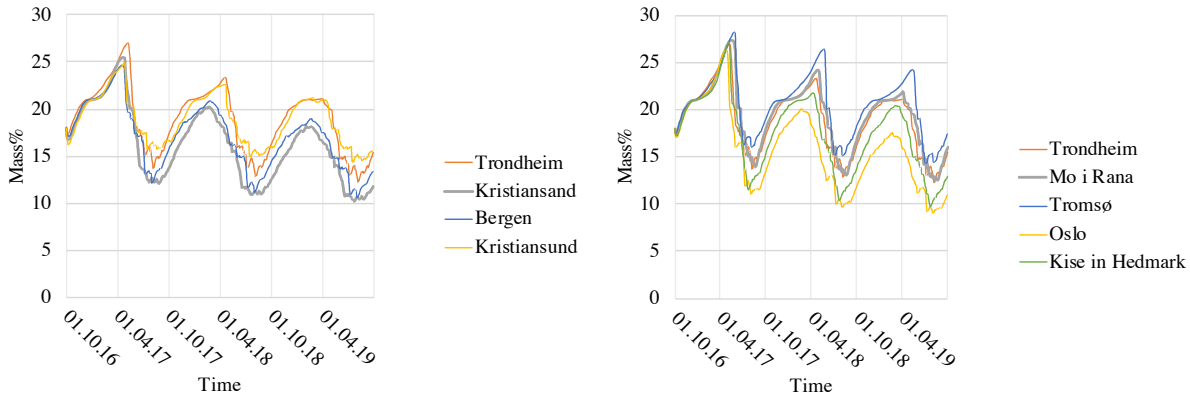

(k) Comparison of the climates

(l) Comparison of the climates

Figure B.1: Moisture content in the middle of the wooden sheathing, monitor point 12 (*Continued*)

B.2 Moisture content in the top beam

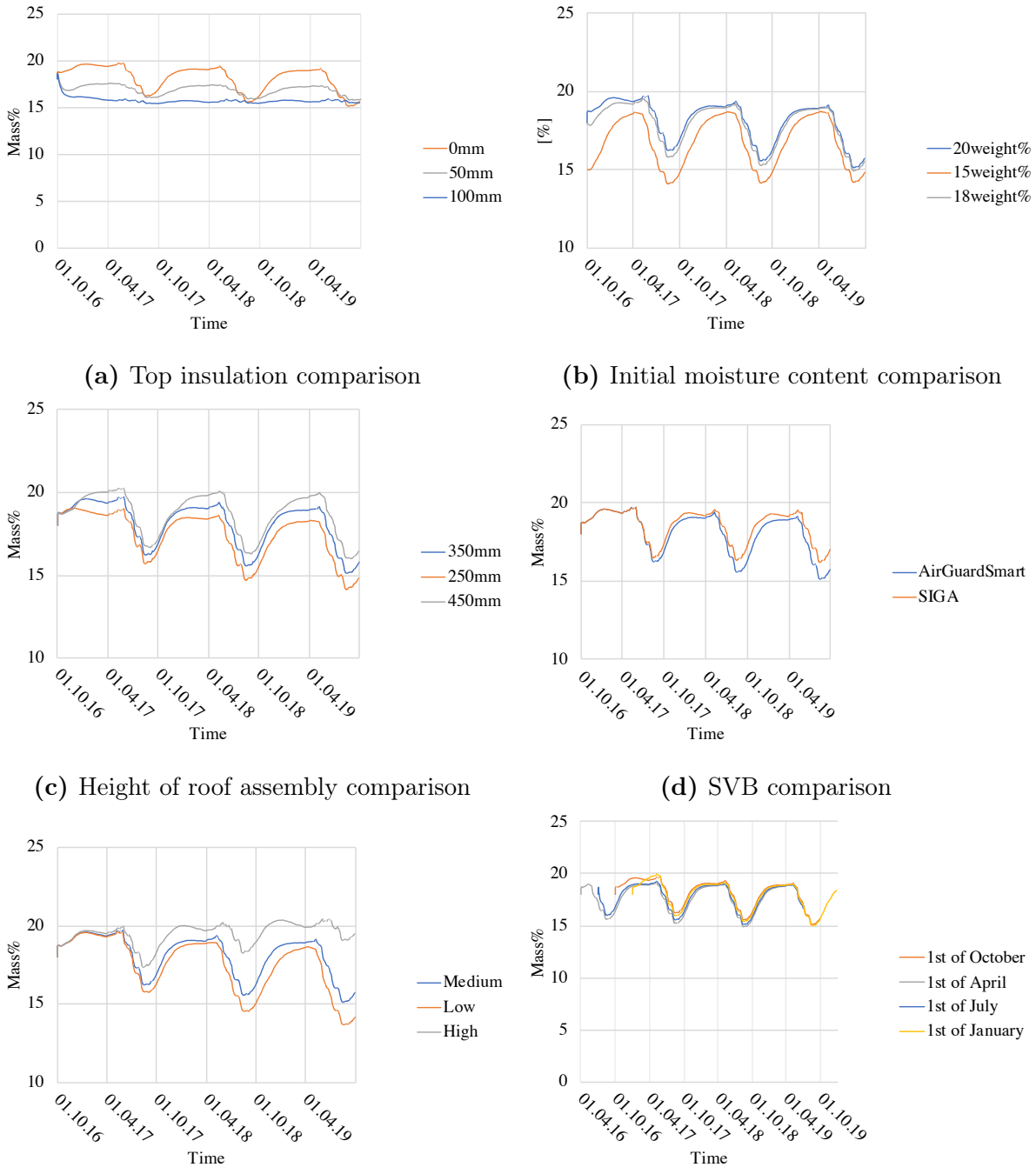

(a) Top insulation comparison

(b) Initial moisture content comparison

(c) Height of roof assembly comparison

(d) SVB comparison

(e) Internal moisture load comparison

(f) Closing of the construction comparison

Figure B.2: Moisture content in the middle of the top beam, monitor point 4

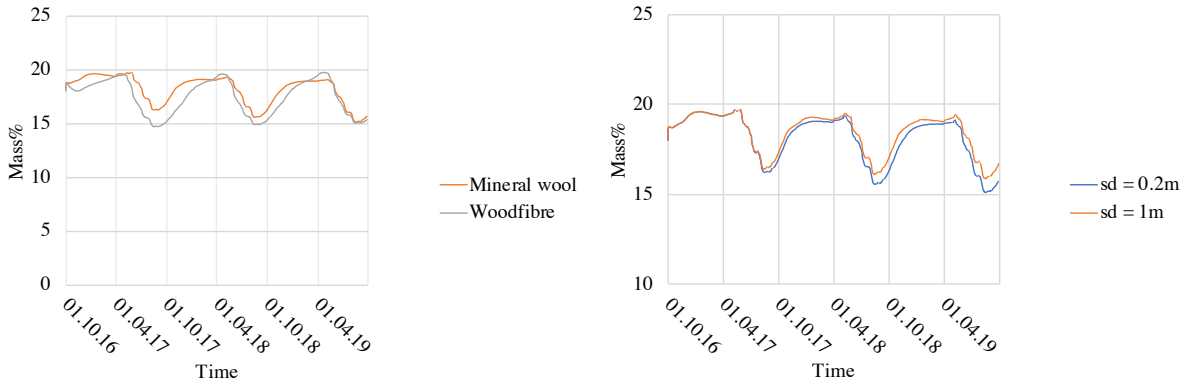

(g) Comparing insulating materials

(h) Internal diffusion resistance comparison

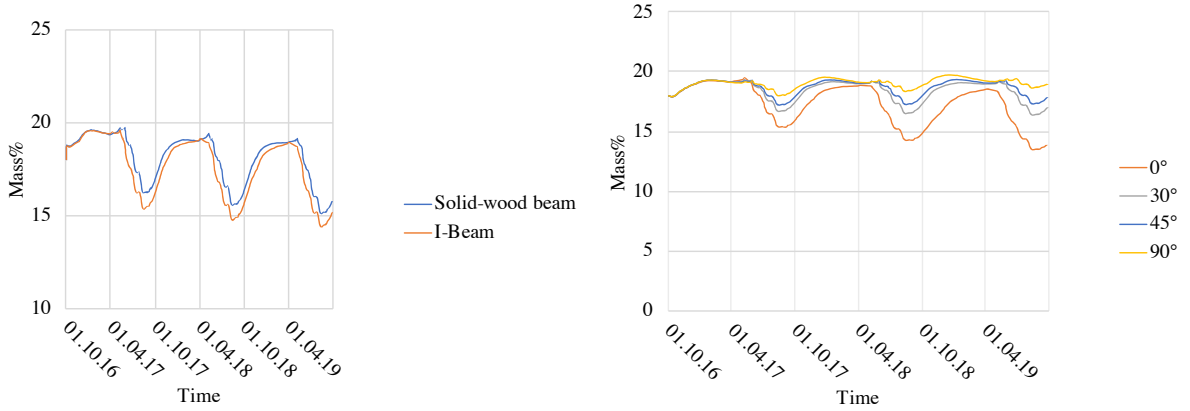

(i) Type of beam comparison

(j) Inclination comparison

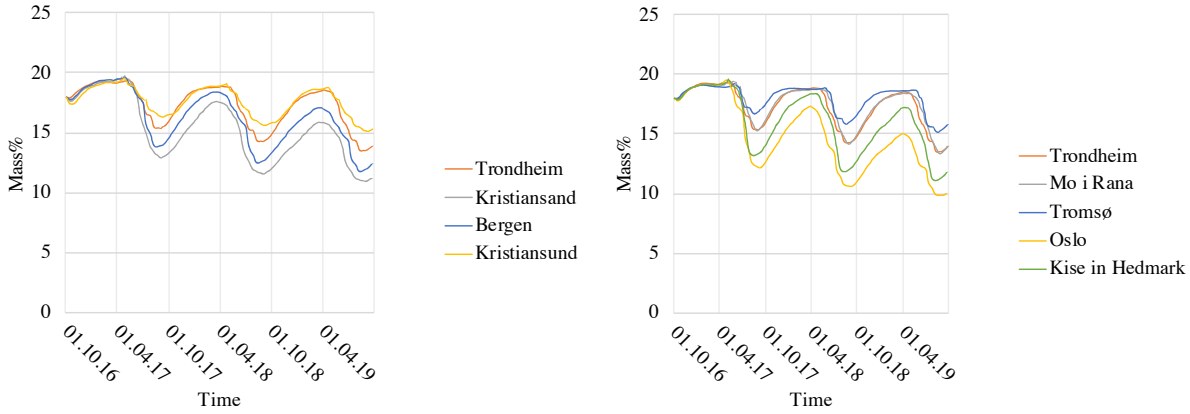

(k) Comparison of the climates

(l) Comparison of the climates

Figure B.2: Moisture content in the middle of the top beam, monitor point 4 (*Continued*)

Appendix C: Temperature correlation

The temperature correlation is calculated with WUFI using the measured internal climate and standard climate files from WUFI and IDA ICE. The area where the temperature is being extracted from is in the insulation close to the beam, 1cm below the wooden sheathing and a thin layer on the surface of the wooden sheathing. This resembles the areas where the sensors are placed in the pilot projects. As shown in figure C.1, the climate of Longyearbyen has a higher spread of points, which means that the uncertainties of this correlation are higher. Figure C.2 shows a day the roof is exposed to solar radiation. Here it is possible to see how the surface temperature is increased above the temperature 1 cm below the wooden sheathing.

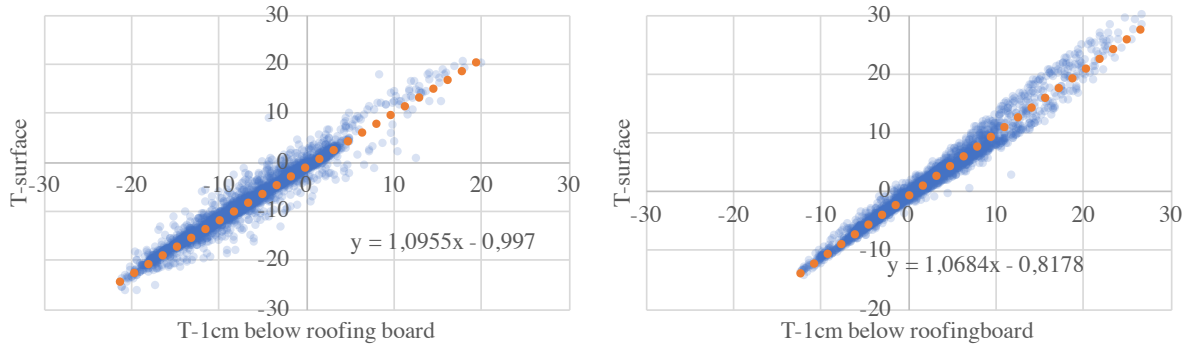

(a) Longyearbyen **(b)** Lund Vest

Figure C.1: Temperature correlation

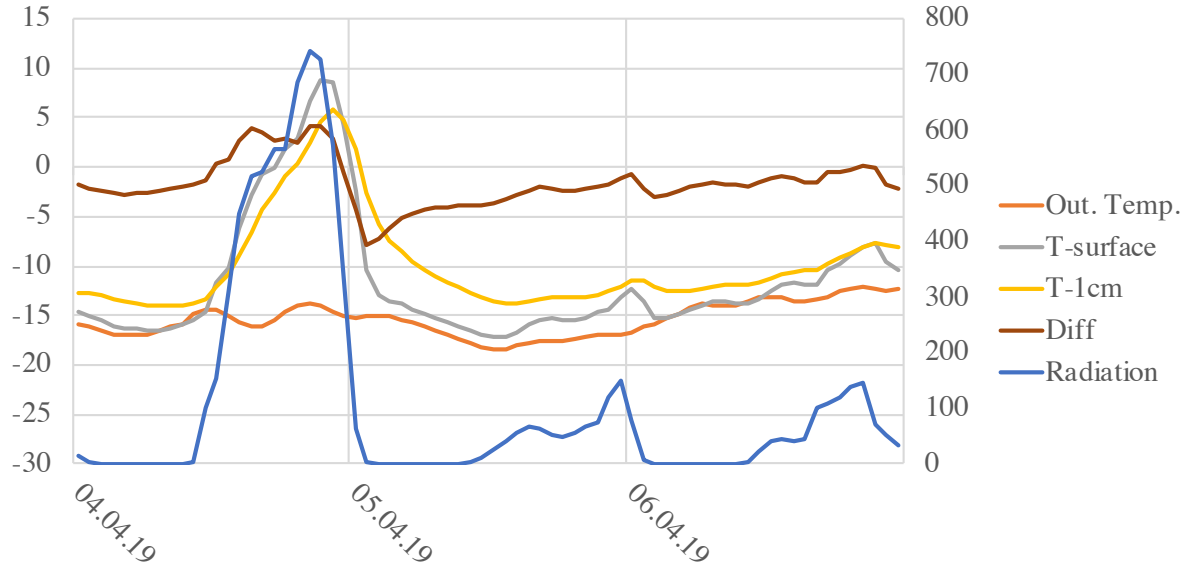

Figure C.2: Temperature correlation over 3 days in Longyearbyen

Appendix D: Pilot project

D.1 Measurements before inhabitation

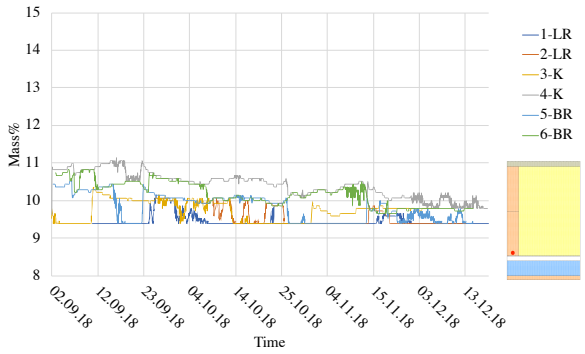

(a) Longyearbyen A33/34, 1 cm above the SVB

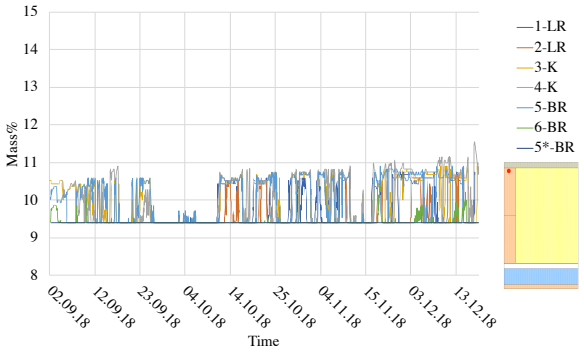

(b) Longyearbyen A33/34, 1cm beneath the wooden sheathing

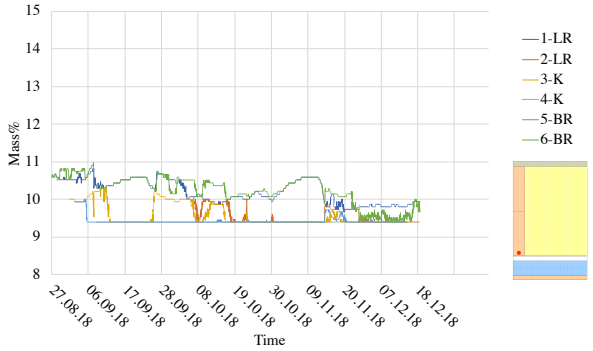

(c) Longyearbyen A35/36, 1 cm above the SVB

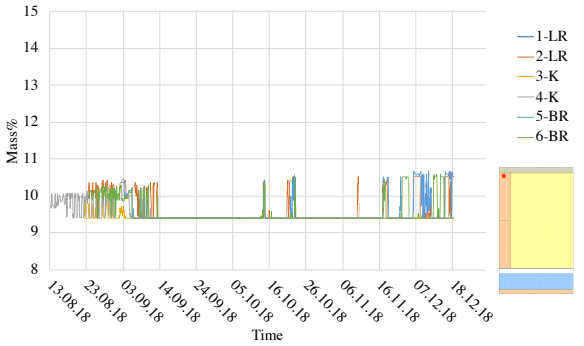

(d) Longyearbyen A35/36, 1cm beneath the wooden sheathing

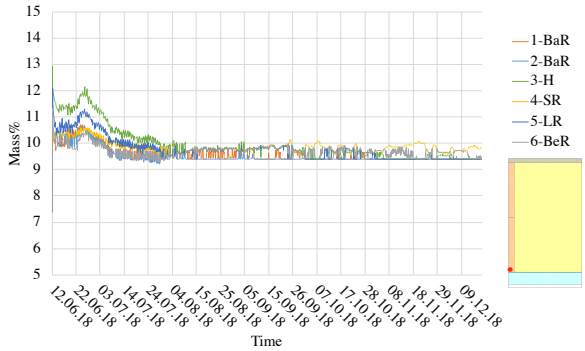

(e) Lund Vest, 1 cm above the SVB

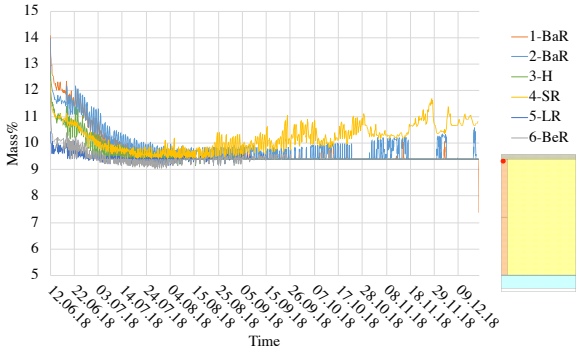

(f) Lund Vest, 1cm beneath the wooden sheathing

Figure D.1: Moisture content measured in the beam before inhabitation of the house

D.1.1 Longyearbyen-A35/36

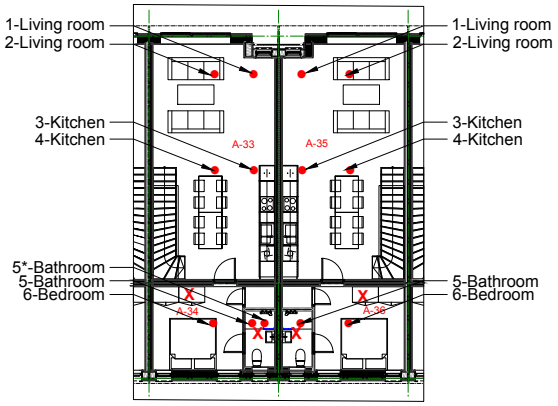

(a) Floor plan

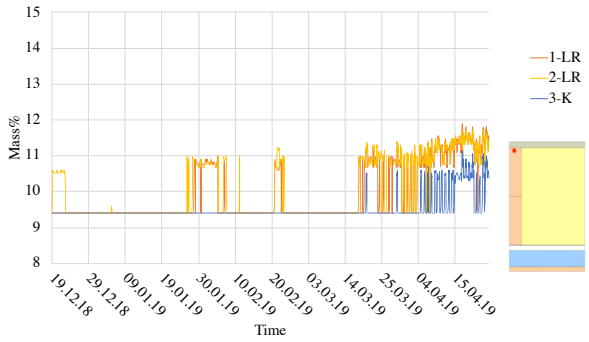

(b) Sensors 1-4 (A35), 1cm beneath the wooden sheathing

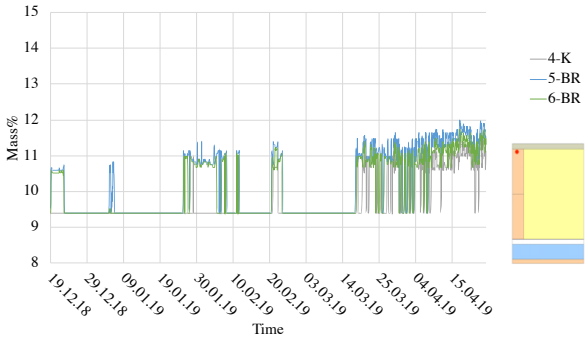

(c) Sensors 5-6 (A36), 1cm beneath the wooden sheathing

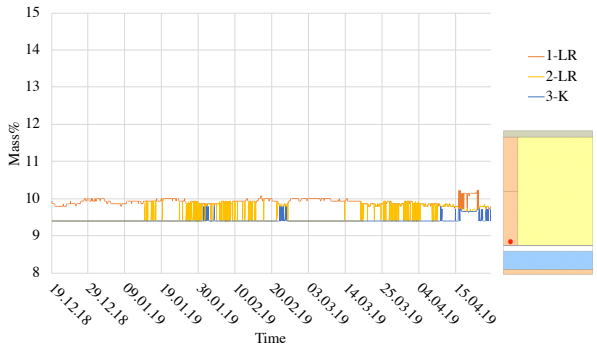

(d) Sensors 1-4 (A35), 1cm above the SVB

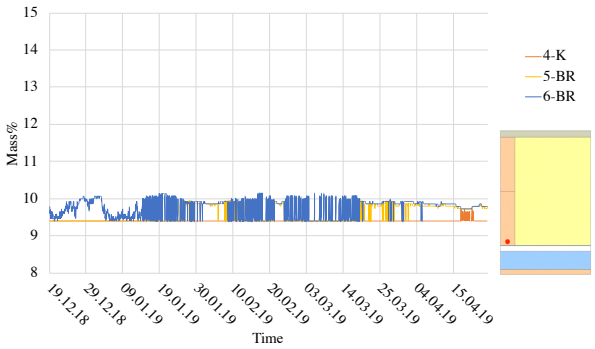

(e) Sensors 5-6 (A36), 1cm above the SVB

Figure D.2: Moisture content measured by sensors 1-6 in the project in Longyearbyen house A35/36

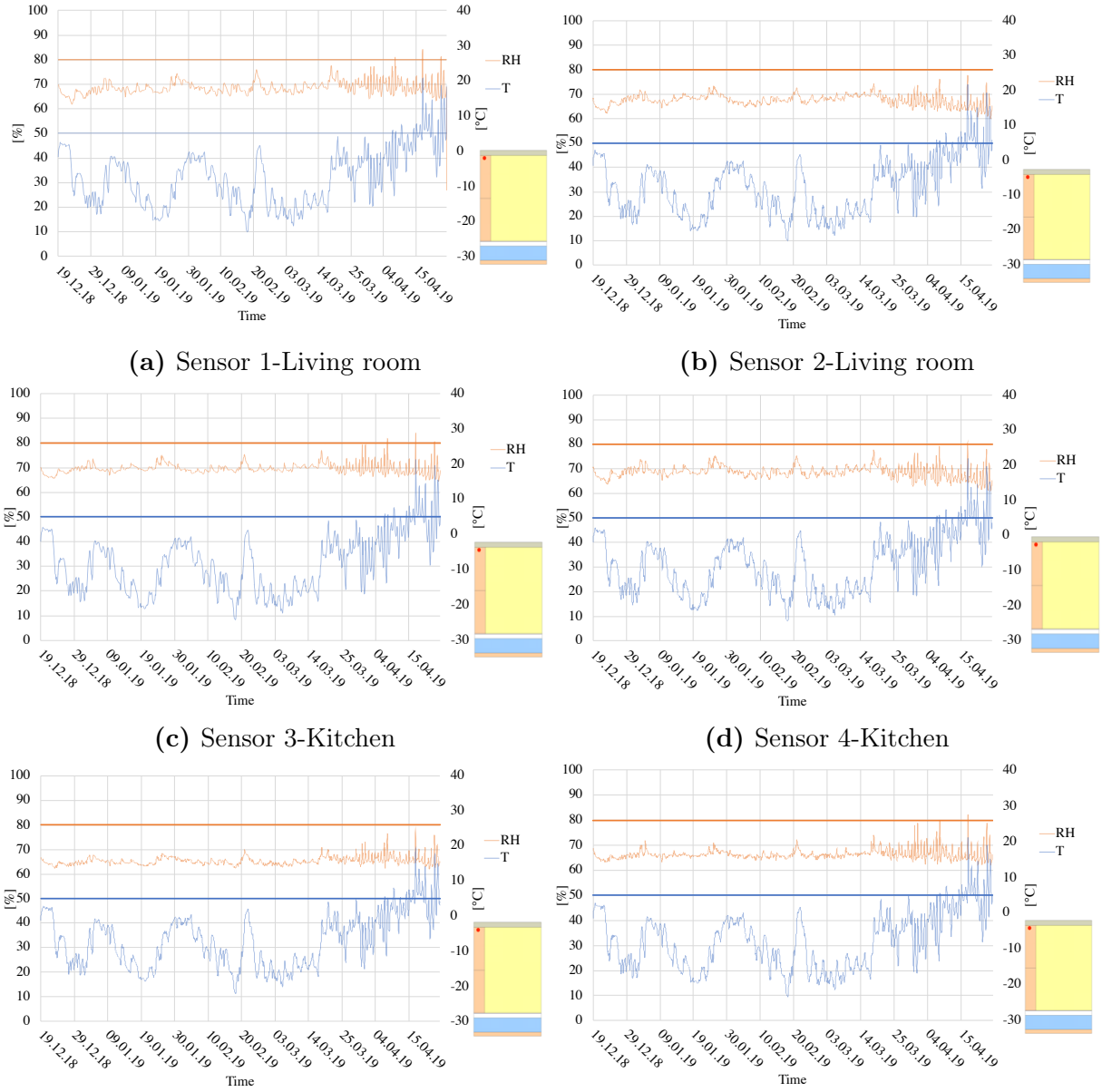

(a) Sensor 1-Living room

(b) Sensor 2-Living room

(c) Sensor 3-Kitchen

(d) Sensor 4-Kitchen

(e) Sensor 5-Bathroom

(f) Sensor 6-Bedroom

Figure D.3: RH-T for each sensor in the project in Longyearbyen A35/36, measured 1cm beneath the wooden sheathing

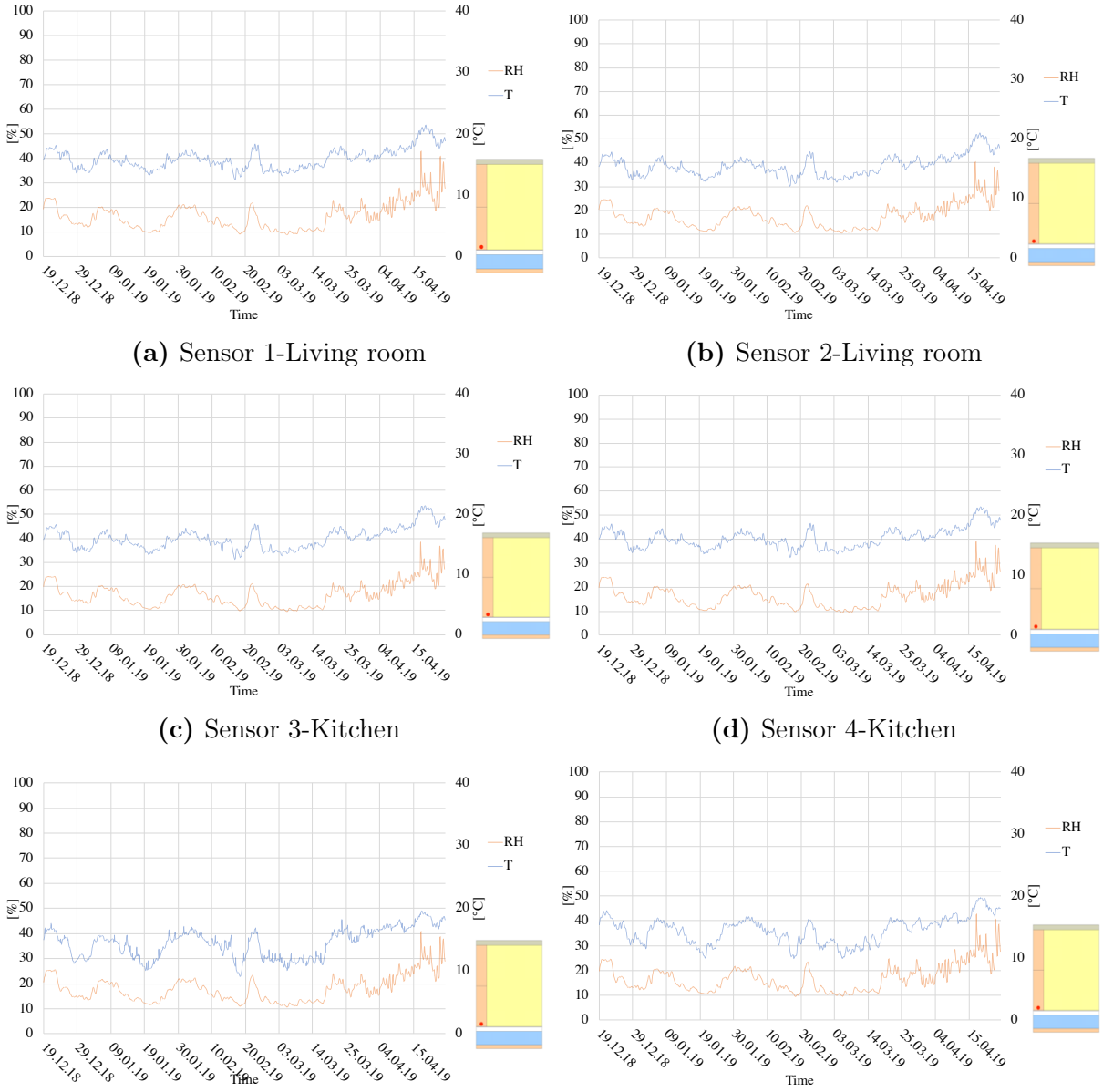

(a) Sensor 1-Living room

(b) Sensor 2-Living room

(c) Sensor 3-Kitchen

(d) Sensor 4-Kitchen

(e) Sensor 5-Bathroom

(f) Sensor 6-Bedroom

Figure D.4: RH-T for each sensor in the project in Longyearbyen A35/36, measured 1cm above the SVB